


Cite this: *RSC Adv.*, 2025, **15**, 3607

Recent advances in the synthesis, reaction, and bio-evaluation potential of purines as precursor pharmacophores in chemical reactions: a review

Ahmed Ragab  ^{*ab}

Purines are nitrogenous heterocyclic compounds characterized by the presence of two fused rings: pyrimidine and imidazole. Their significance is underscored by their widespread occurrence in natural products as the metabolic processes of all living organisms heavily rely on purines and their synthetic derivatives. Furthermore, purines exhibit considerable bioactivity, highlighting their importance in biological systems. Given their unique structural characteristics and ability to yield a diverse array of bioactive molecules, purines have attracted substantial attention from researchers. This review illustrates the recent methods for the synthesis of purines from diaminomaleonitrile, urea derivatives, imidazole, and pyrimidine derivatives reported from 2019 to 2024. Additionally, it elucidates the various chemical modifications applied to the purine nucleus, including benzoylation, alkylation, halogenation, amination, selenylation, thiolation, condensation, diazotization, coupling reactions, and other miscellaneous reactions. Moreover, this review discusses several biological evaluations, including the mechanisms of action of purine derivatives as anticancer, antimicrobial, anti-inflammatory, antiviral, antioxidant, and anti-Alzheimer agents. This review aims to assist researchers in synthetic organic and medicinal chemistry toward the development and enhancement of novel methodologies for the synthesis of new purine molecules while supporting biologists in the identification of new targets for bio-evaluation.

Received 21st November 2024
Accepted 22nd January 2025

DOI: 10.1039/d4ra08271k
rsc.li/rsc-advances

1. Introduction

Purine (imidazo[4,5-*d*]pyrimidine) is a heterocyclic aromatic system composed of fused pyrimidine and imidazole rings. It is

found in four tautomeric N-H forms. Purine tautomer stability increases with increasing aromaticity, and the order is as follows: 9-H > 7-H > 3-H > 1-H. It has been reported that deprotonated NH-pyrimidine (H9 and H7) displays higher

^aChemistry Department, Faculty of Science, Galala University, Galala City, Suez, 43511, Egypt. E-mail: ahmed.abdelwahab@gu.edu.eg

^bDepartment of Chemistry, Faculty of Science (Boys), Al-Azhar University, Nasr City, Cairo, 11884, Egypt. E-mail: Ahmed_ragab@azhar.edu.eg

Ahmed Ragab

Ahmed Ragab is recognized as a prominent figure in the field of organic chemistry, particularly in pharmaceutical organic chemistry. He serves as an associate professor of organic chemistry in the Chemistry Department at the Faculty of Science, Al-Azhar University, Cairo, Egypt. Currently, he is on secondment to the Chemistry Department, Faculty of Science, Galala University, where he continues his academic pursuits. Ahmed obtained his bachelor's degree in special chemistry from the Faculty of Science. Subsequently, he earned both a master's degree and a PhD in organic chemistry, specializing in the synthesis of heterocyclic organic compounds, from Al-Azhar University, Cairo. His master's and doctoral research were conducted under the supervision of Professor Dr Ahmed Shehab El-Sherief, Professor Dr Yousry Ammar, and Professor Dr Yahya M. Abdelfatah. His research interests are focused on the synthesis of novel heterocyclic compounds with significant biological activity, particularly drug derivatives and natural products, along with the evaluation of their biological activities as antifungal, antimicrobial, and anticancer agents. He also engages in organic process development, drug design, as well as medicinal and pharmaceutical chemistry. In the past five years, his work has concentrated on synthesizing new hybrid bioactive heterocyclic compounds for biological evaluation, covering areas such as antimicrobial, anticancer, anti-inflammatory, and antidiabetic activities,

all based on the active core of the synthesized compounds. Furthermore, he is involved in the design of new dyes and sensors. His research has included many computational studies, such as density functional theory (DFT) and molecular docking simulations, and he has collaborated with various research teams. In 2023, he contributed to the modification of novel polymeric materials by designing new polymer-drug conjugations at the Department for Biomaterials Research, Polymer Institute, Slovak Academy of Sciences, Bratislava, Slovakia.



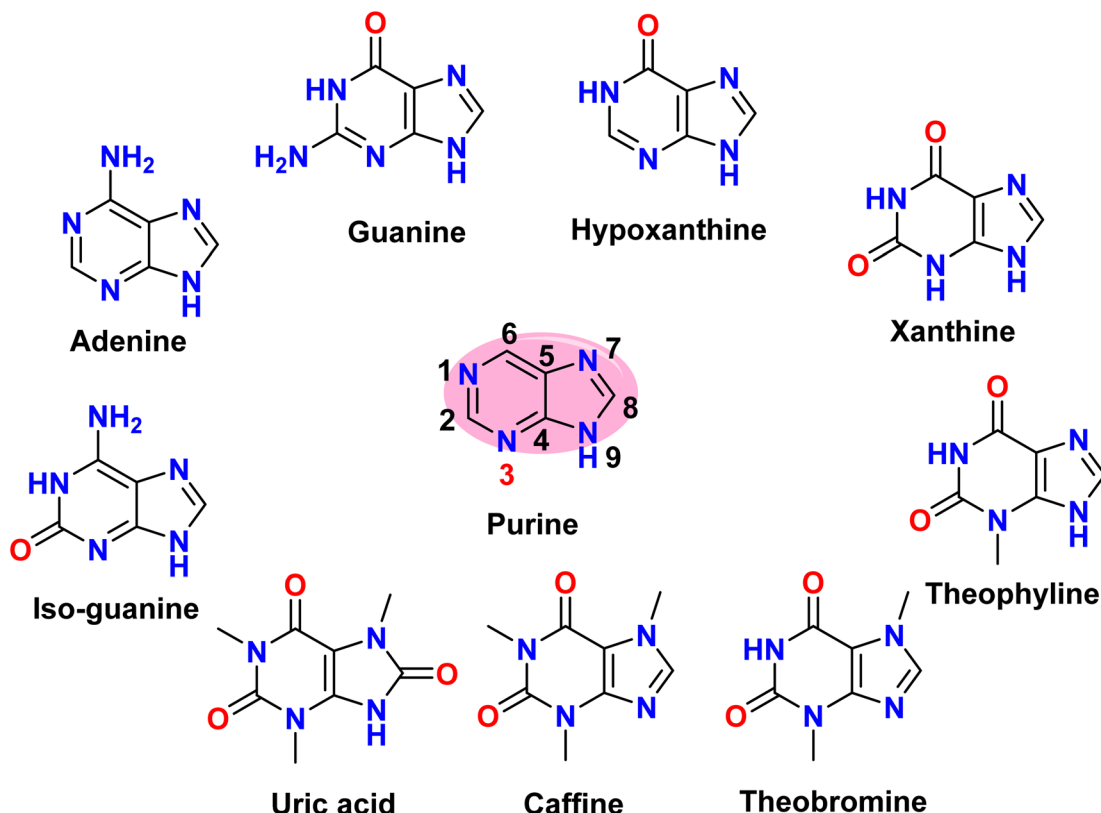


Fig. 1 Structure of purine and its analogues.

aromaticity, while its aromaticity decreases in imidazole (H1 and H3).¹ These results were confirmed by the harmonic oscillator model of aromaticity (HOMA). Pyrimidine without NH showed an HOMA of 0.971, and imidazole showed an HOMA of 0.742. The structure of purine serves as a basis for synthesizing many biologically significant compounds, including guanine, adenine, isoguanine, xanthine, caffeine, hypoxanthine, and uric acid. Moreover, adenine and guanine are important because they are the fundamental building blocks of DNA, RNA, and ATP systems, which are vital to life processes (Fig. 1).¹

Purine is a nine-atom compound with four nitrogen atoms at positions 1, 3, 7, and 9. Numbering in purines starts with nitrogen 1 of the six-membered ring and moves in an anti-clockwise direction, and it continues on the imidazole ring but in a clockwise manner.¹ Additionally, purines are essential components of nucleic acids and play a role as energy cofactors for coenzymes involved in redox processes. They are also involved in several intracellular signal transduction processes and function as direct neurotransmitters.² Purines have received significant research attention owing to their distinct properties and their value as a valuable source of various bioactive molecules in medicinal chemistry.³ Moreover, the importance of purine derivatives originates from their abundant presence in natural products and synthetic compounds, as well as their potential for bioactivity. The metabolism of all living organisms heavily depends on purine and purine bases, such as adenine, guanine, and xanthine (Fig. 1).⁴

Furthermore, the purine scaffold is has been synthesized and analyzed to develop beneficial drugs with broad biological activity, such as anti-cancer drugs with different targets (m-TOR, EGFR, FGFR, VEGFR, PI3K α , and B-RafV600E), anti-bacterial (standard strains, clinical isolates, and *Helicobacter pylori*), anti-inflammatory (JAK2/BRD4, COX-2, and 15-LOX), anti-fungal, anti-oxidant, anti-tuberculosis, anti-HSV, anti-diabetic, anti-viral, and anti-Alzheimer's (AChE and BChE) activities.⁵⁻¹⁵ Additionally, many purine-based medications, including 6-thio-purine (mercaptopurine) and derivatives, cladribine, fludarabine, nelarabine, clofarabine, fadriciclib (CYC065), seliciclib, sapanisertib, and AZD-7648 (Fig. 2) are used in clinical trials.^{16,17} Most of them are used to treat cancers and inflammation, and their mode of action involves the impairment of the ability to synthesize nucleic acids or the inhibition of important metabolic enzymes.^{6,18} Moreover, numerous review articles have previously addressed the synthesis, reactions, and bio-evaluation of the purine scaffold in various contexts, including the utilization of purine-containing compounds as anticancer agents^{19,20} and cancer-targeting kinase inhibitors.²¹ Furthermore, the role of purines in inflammatory responses, encompassing their release, metabolism, and signaling, has been extensively explored.²² Purine nucleotides have also been identified as signaling molecules²³ and promising scaffolds in drug discovery.²⁴ Additionally, the chemistry and biosynthetic pathways of purines, as well as related reactions, biomedical prospects, and clinical applications, are discussed.²⁵ Furthermore, the synthetic routes and pharmaceutical activities



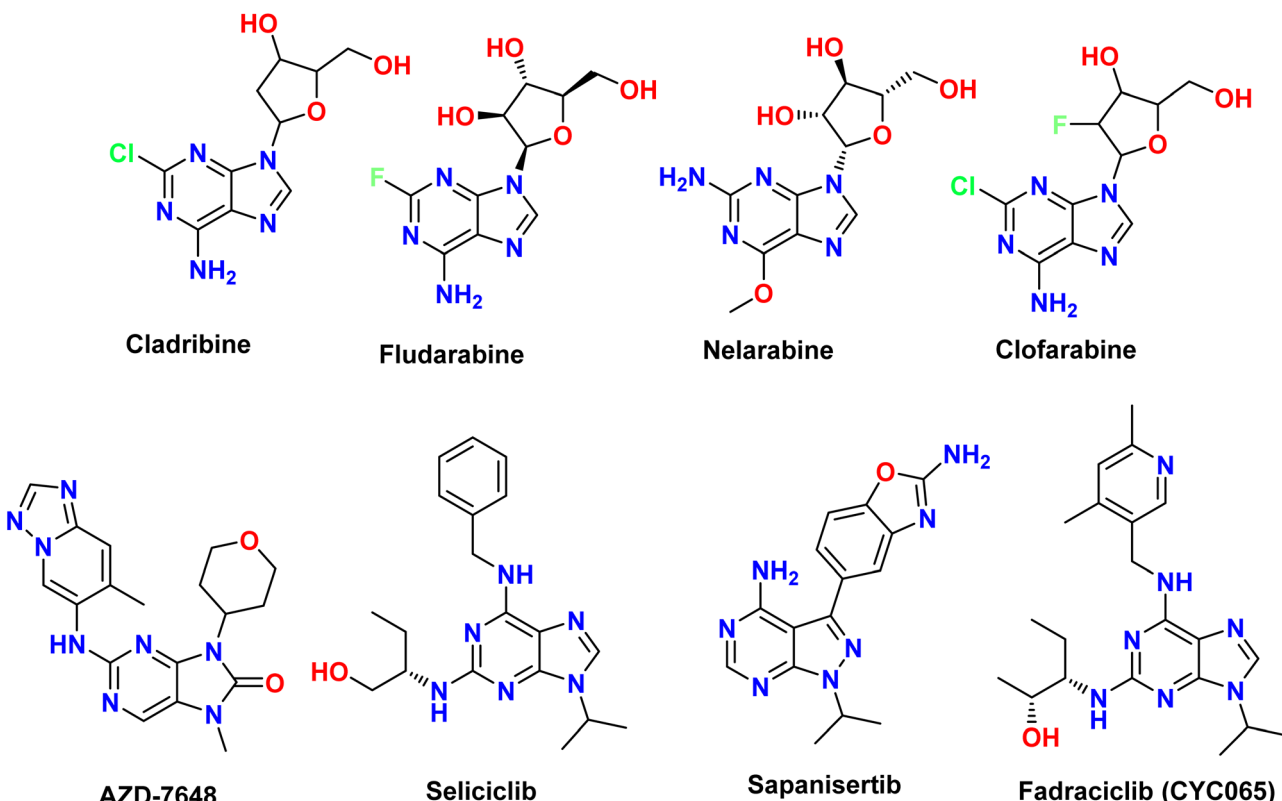


Fig. 2 Structures of purine-based FDA-approved drugs and those under clinical trials.

of purine derivatives have been examined,²⁶ alongside their neurotoxic effects.²⁷ However, the advantage of this review over the others is that it presents several examples from recent studies, newer synthetic methods, and some bio-evaluation from the perspective of SAR studies in a simple way.

Overall, this review article provides a comprehensive overview and summary of various methods employed for synthesizing purine derivatives over the past five years (2019–2024). In addition, this review article is one of my continuous efforts to gain insights into the design, synthesis, and bio-evaluation of heterocyclic scaffolds that are designed to modify and develop the bio-evaluation based on their structure or based on a hybridization approach for more than one nucleus to obtain one bioactive molecule, as described in my articles with my group.^{28–32} This review highlights numerous approaches and reagents utilized in these syntheses, including 2,3-diaminomaleonitrile, urea derivatives, imidazole derivatives, and pyrimidine derivatives. Furthermore, the article details an array of reactions involving purine derivatives, such as benzoylation, alkylation (mono-, di-, and tri-), halogenation (bromination), amination (nucleophilic substitution reactions), selenylation, thiolation, condensation, and cyclization, which facilitate the formation of new heterocyclic rings. Additional reactions discussed include diazotization and coupling reactions, among others. In conclusion, the article presents an overview of the biological evaluation of purine derivatives, which are categorized according to their activities, including anticancer, antimicrobial, anti-inflammatory, antiviral, antioxidant, and anti-

Alzheimer effects. It is anticipated that this review can guide future researchers in exploring rational approaches to the application of purine scaffolds as pharmaceuticals targeting various biological pathways in clinical trials.

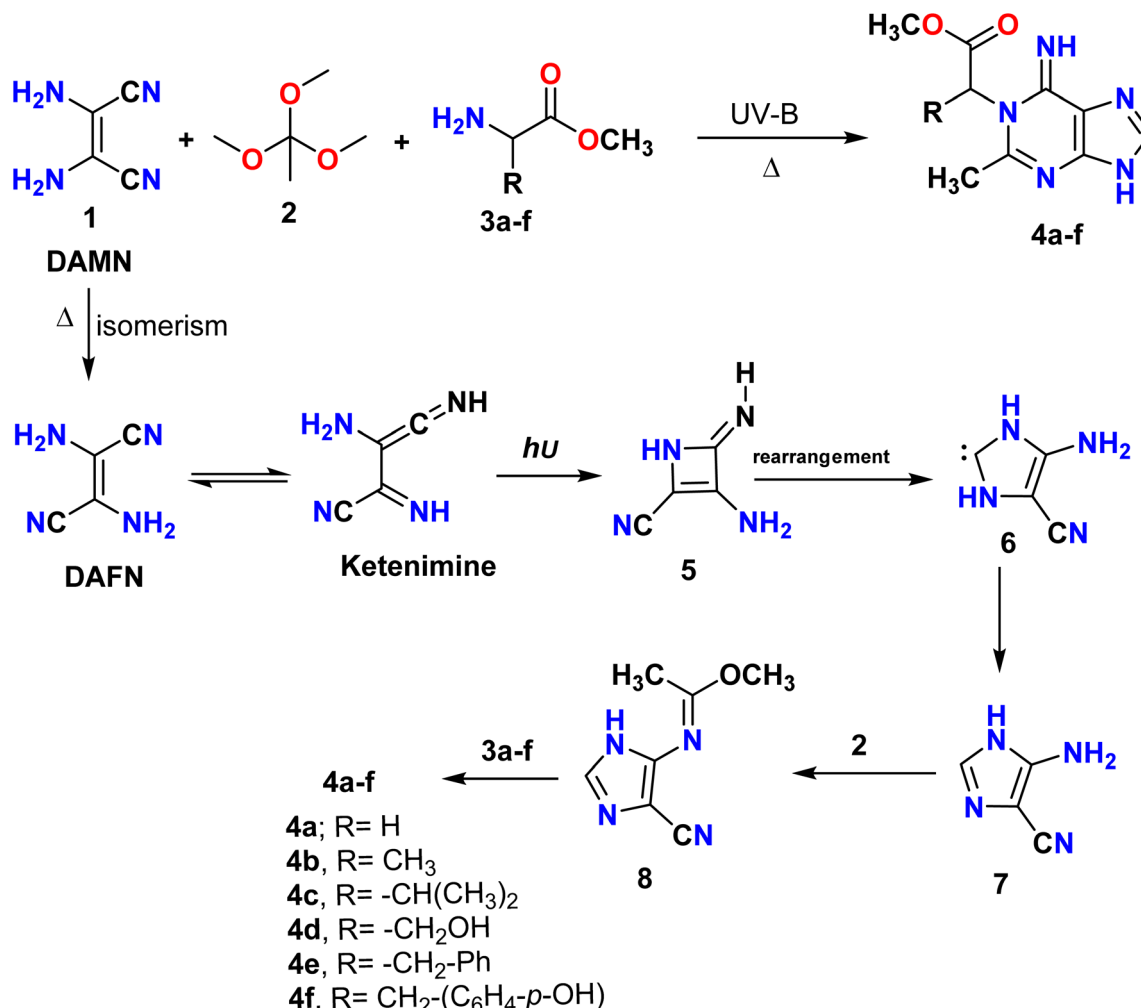
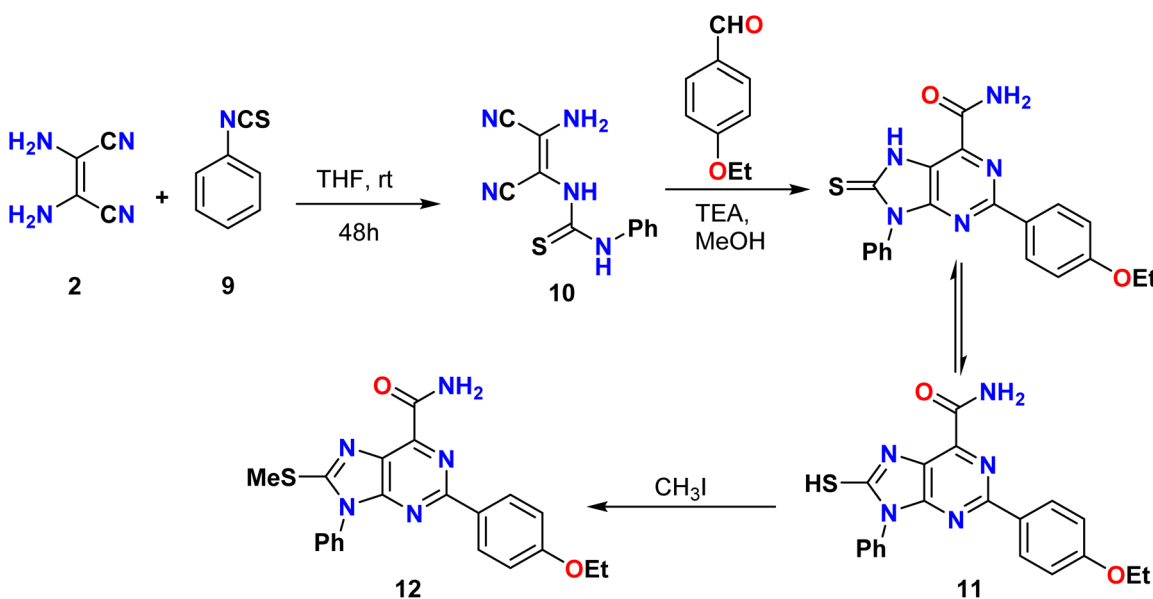
2. Synthesis of purine derivatives

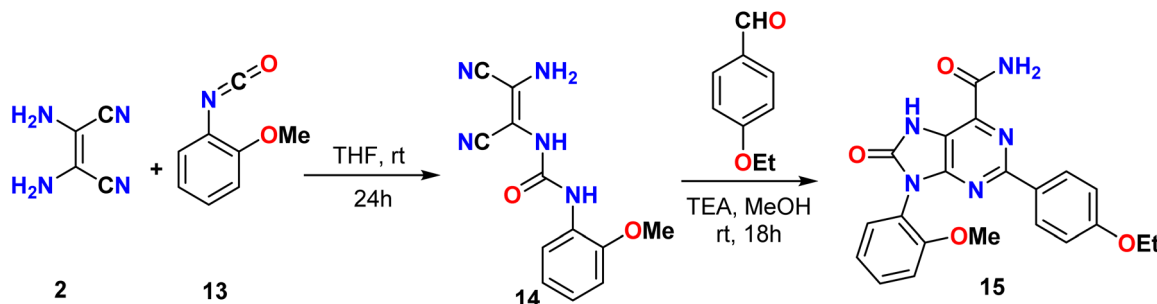
2.1. From diaminomaleonitrile and urea derivatives

Bizzarri *et al.* illustrated the synthesis of amino-acid-decorated purines **4a–f**, which were obtained as the main products in the multicomponent reaction between 2,3-diaminomaleonitrile (DAMN) **1**, trimethyl orthoacetate **2**, and α -amino acid derivatives **3a–f** in acetonitrile containing triethyl amine (TEA) under reflux conditions and photon irradiation (290–315 nm) for 15 h. This way, they combined thermal and photochemical conditions to improve the complexity of the reaction pathway.³³

Moreover, the reaction can be described by the photoisomerization of diaminomaleonitrile (DAMN) to diaminofumaronitrile (DAFN), followed by the cyclization of diaminofumaronitrile (DAFN) to amino imidazole carbonitrile (AICN) **7** (ref. 34) *via* an unstable azetidine intermediate **5**.³⁵ The azetenes **5** undergo C–C bond cleavage and ultimate rearrangement to give N-heterocyclic carbene **6**, which tautomerizes readily to form AICN **7**. Additionally, amino imidazole carbonitrile (AICN) reacts with trimethyl orthoacetate **2** and produces the imidazole imino ether derivative **8**, which subsequently reacts with amino acid derivatives to give the desired purine derivatives, as shown in Scheme 1.³³



Scheme 1 Synthesis of 6-imino-6,9-dihydro-1*H*-purine derivatives **4a–f** decorated with amino acids.Scheme 2 Synthesis of 8-(methylthio)-9-phenyl-9*H*-purine-6-carboxamide derivatives **11** and **12** from diaminomaleonitrile.



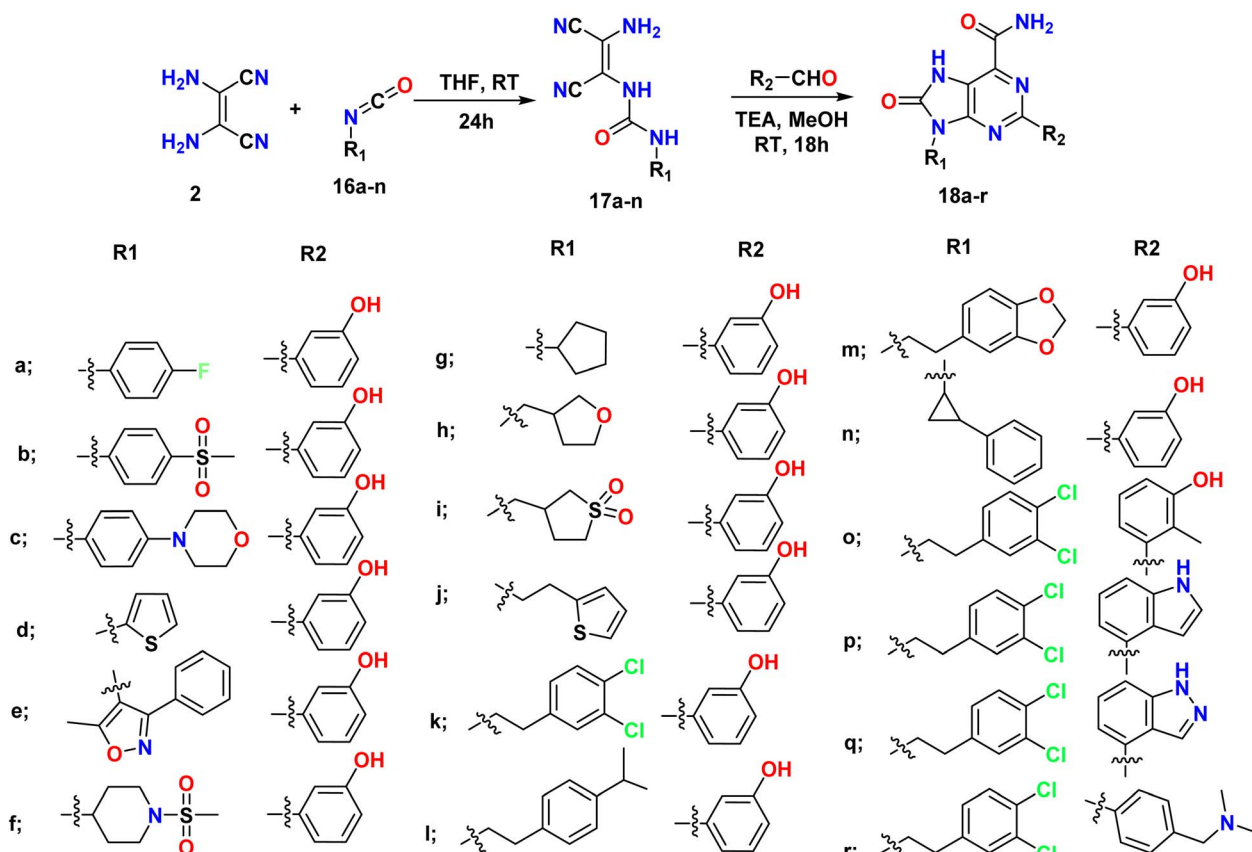
Scheme 3 Synthesis of 2,9-(substituted-phenyl)-8-oxo-7H-purine-6-carboxamide derivative 15.

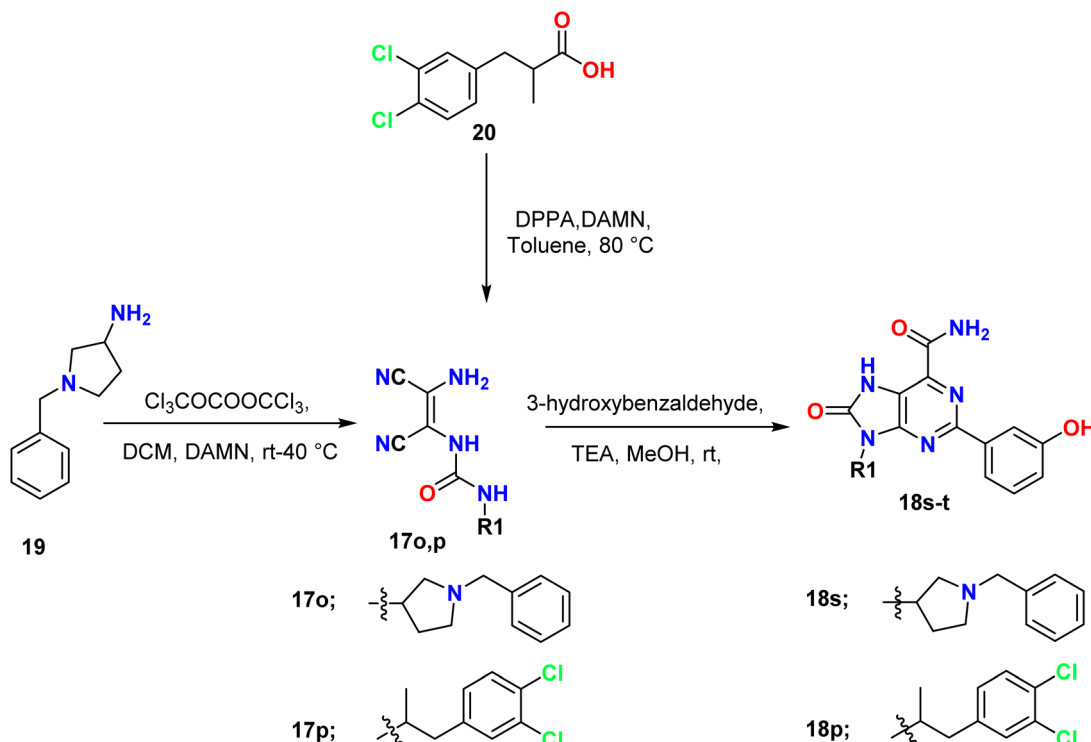
Huang *et al.* described the synthesis of a new 8-(methylthio)-9-phenyl-9*H*-purine-6-carboxamide derivative **12** by treating phenyl isothiocyanate **9** with diaminomaleonitrile (**2**) in the presence of THF as the solvent. The as-formed thiourea derivative then reacted with 4-ethoxybenzaldehyde to provide the 8-mercaptopurine-6-carboxamide derivative **11** as the desired product. The reaction between **11** and iodo-methane occurred exclusively at the relatively soft sulfur atom, yielding the *S*-alkylation product **12** (Scheme 2).³⁶

In the same way, Tseng *et al.* reported a synthetic method for the 2,9-(substituted-phenyl)-8-oxo-7*H*-purine-6-carboxamide derivative **15** based on the condensation reaction between 2-methoxyphenyl isocyanate **13** and diaminomaleonitrile (DAMN)

2, which yielded a urea derivative **14**. This urea compound was then treated with 4-ethoxybenzaldehyde to synthesize a series of purine derivatives **15** that could be used as dual-target anti-cancer agents, as illustrated in Scheme 3.³⁷

Mazzucato *et al.*, synthesized 7*H*-purin-8(9*H*)-one derivatives **18a–r** in two steps; the first step involved the reaction of 2,3-diaminomaleonitrile (DAMN) **2** and commercial isocyanate **16a–n** to afford ureic intermediates **17a–n** with the first substituent **R**₁. The second step involved the formation of a core and the addition of a second substituent (**R**₂) through the reaction of the intermediates with different aldehydes in the presence of TEA and catalytic quantities of I_2 , as shown in Scheme 4.³⁸

Scheme 4 Synthesis of 7*H*-purin-8(9*H*)-one from alkyl/aryl isocyanate using 2,3-diaminomaleonitrile (DAMN) and aldehyde.

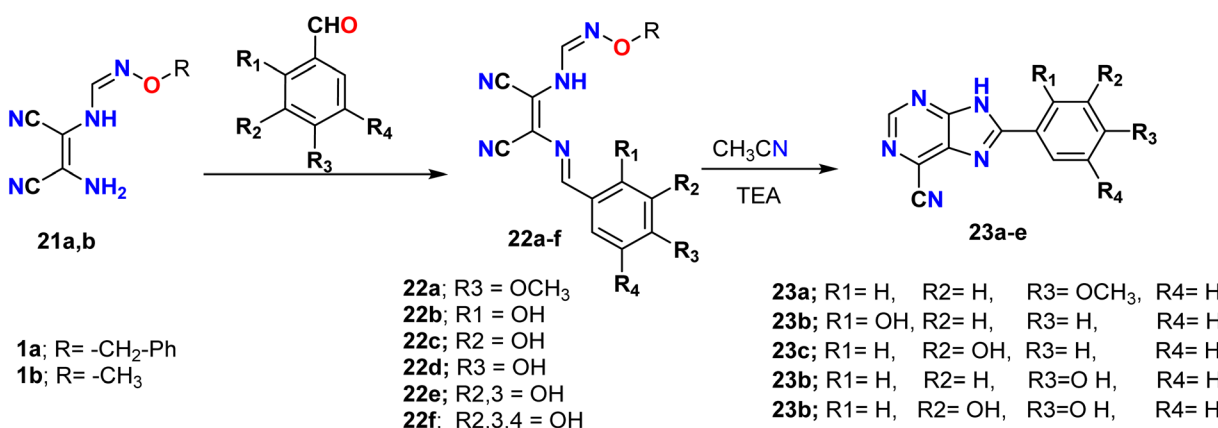


Scheme 5 Synthesis of 2,9-diaryl-8-oxo-7H-purine-6-carboxamide derivative 18s-t.

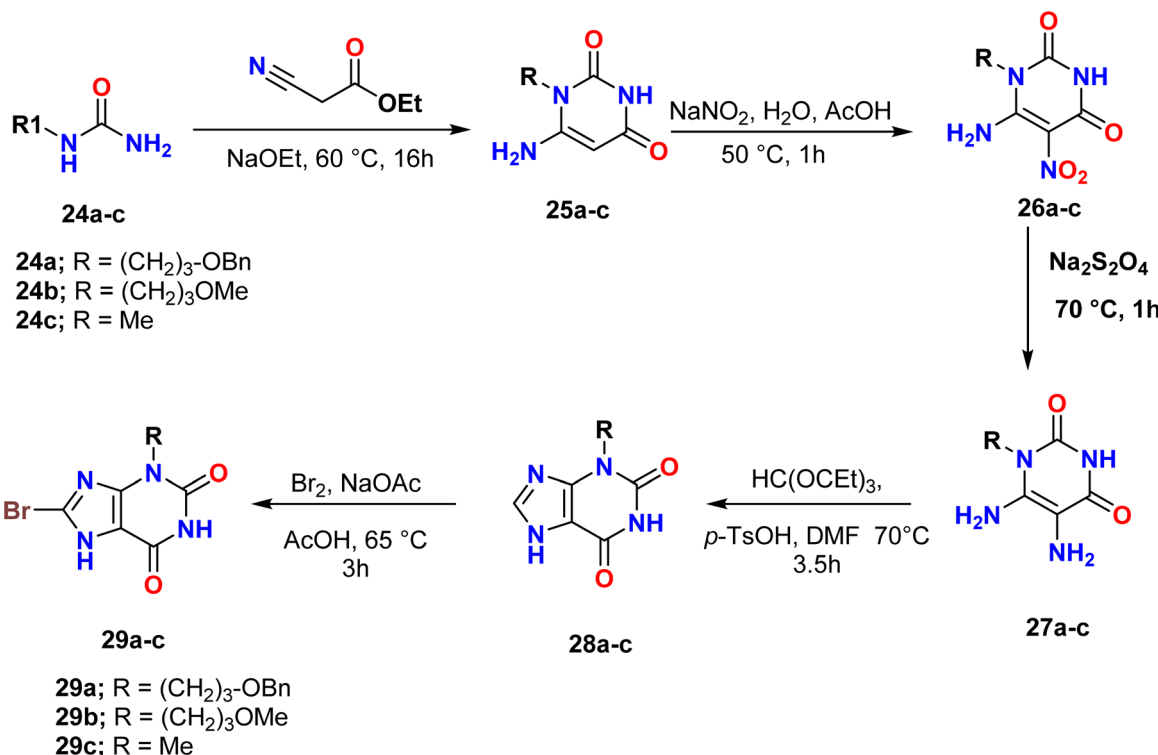
Moreover, 1-benzyl-3-isocyanatopyrrolidine was prepared by the reaction of 1-benzylpyrrolidin-3-amine **19** with triphosgene [$O=C(OCCl_3)_2$]; then the obtained isocyanate was reacted *in situ* with diaminomaleonitrile **1** (DAMN) to afford the corresponding urea derivative **17o**, which when treated with 3-hydroxybenzaldehyde and TEA gave the final product **18s**. Additionally, 2-benzylpropionic acid **20** was converted to an isocyanate (R-NCO) through Curtius rearrangement by using diphenylphosphoryl azide (DPPA) to convert the acid to azide and further to isocyanate. R-NCO then reacted *in situ* with diaminomaleonitrile (DAMN) **2** to give the urea derivative **17p**, which was treated with 3-hydroxybenzaldehyde to form the 2,9-diaryl-8-oxo-7H-purine-6-carboxamide derivative **18t** (Scheme 5).³⁸

Bettencourt *et al.* synthesized 6-cyanopurine derivatives **23a-e** containing a phenolic moiety through the reaction of *O*-alkylformamidoximes **21a, b** [*O*-benzylformamidoxime **21a** and *O*-methylformamidoxime **21b**] with phenolic aldehyde and triethyl amine TEA (cat.) in an ether solution for 15 minutes on an ice bath under stirring. The reaction proceeded *via* the formation of amidoxime **22a-f** by intramolecular cyclization and the elimination of an alcohol molecule. The elimination of methanol resulted in a simpler isolation process than benzoyl alcohol due to its high boiling point (Scheme 6).³⁹

Pretze *et al.* reported the synthesis of 3-substituted-8-bromo-1*H*-purine-2,6(3*H*,7*H*)-diones **29a-c** from urea derivatives. The alkylated urea derivatives **24a-c** were prepared from primary



Scheme 6 Synthesis of 6-cyanopurine derivatives 23a-e containing a phenolic moiety.



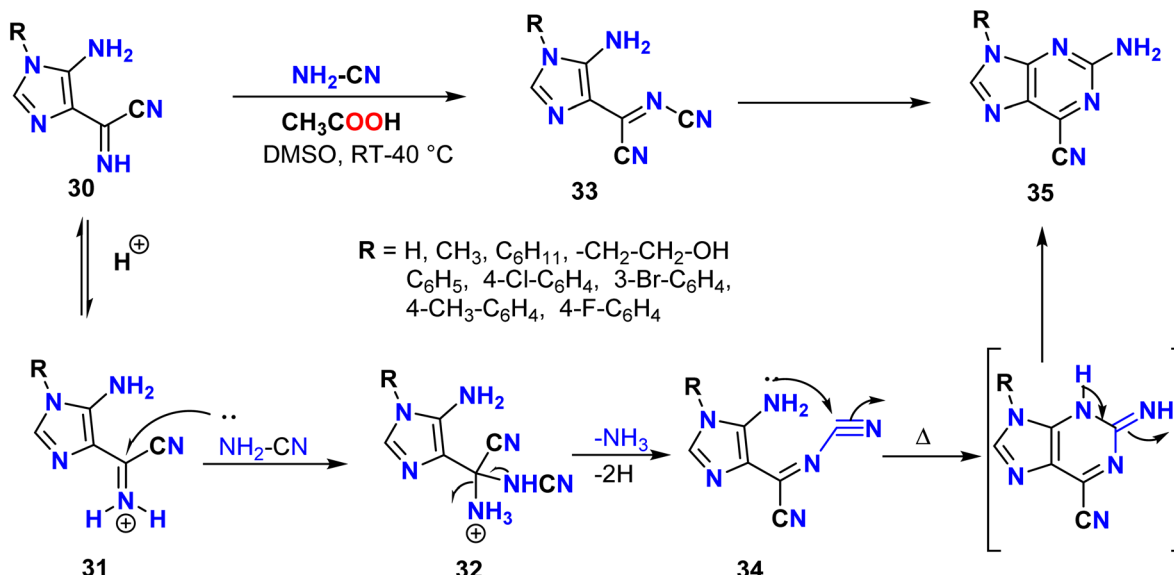
Scheme 7 Synthesis of brominated purine derivatives starting from alkylated urea.

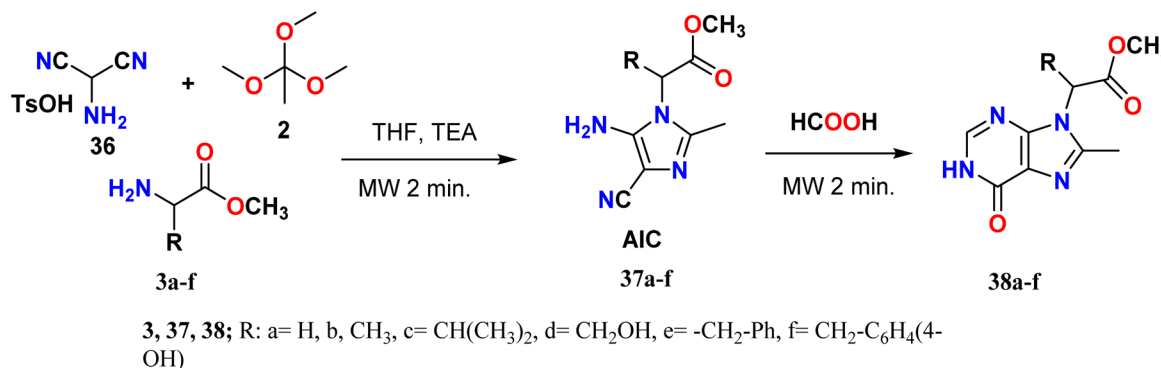
amines using sodium cyanate. Additionally, the asymmetrically alkylated urea derivatives **24a-c** reacted with ethyl 2-cyanoacetate in the presence of sodium ethoxide to afford *N*-substituted uracil derivatives **25a-c**, which were subsequently treated with sodium nitrite (NaNO_2) to produce the nitroso-uracil derivatives **26a-c** under acidic conditions. These derivatives then underwent a reduction reaction with sodium dithionite to give 5,6-diamino-pyrimidine-2,4(1*H*,3*H*)-diones **27a-c**. Moreover, the treatment of the diamino-pyrimidine-2,4-ones with triethyl

orthoformate in the presence of toluenesulfonic acid (*p*-TsOH) produced 3-substituted-1*H*-purine-2,6(3*H*,7*H*)-diones **28a-c**, which were then brominated using bromine for 3 hours at 65 °C to give the desired purine derivatives (Scheme 7).⁴⁰

2.2. From imidazole derivatives

Gonçalves *et al.* reported the synthesis 2-amino-6-cyano-purine **35** by treating 5-amino-4-cyanoformimidoyl imidazoles **30** with cyanamide in acetic acid and a small volume of DMSO, which

Scheme 8 Synthesis of 2-amino-6-cyano-purine **35** from 5-amino-4-cyanoformimidoyl imidazoles **30** using cyanamide.

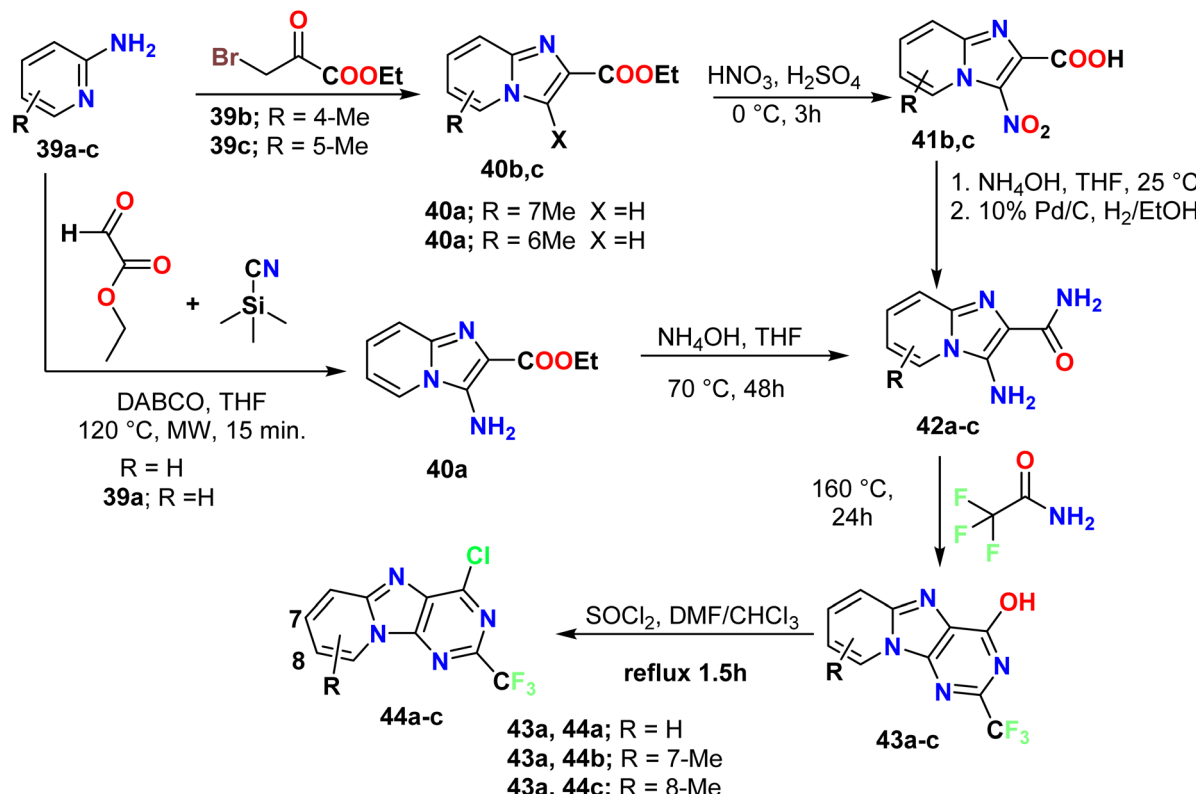
Scheme 9 Synthesis of 8,9-disubstituted-1*H*-purin-6-one derivatives 38a-f from enaminonitrile-imidazole using microwave irradiation.

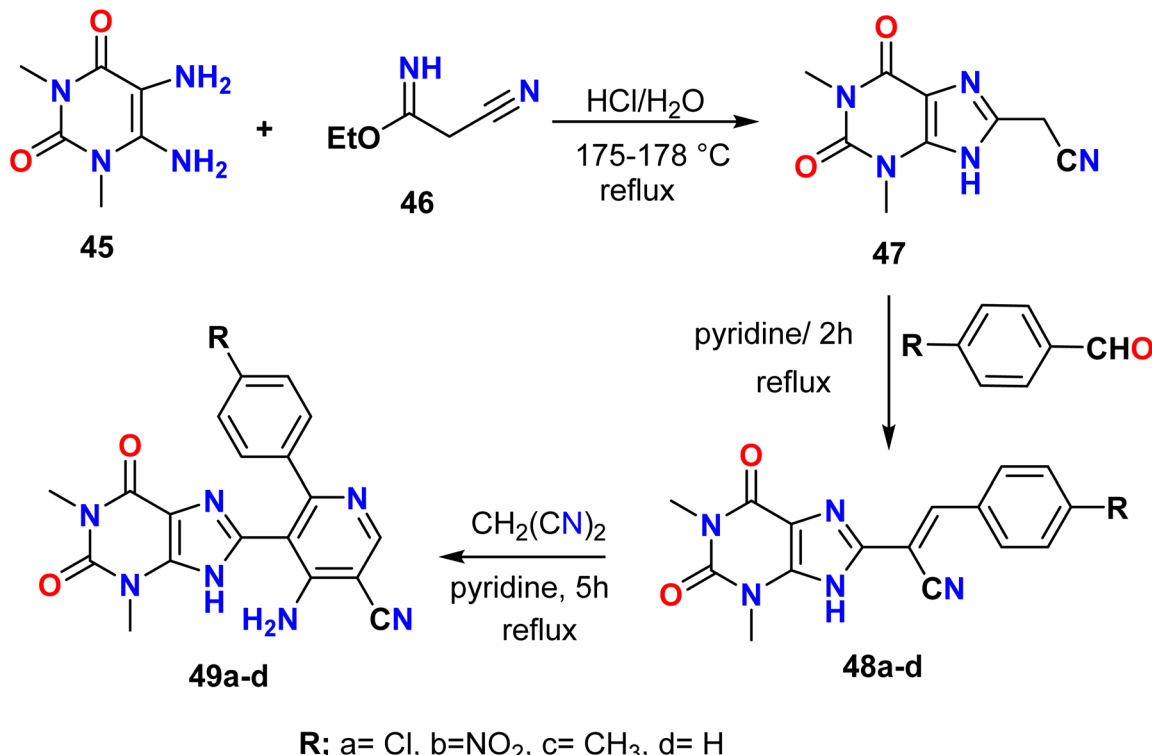
afforded the *N*-cyanoimidoyl cyanide intermediates 33; these underwent intramolecular cyclization and finally generated 2-amino-6-cyano-purine 35. The reaction mechanism involved the attack of the cyanamide on the imino group of 4-cyanoformimidoyl, leading to the loss of an ammonia molecule (NH₃) and the formation of a new intermediate 34. Finally, the amino group of imidazole at C5 attacks the nitrile group and the subsequent proton transfer affords the desired product 35 (Scheme 8).⁴¹

Bizzarri *et al.* synthesized 8,9-disubstituted-1*H*-purin-6-one derivatives 38a-f via a one-pot multicomponent reaction using microwave irradiation (250 W, 250 psi, 2.0 min at 200 °C). First, the enaminonitrile-imidazole derivatives 37a-f (AIC) were

prepared by the condensation of aminomalononitrile *p*-toluenesulfonate (AMNS) 36, triethyl orthoacetate (TOA) 2 and methyl esters of amino acids 3a-f (glycine, alanine, valine, serine, phenylalanine, and tyrosine). Eventually, the amino group of AIC reacted with formic acid, leading to the loss of a water molecule under MW irradiation, and the cyano group hydrolyzed to amide (CONH₂) and cyclized to give compound 38 (Scheme 9).⁴²

Tber *et al.* described a multi-step method for synthesizing 2-(trifluoromethyl)pyrido[1,2-*e*]purine derivatives from 2-amino-pyridine. First, they used a desilylative Strecker-Ugi type multicomponent reaction to prepare 3-aminoimidazo[1,2-*a*]pyridine-2-carboxylate 40a. This involved treating 2-

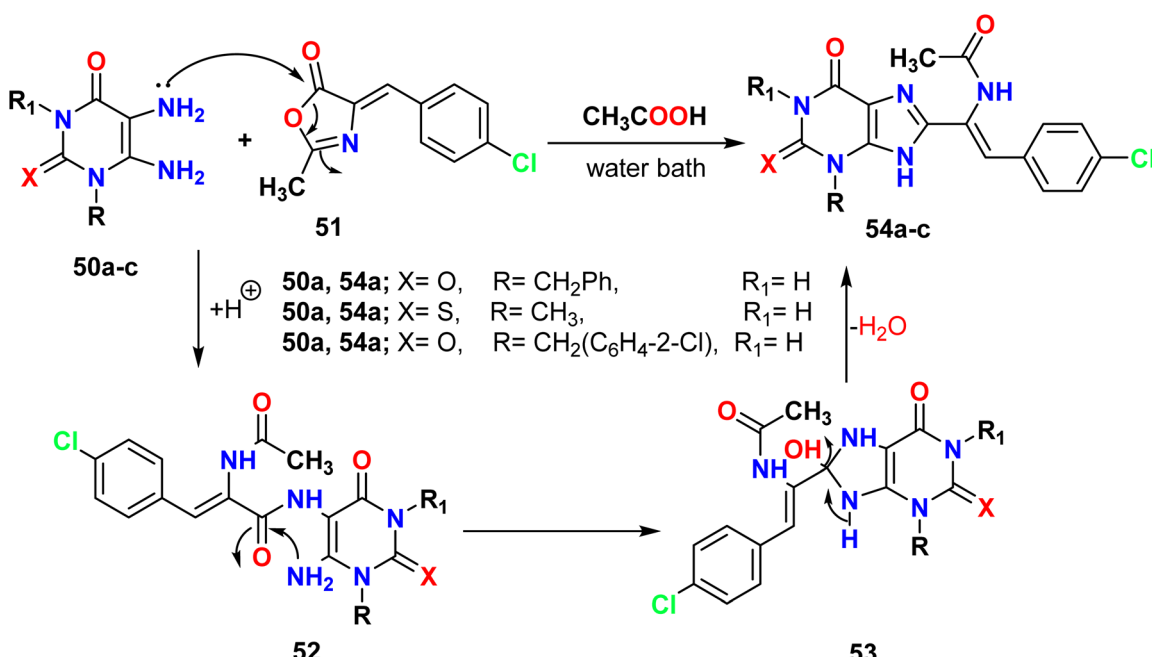
Scheme 10 Synthesis of 2-(trifluoromethyl)pyrido[1,2-*e*]purine derivatives 43 and 44 from 2-aminopyridine derivatives.



Scheme 11 Synthesis of 1,3-dimethyl-2,6-dioxo-1*H*-purine derivatives **49a–d** from diaminopyrimidine.

aminopyridine with ethyl glyoxylate in the presence of trimethylsilyl cyanide (TMSCN) as a source of cyanide and 1,4-diazabicyclo[2.2.2]octane (DABCO) as a strong base under microwave irradiation. Then, they heated the ester imidazole

with an ammonia solution at 70 °C for 48 hours to produce the 3-aminoimidazo[1,2-*a*]pyridine-2-carboxamide derivative **42a**. This compound was then reacted with 2,2,2-trifluoroacetamide (10 equiv.) under argon at 160 °C for 24 hours to yield 2-



Scheme 12 Synthesis of *N*-substituted-8-purine derivatives **54a–c** via the cyclo-condensation of 5,6-diaminouracils **50a–c** with the oxazolone derivative **51**.



(trifluoromethyl)pyrido[1,2-*e*]purin-4-ol **43a**. Finally, this compound was treated with thionyl chloride to obtain the dehydroxychlorinated pyrido[1,2-*e*]purin-4-ol derivatives **44a-c**. In the same way, the authors also described the synthesis of imidazo[1,2-*a*]pyridine-2-carboxylates **40b, c** from 2-amino-pyrimidine and ethyl bromopyruvate. The product was then nitrated, and the ester group was converted to an amide. Finally, the nitro group was reduced to afford 3-aminoimidazo[1,2-*a*]pyridine-2-carboxamides **42b, c** (Scheme 10).⁴³

2.3. From pyrimidine derivatives

Verma *et al.* described a new strategy for the synthesis of 1,3-dimethyl-2,6-dioxo-1*H*-purine derivatives containing the acetonitrile group. The reaction involved treating 1,3-dimethyl-5,6-diaminopyrimidine **45** with ethyl 2-cyanoacetimidate **46** in the presence of HCl under reflux conditions. Additionally, these materials were used as the starting material to prepare new purine derivatives attached to a pyridine moiety *via* a two-step reaction. The first step involved the Claisen–Schmidt condensation of 1,3-dimethyl-8-(acetonitrilyl)-3,9-dihydro-1*H*-purine-2,6-dione **47** with substituted benzaldehyde in pyridine, which acted as a basic medium, to afford acrylonitrile-purine derivatives **48a-d**. These were then reacted with malononitrile in ethanol and in the presence of a few drops of pyridine to afford 4-amino-5-(2,6-dioxo-1*H*-purin-8-yl)pyridine-3-carbonitriles **49a-d** (Scheme 11).⁴⁴

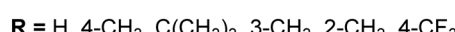
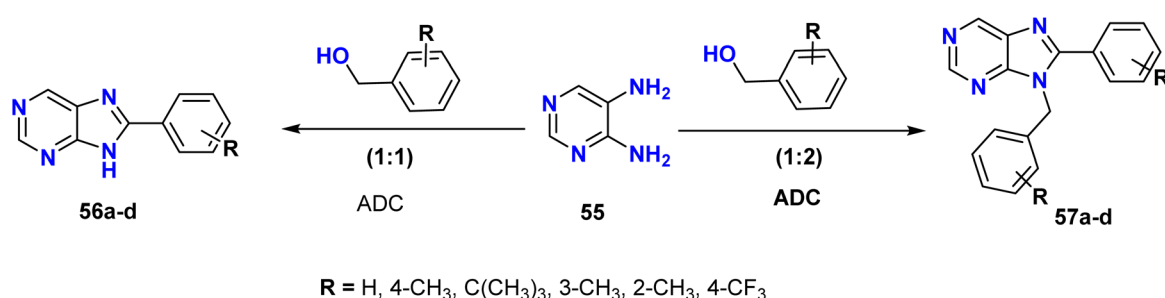
El-Kalyoubi *et al.* described the synthesis of *N*-substituted-8-purines **54a-c** by the cyclo-condensation of 5,6-diaminouracils **50a-c** with an oxazolone derivative **51** in acetic acid on a water bath for 1 hour. The mechanistic pathway illustrated that the oxazolone derivative **51** was protonated at the carbonyl moiety, and the C5 amino group of the uracil derivatives **54a-c** attached with the carbonyl, which led to ring opening; then, the second

amino group C6 attached with the amidic adjacent carbonyl, leading to the formation of imidazopyridine derivatives (Scheme 12).⁴⁵

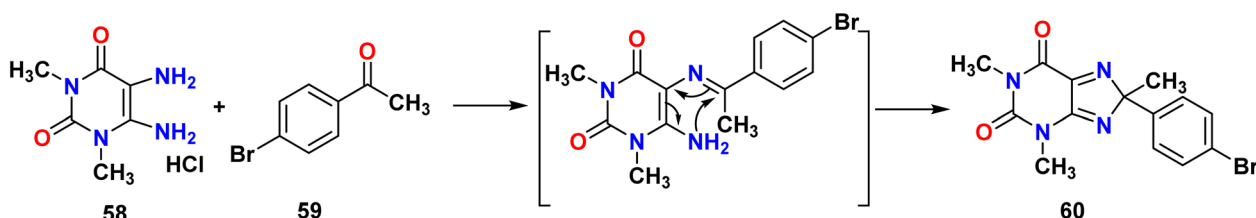
Chakraborty *et al.* explored the synthesis of 8-substituted purines **56a-d** and 8,9-disubstituted purines **57a-d** *via* an acceptor-less dehydrogenative coupling reaction of benzyl alcohol with 4,5-diaminopyrimidine and Ni(II)-catalyst [Ni(Me-TAA)] under aerobic conditions in toluene and potassium *tert*-butoxide (KO*t*Bu), and the reaction was dependent on their molar ratio.¹ The reaction required prolonged time rather than the formation of benzimidazole, and the yield obtained ranged from moderate to good (Scheme 13).

El-Kalyoubi *et al.* achieved purine derivatives through the formation of Schiff bases followed by aza-Michael addition. The substituted purines were obtained in a high yield by subjecting 1,3-dimethyl-5,6-diaminouracil **58** to heat in the presence of *p*-bromoacetophenone **59** in DMF (1 mL). Although most of their synthesized derivatives were screened against four cancer cell lines (HepG2, Huh7, MCF7, and A549), the anti-cancer activity of 8-(4-bromophenyl)-1*H*-purine-2,6-dione **60** (ref. 46) (Scheme 14) was not evaluated.

Doganc *et al.* described the synthesis of 2-chloro-8-(substituted phenyl)-9*H*-purine *via* two steps; the first step involved the formation of Schiff bases **62a, b** from 2-chloropyrimidine-4,5-diamine **61** and benzaldehyde derivatives, especially those with 4-fluoro or 3,4-dimethoxy phenyl substituents, under reflux conditions for 1 hour in ethanol. Moreover, the as-formed Schiff base was treated with *N*-bromosuccinamide in chloroform under reflux, and the product was separated from the solvent under reduced pressure as two isomers N9 and N7. Additionally, they reported that the reaction of 4,5-diaminopyrimidine with 4-fluorobenzoyl chloride afforded 6-chloro-8-(4-fluorophenyl)-3*H*-purine **64** as the sole product. The structures of the designed purine derivatives were confirmed by

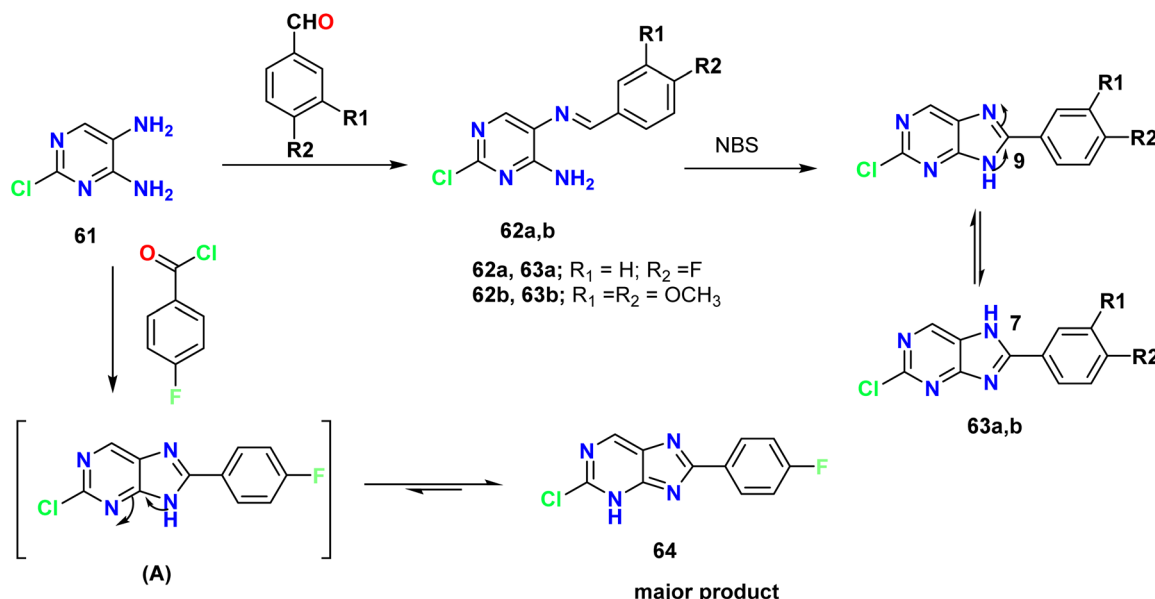


Scheme 13 Synthesis of 8-substituted purines **56a-d** and 8,9-disubstituted purines **57a-d** *via* acceptorless dehydrogenative coupling (ADC).



Scheme 14 Synthesis of 8-(4-bromophenyl)-1*H*-purine-2,6-dione **60** from 1,3-dimethyl-5,6-diaminouracil **58** and acetophenone derivative.





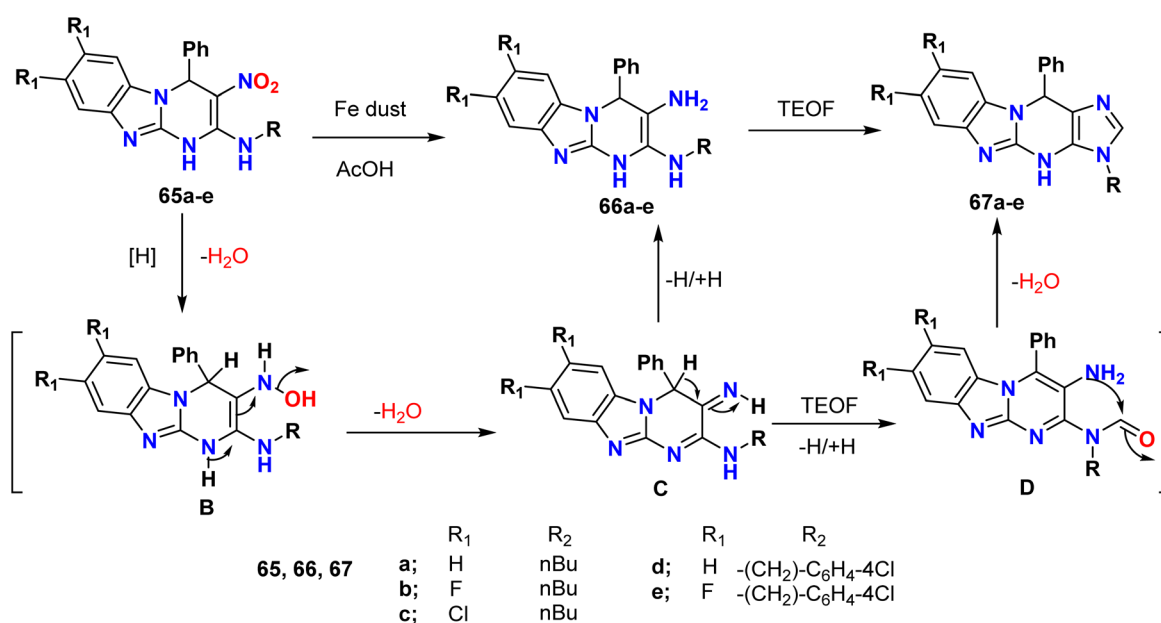
Scheme 15 Synthesis of 2-chloro-8-(substituted phenyl)-9H-purine derivatives **63** and **64** from a Schiff base, *N*-bromosuccinimide, and benzoyl chloride derivatives.

¹H-¹H NOE (nuclear Overhauser effect spectroscopy, NOESY), ¹H-¹³C/¹⁵N HMBC (heteronuclear multiple bond correlation) methods and X-ray crystallographic data (Scheme 15).²

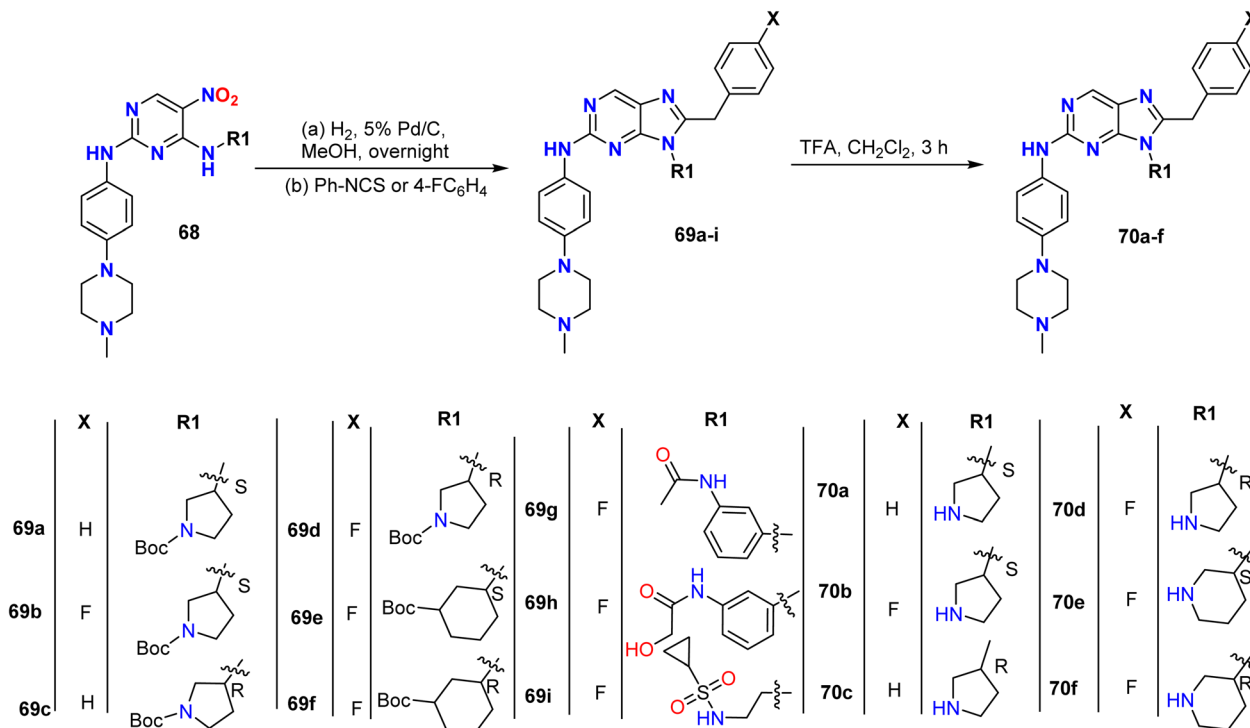
Fedotov *et al.* synthesized benzimidazopurines **67a-e** as poly-condensed purine derivatives through many pathways. Several trials of treating nitrobenzimidazo-pyrimidines **65a-e** with sodium dithionite and catalytic hydrogenation in different reaction media did not result in the desired diamines. Therefore, the starting material was isolated in all cases. Additionally, the target compounds were produced by the reduction of the nitro group using iron dust in a mixture of triethyl orthoformate

and acetic acid; the reduction was followed by the aromatization of the pyrimidine cycle, leading to the formation of tetracyclic benzimidazopurines **67a-e** with yields up to 85%. The mechanistic studies illustrated that the reaction proceeded through hydroxylamine **B** formation, followed by the aromatization of the pyrimidine ring **C** and then the final product. Finally, they proposed that metals in acidic media reduce nitroamines more efficiently than heterogeneous hydrogenation, which is uncommon (Scheme 16).⁴⁷

Lei *et al.* prepared 9-heterocycl-substituted 9H-purine derivatives **71a-l** by the reduction of 5-nitropyrimidine



Scheme 16 Synthesis of poly-condensed purine derivatives **67a-e** from nitro-benzimidazopyrimidines **65a-e** via reduction and cyclization.

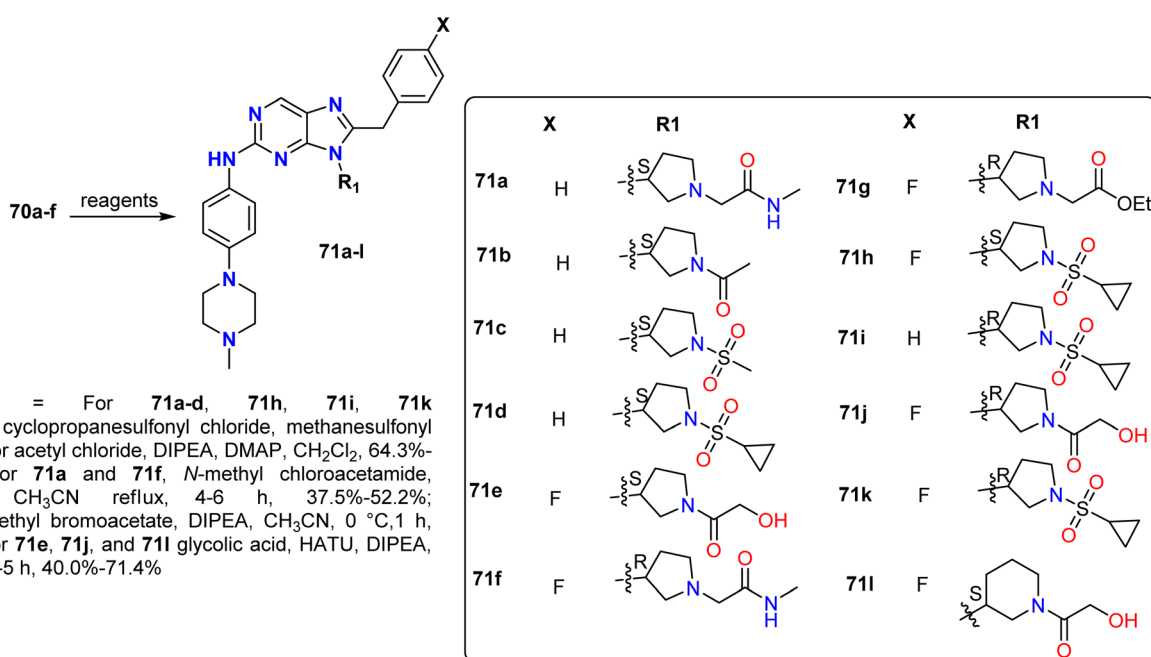


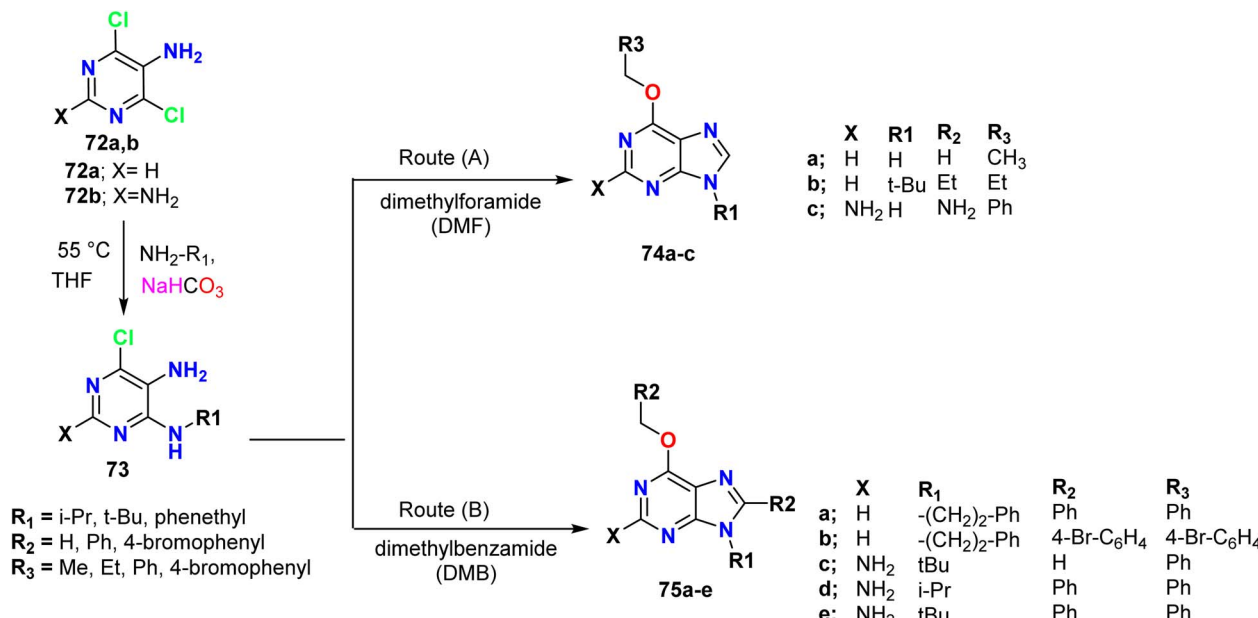
Scheme 17 Synthesis of 9-heterocyclyl substituted 9H-purine derivatives 69 and 70.

derivatives **68** using palladium on carbon (Pd/C) (5%) to afford the corresponding amines. Additionally, the intermediate amines **68** were treated with phenyl isothiocyanate or 4-fluorophenyl isothiocyanate to generate 9*H*-purine-2,8-diamines **69a–i**, some of which contained the *tert*-butoxycarbonyl protecting group (BOC group), which was removed using

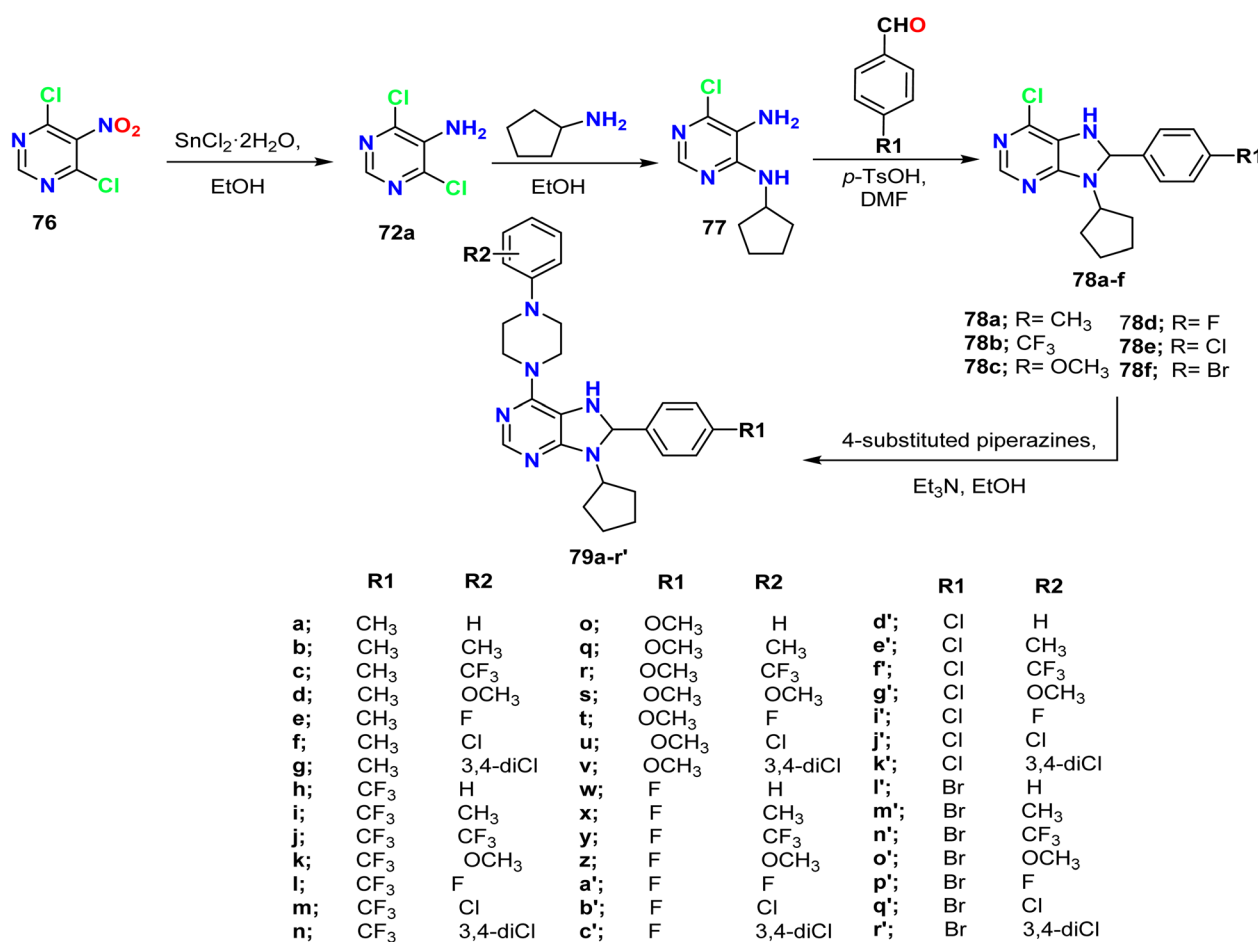
trifluoroacetic acid to generate **70a–f**; these were subsequently reacted with sulfonyl chloride and glycolic acid or ethyl bromoacetate to give compounds **71a–l** (Schemes 17 and 18).⁴⁸

Lorente-Macías *et al.* explored 6-alkoxy purine as a Jurkat-selective proapoptotic agent. The 6-alkoxy purine derivatives were prepared in two steps; reacting dichloropyrimidines

Scheme 18 Synthesis of 9-heterocyclyl substituted 9*H*-purine derivatives **71a–l**.



Scheme 19 Synthesis of 6-alkoxy purine derivatives 74a-c and 75a-e from dichloropyrimidines.



Scheme 20 Synthesis of di- and tri-substituted purines from 4,6-dichloro-5-nitropyrimidine.

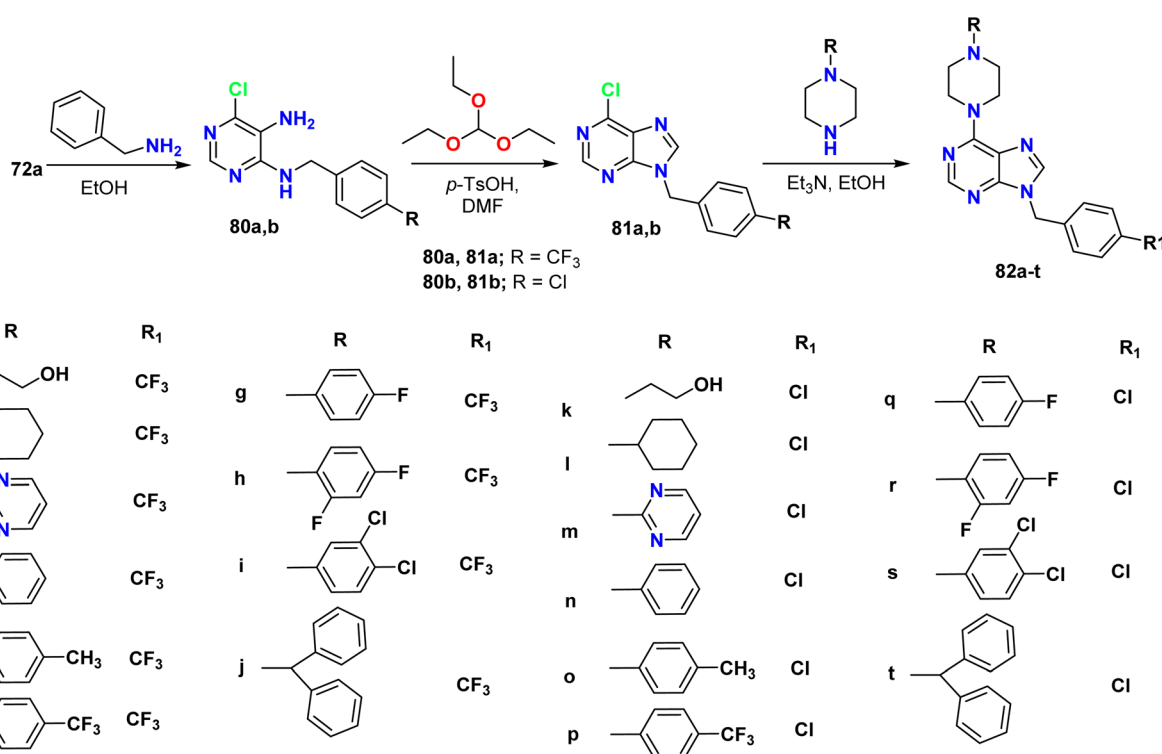
with various alkyl amines in the first step yielded 6-chloro diaaminopyrimidine derivatives **73**. Subsequently, the chloropyrimidines were displaced at C6 with suitable alcohols under strong basic conditions in the presence of *N,N*-dimethylamide. This synthetic process led to the production of purine analogs **74a–c**. The reaction was controlled by the type of *N,N*-dimethylamide used as the solvent and reagent. For example, using dimethylformamide (DMF) facilitated the synthesis of 6,9-disubstituted purines with nonsubstituted C8 (route A). On the other hand, the presence of sterically hindered *N,N*-dimethylamides like dimethylbenzamide (DMB) resulted in the synthesis of tri-substituted purines **75a–e** (route B), where the alcohols (benzyl alcohol and 4-bromobenzyl alcohol) generated fragments at both C6 and C8. Additionally, microwave irradiation at higher temperatures was used for the 2,5-diaminopyrimidine core due to its lower reactivity than the 5-amino-2-chloropyrimidine core (Scheme 19).⁴⁹

Polat *et al.* synthesized a series of 6,8,9-trisubstituted purine derivatives **79** starting from 4,6-dichloro-5-nitropyrimidine **76**. 5-Nitropyrimidine **76** was reduced in the presence of tin(II) chloride to produce 6-dichloropyrimidin-5-amine **72a**, then the chlorine atom at C4 of pyrimidine was substituted with cyclopentyl amine in the presence of triethyl amine *via* a nucleophilic substitution reaction to afford 6-chloro-*N*4-cyclopentylpyrimidine-4,5-diamine **77**, which was subsequently reacted with substituted benzaldehyde under *p*-TSA catalysis and cyclized to obtain 6-chloro-8,9-disubstituted **7H**-purine derivatives **78a–f**. Finally, the tri-substituted purines **79a–r'** were obtained by the reaction of 6-chloropurine derivatives **78a–f** with appropriate *N*-substituted piperazines (Scheme 20).⁵⁰

In the same way, Kucukdumlu *et al.* reported the synthesis of 5-amino-4,6-dichloro pyrimidine **72a** by the reduction of 4,6-dichloro-5-nitro-pyrimidine **76** using *SnCl*₂, followed by amination with benzylamine to give 4-(4-substituted benzyl)pyrimidines **80a, b**. The 6-chloro purines **81a, b** were prepared by the condensation of compounds **80a, b** with triethyl orthoformate in the presence of toluenesulfonic acid to afford intermediates **81a, b**, which underwent amination to afford 6,9-disubstituted purine derivatives **82a–t** (Scheme 21).⁵¹

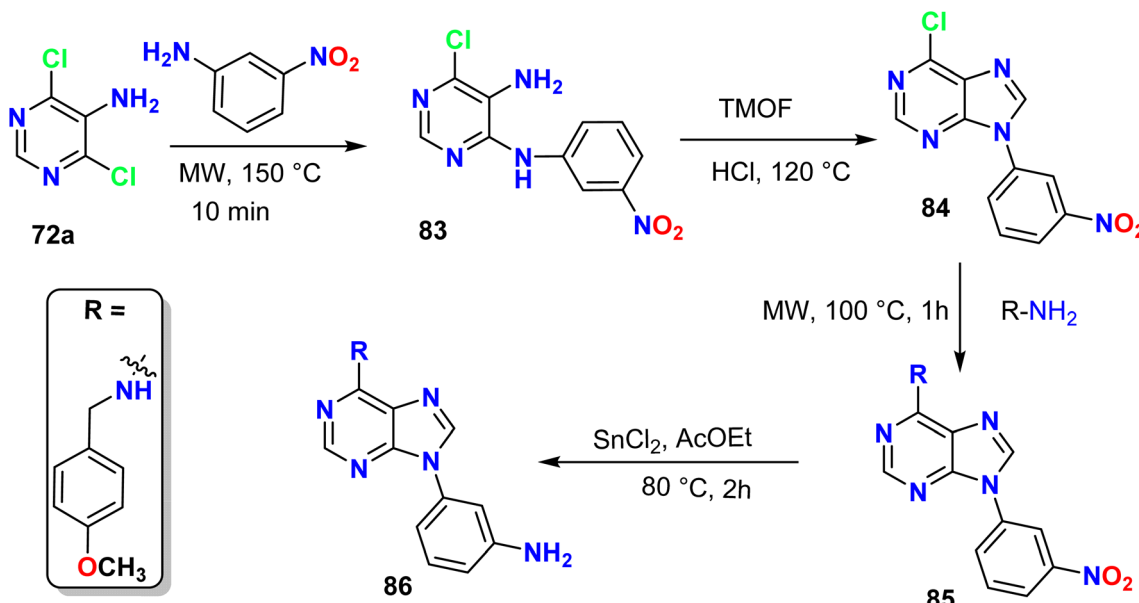
Orduña *et al.* illustrated the synthesis of new substituted purine derivatives containing amino groups using a low-power microwave. They synthesized a 5,6-diamino-pyrimidine derivative **83** from 4,6-dichloropyrimidin-5-amine **72a** *via* amination using 3-nitro aniline under MWI at 150 °C for 10 minutes, which afforded the corresponding 9-substituted purine derivative **84** in a good yield (67%). Additionally, the second amination process was performed with *p*-methoxy benzylamine under MWI at 100 °C for 1 hour, and finally, the nitro group of the 6,9-disubstituted purine derivative **85** was treated with *SnCl*₂ in a mixture of ethanol and ethyl acetate under reflux conditions for 2 h to afford the purine derivative **86** containing an amino group (Scheme 22).⁵²

Bigonah-Rasti *et al.* synthesized a triazolo[5,1-*f*]purine derivative **91** starting from 5-amino-3-(methylthio)-1*H*-1,2,4-triazole **87**, which was used as a bi-nucleophile with the 5-dichloropyrimidine derivative **88** under heating conditions and TEA as the catalyst to afford the 5-bromo-2-chloro-6-methyl-pyrimidin-4-amine derivative **89**. Additionally, the tricyclic heterocyclic core was alkoxylated using several aliphatic alcohols in KOH. The reaction then progressed through two



Scheme 21 Synthesis of 6,9-disubstituted purine derivatives **82a, b**.





Scheme 22 Synthesis of 6,9-disubstituted purine derivative 86 from 4,6-dichloropyrimidin-5-amine 72a.

consecutive aromatic nucleophilic substitutions (SNAr), which involved intramolecular cyclocondensation and the formation of a non-isolated adduct intermediate, leading to the elimination of HBr and MeSH in two successive steps (Scheme 23).⁵³

3. Reactions of purine derivatives

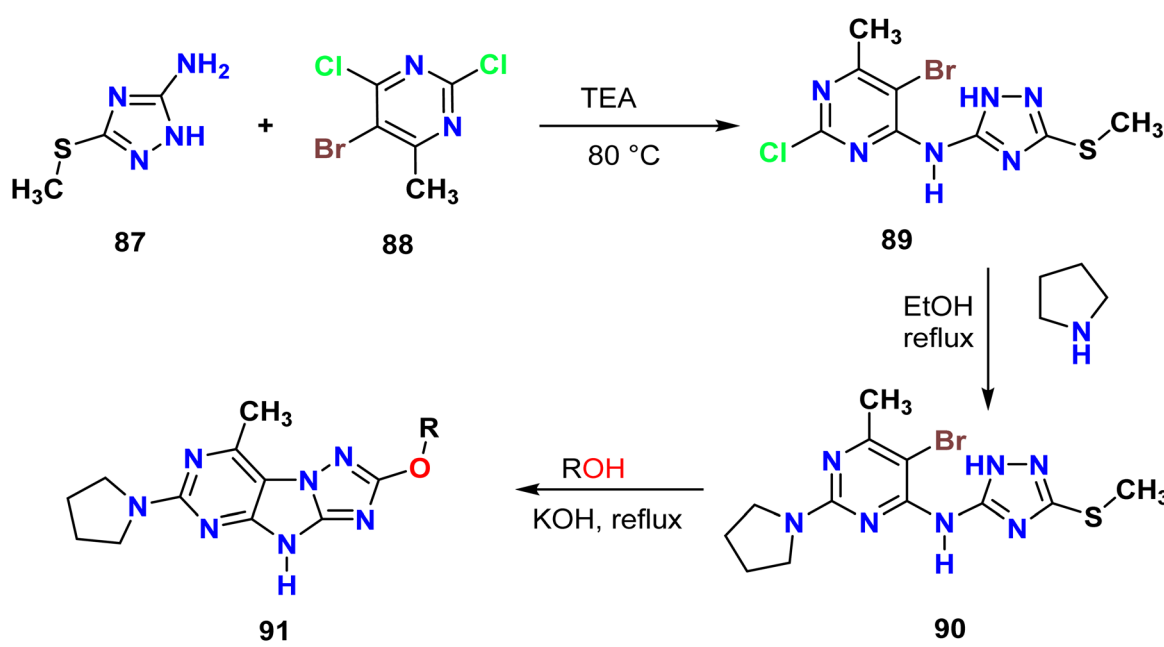
The reaction of purines can proceed *via* more than one functional group and therefore, can be classified as follows.

3.1. Benzoylation

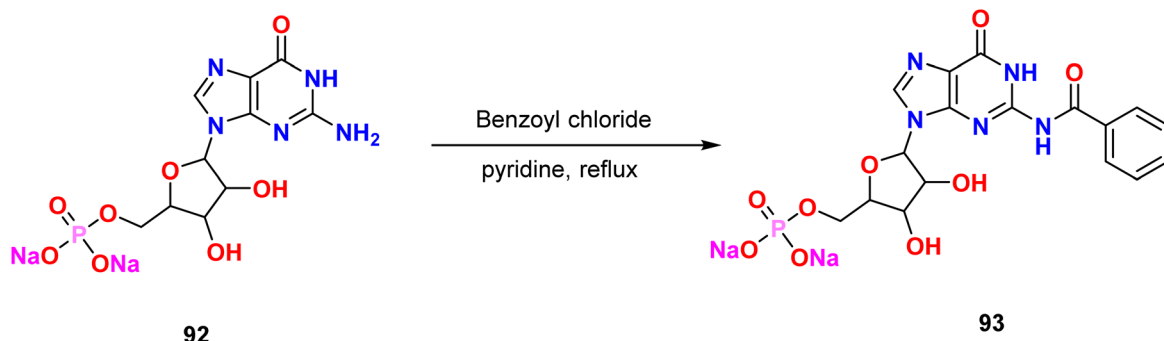
Attia *et al.* described the formation of a new guanosine monophosphate **93** with an amide linker by modifying the amino group of guanosine monophosphate **92** using benzoyl chloride (Scheme 24).⁵⁴

3.2. Alkylation

The alkylation of purine derivatives can be of three types based on the substitution of the nitrogen atom and therefore, can be



Scheme 23 Synthesis of tricyclic 2-alkoxy-4H-[1,2,4]triazolo[5,1-f]purine derivatives.



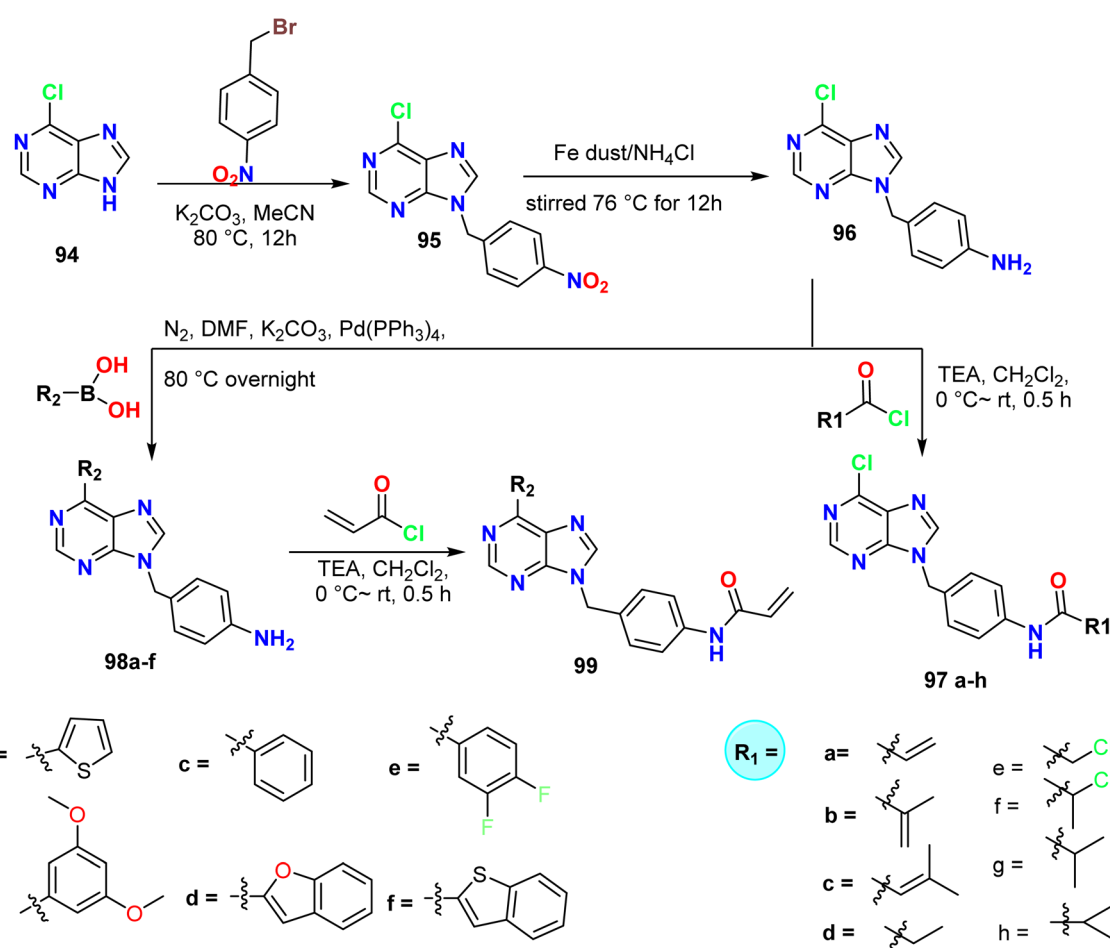
Scheme 24 Benzoylation of the 2-amino-9-alkyl purine derivative.

classified as mono, di, and tri-substituted purines. Wang *et al.* synthesized new 9-substituted-9*H*-purine derivatives **97a–h**, **98a–f**, and **99** through the reaction of 6-chloro-9*H*-purine **94** with 4-nitrobenzyl bromide to afford 6-chloro-9-(4-nitrobenzyl)-9*H*-purine **95**, which underwent a reduction reaction in the presence of Fe powder and ammonium chloride (NH₄Cl) to give the corresponding amino derivative **96** (Scheme 25).

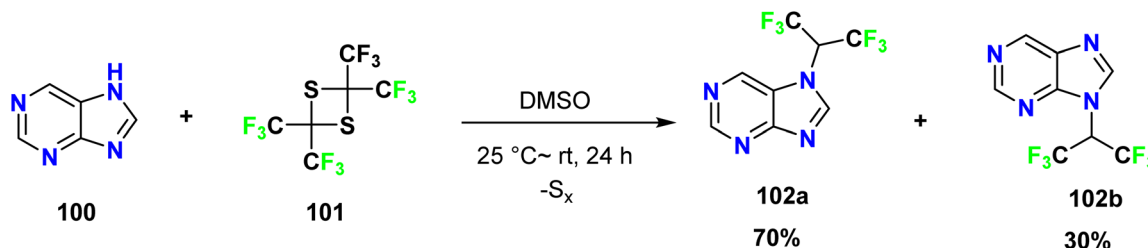
Additionally, amide condensation reactions with Michael receptors, such as acryloyl chloride and analogs, were carried out using the amine derivative in order to obtain the desired products

97a-h. Moreover, compound **96** was first exposed to a Suzuki coupling reaction with compounds containing boronic acid, which produced disubstituted purine intermediates **98a-f**, which subsequently underwent an amide condensation process with acryloyl chloride to produce the target compound **99** (Scheme 25).⁵⁵

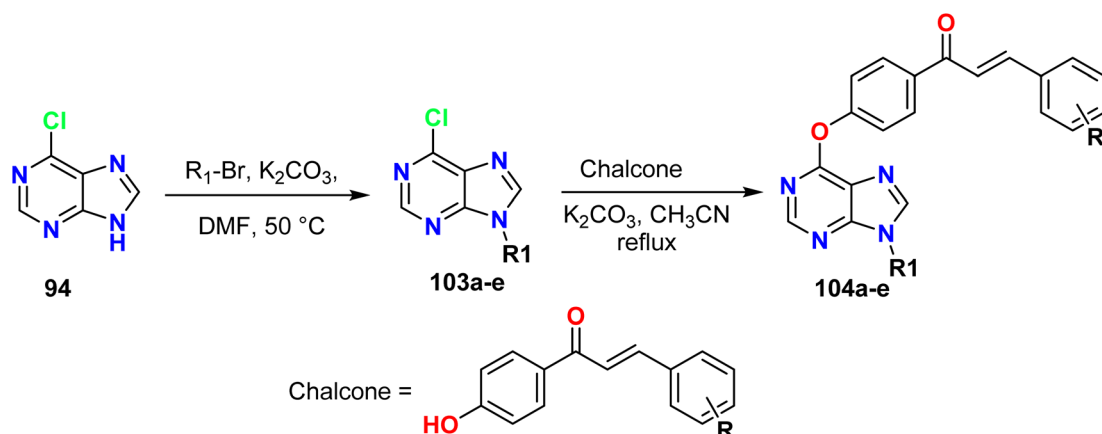
Petrov *et al.* discovered that purine **100** could react with tetrakis(trifluoromethyl)-1,3-dithietane **101** in DMSO in the absence of a catalyst at room temperature, affording 7- and 9-(hexafluoroisopropyl)purines (**102a** and **102b**) in the ratio of 70 : 30% (Scheme 26).⁵⁶



Scheme 25 Synthesis of 9-substituted-9*H*-purine derivatives 97a–h, 98a–f, and 99a–f through alkylation reactions.



Scheme 26 Synthesis of 7- and 9-(hexafluoroisopropyl)purine derivatives 102a and 102b.



Scheme 27 Synthesis of 6,9-disubstituted purine derivatives 104a-e from 6-chloro-9H-purine.

Liu *et al.* outlined the synthesis of 9-substituted purine derivatives **103a-e** from 6-chloro-9H-purine **94** and 1-bromo-propane in the presence of K_2CO_3 ; it was subsequently treated with chalcones containing the phenolic hydroxyl group to afford the corresponding 6,9-bis substituted purine derivatives **104a-e** (Scheme 27).⁵⁷

Villegas *et al.* described the synthesis of 2,6,9-trisubstituted purine derivatives **111** from 6-chloro-2-fluoro-9H-purine **105**. Firstly, the alkylation of 6-chloro-2-fluoro-9H-purine **105** was carried out by treating it with alkyl halide in the presence of K_2CO_3 in DMF at room temperature to give a mixture of N7 and N9 alkylated purine regio-isomers **106a-b** and **106'a, b**. The second alkylation process on N6 of the purine was performed by a Suzuki reaction using trifluoromethoxyphenylboronic acid to afford the 6,9-diaryl purine derivatives **107a-b** (Scheme 28).

At the same time, different piperidine amide derivatives **110a-f** were produced by reacting *tert*-butyl-4-aminopiperidin-1-carboxylate **108** with different acyl chlorides and Et_3N . Moreover, the salts of piperidine amido derivatives **110a-f** were prepared by treating amino piperidine derivatives **109a-f** with trifluoroacetic acid (TFA) in methylene chloride at room temperature. Finally, the diaryl purines were reacted with salts of piperidine amide in the presence of *N,N*-diisopropylethylamine (DIPEA) in butanol to afford the triaryl purine derivatives **111** (Scheme 28).⁵⁸

Popov *et al.* synthesized the diazido derivative **114a** from the reaction of 2-bromoethyl-6-chloropurine **113a-c** with sodium

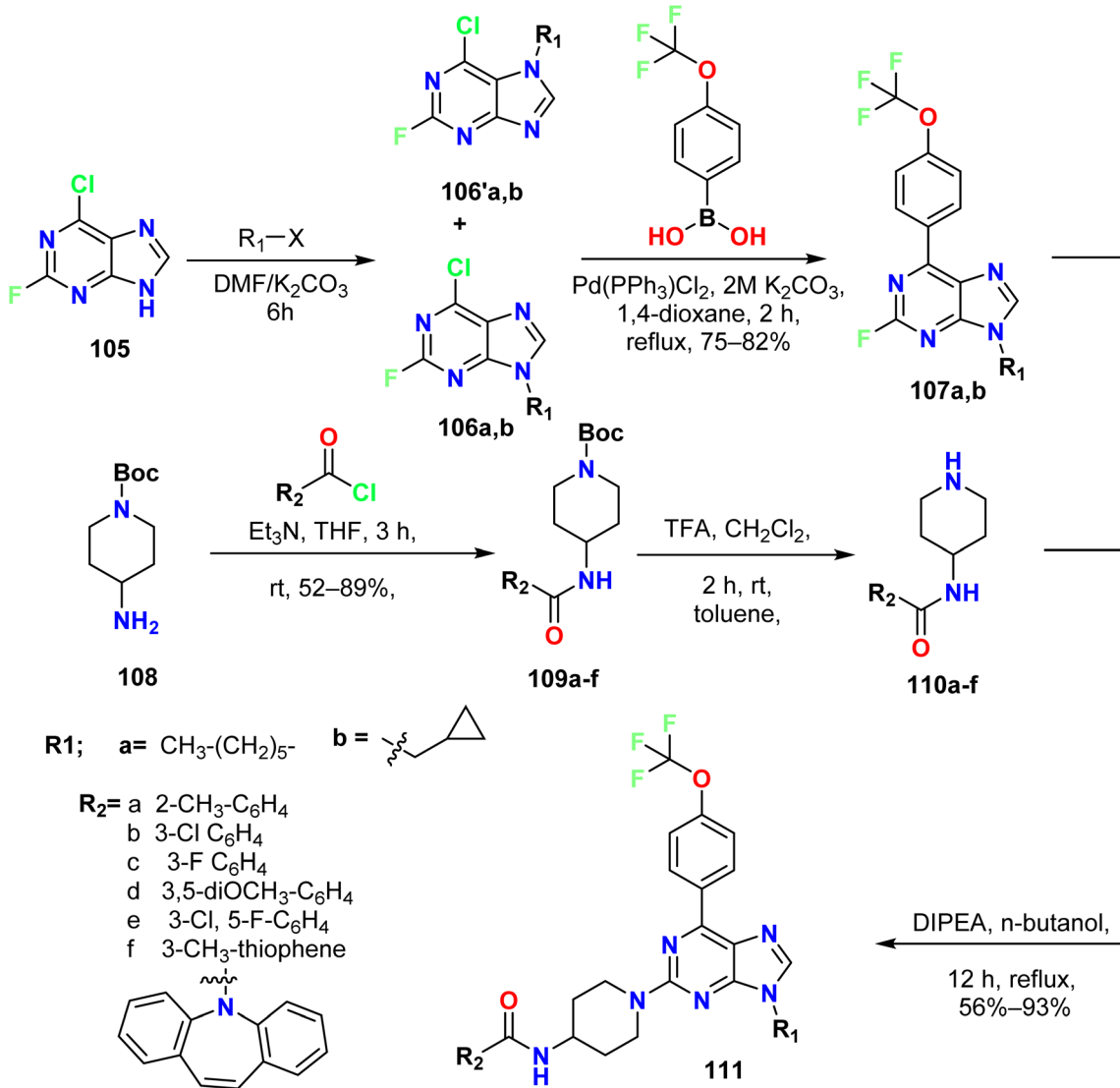
azide, and the product was obtained in two different tautomeric forms. Moreover, this compound was subjected to Cu(i)-catalyzed azide-alkyne cycloaddition (CuAAC) with sodium azide in acetone, yielding the corresponding **115**. The authors also outlined a strategy for the synthesis of 6-substituted bis-purines **118** connected *via* different spacers. Initially, 6-alkyl purine was reacted with sodium azide to afford mono-azide derivatives **116**, which were subsequently reacted with bis-alkynes **117a-c** to obtain the target 6-substituted bis-purine **118** and mono-purine derivatives **119** *via* a CuAAC reaction of the heterocycle. This reaction was carried out, using different catalytic systems and reaction conditions, such as ultrasound irradiation to shorten the reaction time and optimize the synthesis of both mono- and bis-purine compounds (Scheme 29).⁵⁹

Mohamed *et al.* showed the alkylation of theophylline **120** at N7 using benzyl chloride (H and 4-F) *via* a nucleophilic substitution reaction (SN_2) to afford 7-(4-substituted benzyl)-3,7-dihydro-1H-purine-2,6-dione derivatives **121a, b**. The reaction was carried out in the presence of a mixture of potassium carbonate and potassium iodide (K_2CO_3 and KI) in dimethylformamide (DMF) at 80°C for 6 hours (Scheme 30).⁷

3.3. Halogenation (bromination)

Mohamed *et al.* reported the bromination of 1,3-dimethyl-7-(alkyl)-3,7-dihydro-1H-purine-2,6-dione derivatives **121a, b** using *N*-bromosuccinimide (NBS) in DMF under reflux





Scheme 28 Synthesis of 2,6,9-trisubstituted purine derivatives via three-step alkylation.

conditions at 90 °C for 8 h, and bromination occurred at the C8 position (Scheme 31).⁷

Konduri *et al.* described the bromination of the 3-substituted purine derivative **120** by another method. The reaction of the 3-methyl-3,7-dihydro-1*H*-purine-2,6-dione derivative **120** with bromine in acetic acid provided the 8-bromo-3-methyl-1*H*-purine-2,6-dione derivative **123** was 92% yield.⁶⁰ Additionally, Rad *et al.* tried to synthesize bromo-caffeine as a tri-substituted purine **124** using various methods, but the *N*-bromosuccinimide (NBS) in dichloromethane (CH₂Cl₂) and water at room temperature was preferred due to the purity of the product **125** (Scheme 32).⁶¹

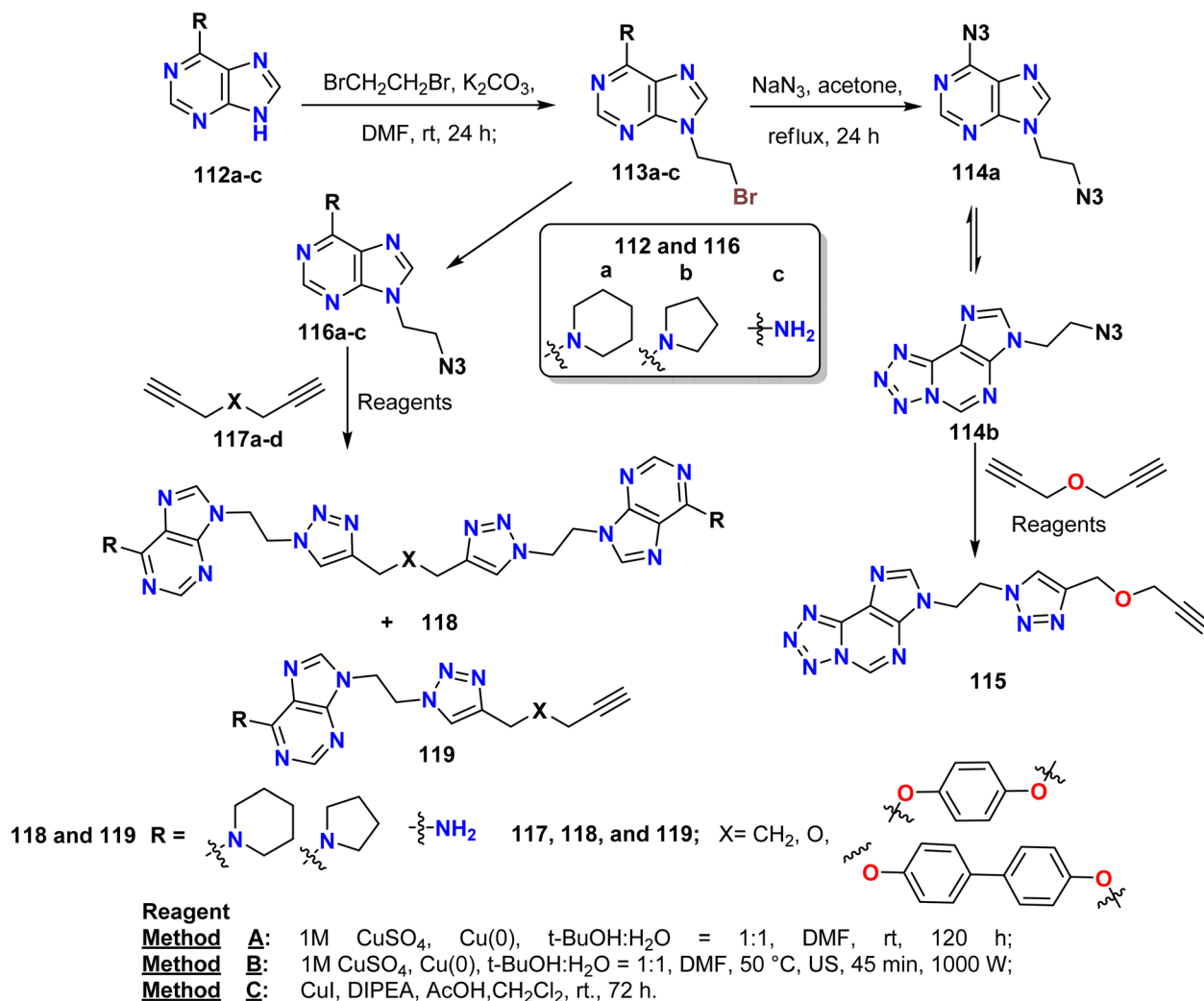
3.4. Amination (nu substitution reaction)

Konduri *et al.* aminated 8-bromo-1,3-disubstituted-1*H*-purine-2,6-dione derivative **126** using 1-BOC-piperazine in the presence of sodium carbonate in DMF solvent, successfully incorporating the piperazine group and forming compound **127**. The

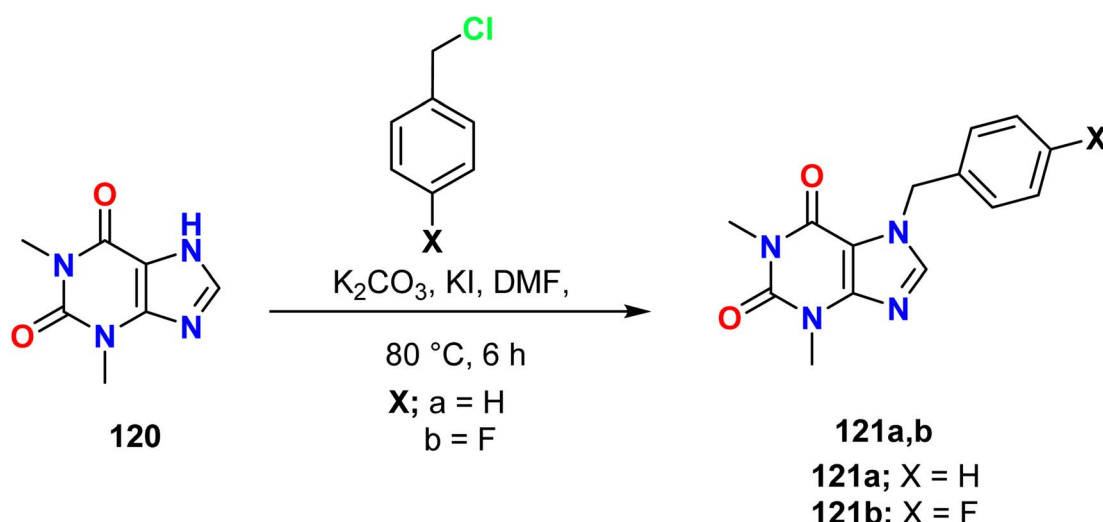
BOC group was cleaved using methanolic HCl in an acid-mediated reaction, resulting in the formation of the important intermediate amine **128** (Scheme 33).⁶⁰

Nadaf *et al.* described the reaction of 6-chloro-9*H*-purine **94** with morpholine to form the 4-(9*H*-purin-6-yl)morpholine **129**, which was then alkylated using different phenyl bromides to obtain the 6,9-disubstituted purine derivatives **132**. On the other hand, alkylating 4-(9*H*-purin-6-yl)morpholine **129** with ethyl chloroacetate afforded an alkylated purine with an ester group, which was treated with hydrazine hydrate to form a new hydrazine derivative **130**. The hydrazine derivative reacted with various aromatic acids in the presence of phosphorous oxychloride to afford purines with alkylated oxadiazoles **131a-f** (Scheme 34).⁶²

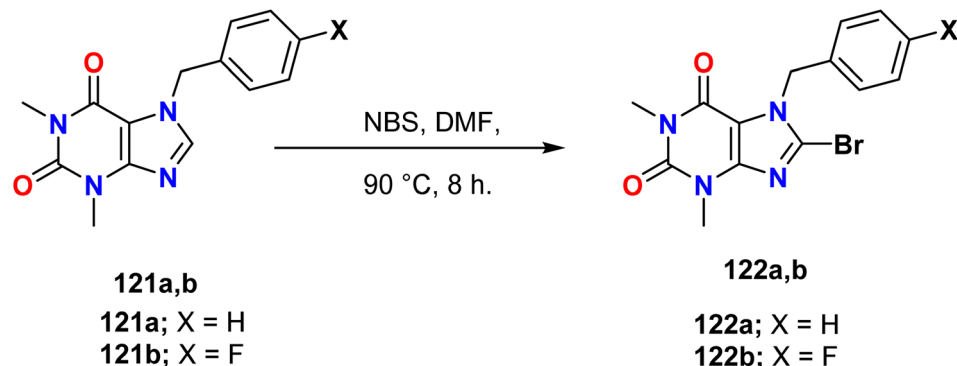
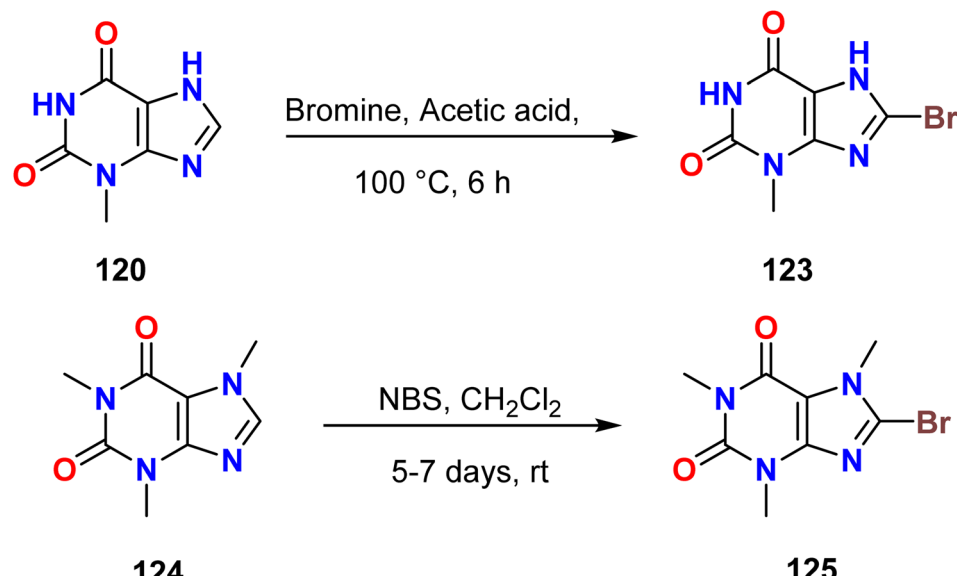
Krasnov *et al.* described the synthesis of novel purine derivatives with amino acids attached to C6. The process involved the treatment of *N*-(6-chloro-9*H*-purin-2-yl)acetamide **133** with *tert*-butyl esters of amino acids **134a-f** in



Scheme 29 Synthesis of 6-substituted bis-purines 118 and mono-purine derivatives 119.



Scheme 30 Alkylation of theophylline using benzyl chloride derivatives.

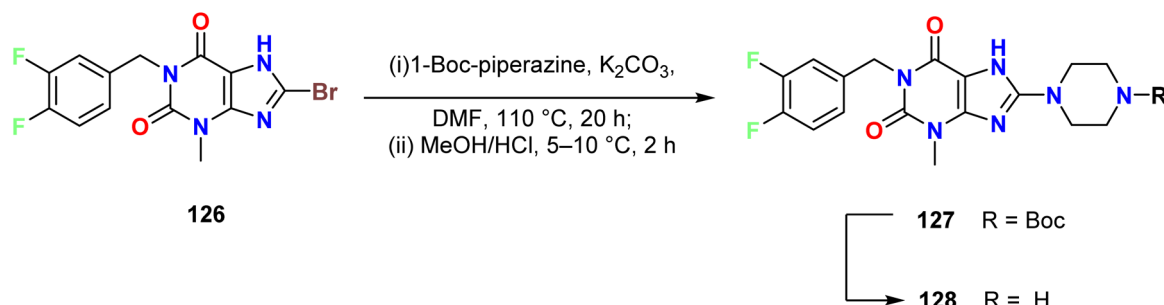
Scheme 31 Bromination of theophylline using *N*-bromosuccinimide.Scheme 32 Synthesis of 8-bromo-1*H*-purine-2,6-dione.

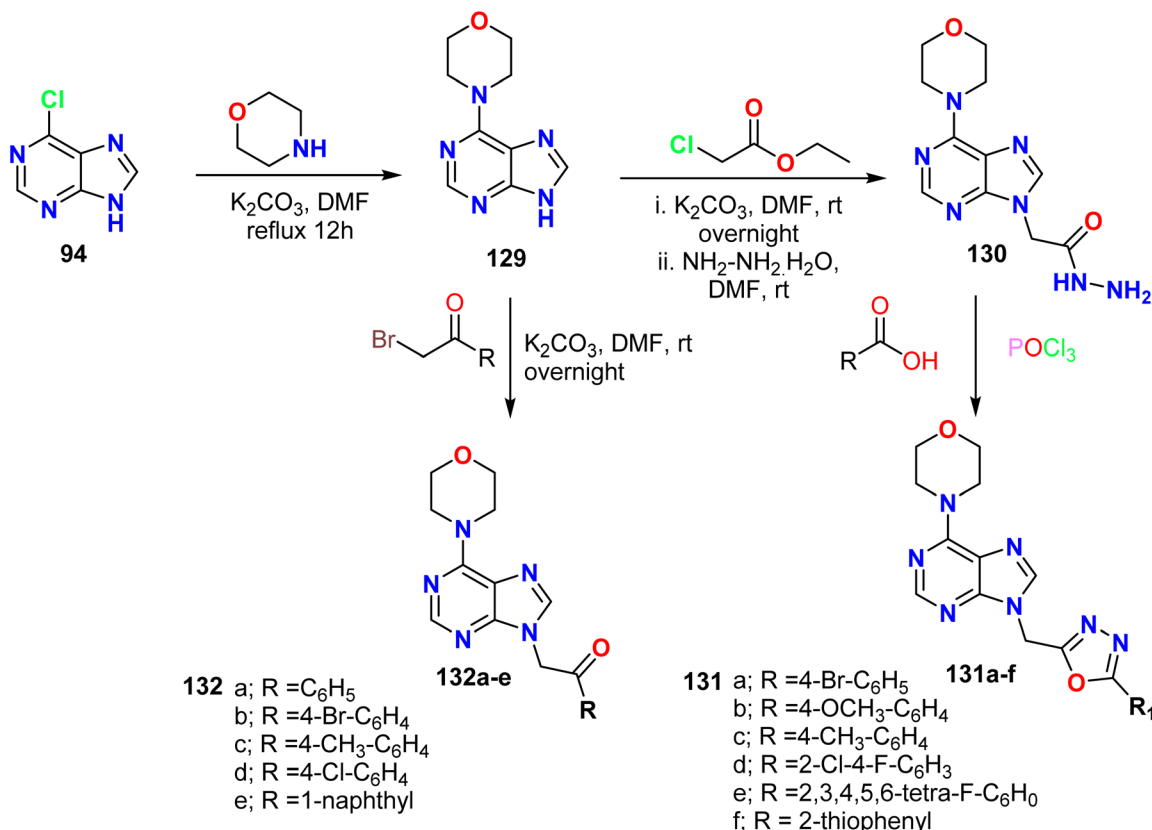
dimethylacetamide (DMA) as the solvent and triethylamine (TEA) as the catalyst at 100 °C under reflux conditions. The products were obtained with yields ranging from 32% to 83%. Subsequently, alkaline hydrolysis was performed to remove the *N*-acetyl and ester groups, resulting in the formation of the desired products **135a–f** (Scheme 35).⁶³

Zagórska *et al.* reported the synthesis of 1*H*-imidazo[2,1-*f*]purine derivatives **138a–c** from 8-bromotheophylline derivatives

136a, b via a reaction with *N*-(aminoalkyl)-4-acetylphenylpiperazine **137** followed by cyclo-condensation. First, 8-bromotheophylline was aminated, and then the 8-amino derivatives spontaneously cyclized through the reaction of NH at C8 with the carbonyl group at N9, resulting in the loss of a water molecule under the reaction conditions (Scheme 36).⁶⁴

On the other hand, Mohamed *et al.* reported the amination of 8-bromo-7-(alkyl)-1*H*-purine-2,6-dione derivatives **122a, b** using 3-

Scheme 33 Synthesis of the 1-alkyl-3-methyl-8-(piperazin-1-yl)-1*H*-purine-2,6-dione derivative.



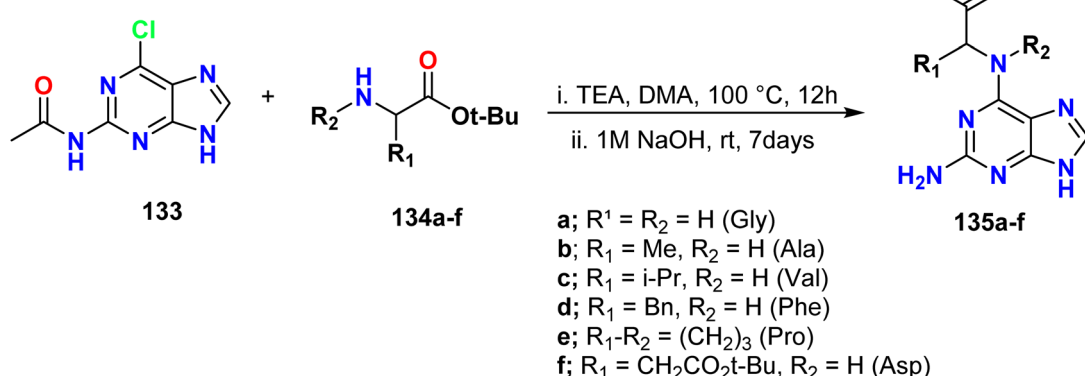
Scheme 34 Amination of 6-chloro-9H-purine with morpholine and subsequent alkylations.

iminosaccharin and sulfathiazole in DMF and in the presence of a catalytic amount of dimethylaminopyridine (DMAP) under reflux conditions to afford **139** and **140**, respectively. Moreover, compounds **141**, **142**, and **143** were readily obtained by the reaction of the 8-bromo-7-(alkyl)-1*H*-purine derivative **122a** with amine derivatives using potassium carbonate in DMF. The authors also described that in order to generate the activity of 2-chloroethylamine-HCl in a mild basic condition, it was necessary to use triethyl amine in DMF to react with **122a**; then the reaction was terminated by the addition of potassium carbonate to give **142**. For the reaction involving 6-aminouracil and **122a**, it was necessary to adjust the pH of the medium in order to facilitate the

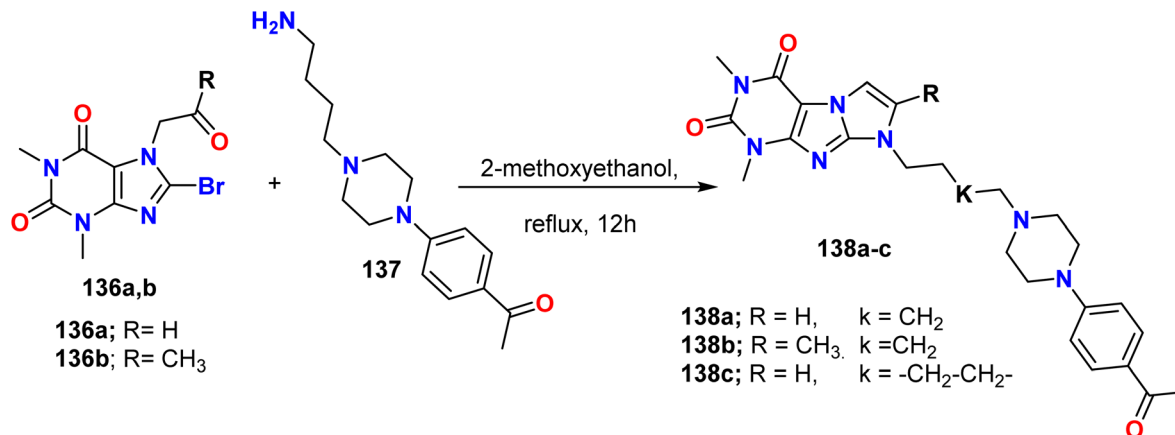
nucleophilic attack using the primary amine. To achieve this, sodium acetate was used as a base in acetic acid. This prevented the de-protonation of uracil NHs and resulted in the formation of compound **143** (Scheme 37).⁷

3.5. Selenylation and thiolation

Dilek *et al.* reported the generation of selenotetrazole-purine derivatives **146a-g** through a three-step synthetic process. Initially, 6-chloropurine was reacted with specific alkyl halides in DMF and K₂CO₃ to afford 6-chloro-9-alkyl-9*H*-purines **144a-g**. Additionally, selenopurines **145a-g** were prepared by reacting



Scheme 35 Synthesis of purine conjugates with natural amino acids.

Scheme 36 Synthesis of 1*H*-imidazo[2,1-*f*]purine derivatives 138a–c.

compounds 144a–g with selenourea in absolute ethanol at room temperature by the Mautner method. The product yields ranged from 30–88%. Compounds 145a–g were allowed to react with 5-chloro-1-phenyl-1*H*-tetrazole to give the desired products 146a–g (Scheme 38).⁶⁵

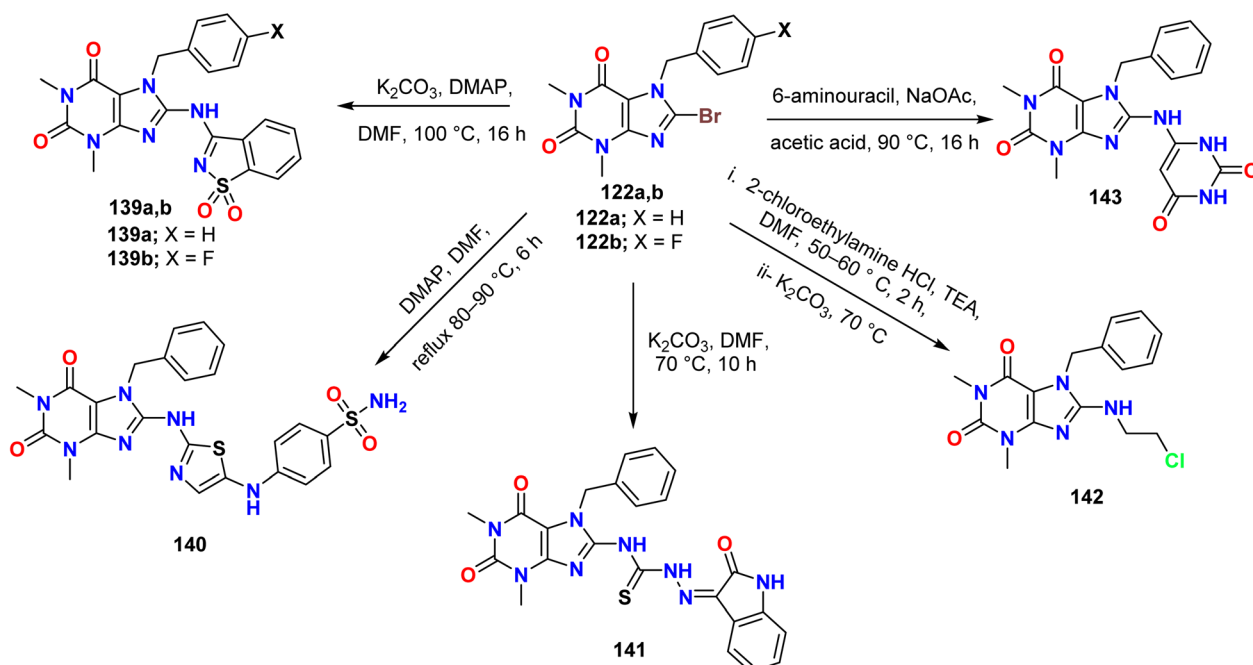
Liu *et al.* outlined the reaction of 6-chloro-9*H*-purine 94 and thiourea under reflux conditions to afford the corresponding 9*H*-purine-6-thiol 147, which reacted with the potassium salt of the phenolate hydroxyl group of a chalcone to afford 6-thioalkyl purine derivatives 148a–f (Scheme 39).⁵⁷

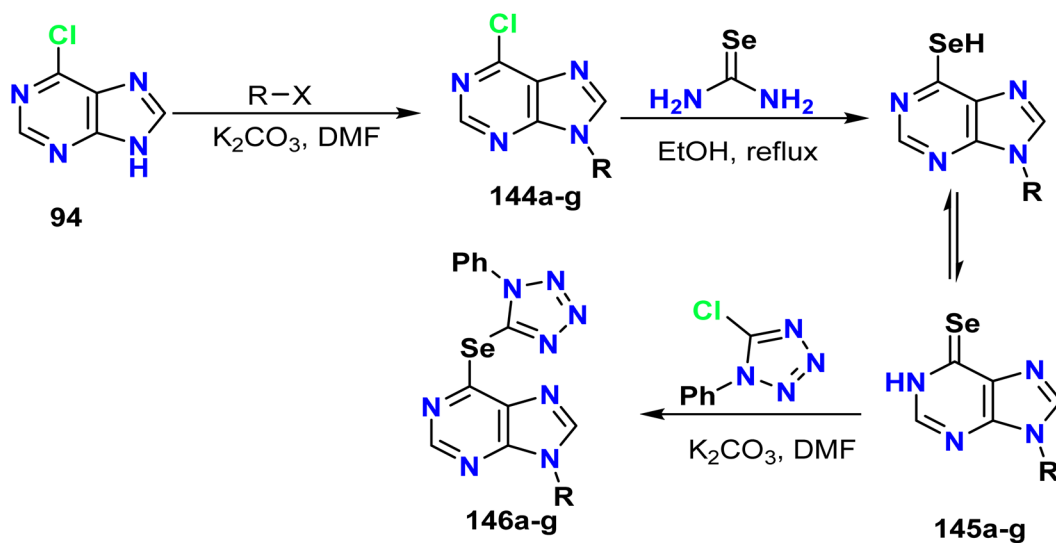
3.6. Condensation and cyclization to form new heterocyclic rings

Singh *et al.* synthesized new Schiff bases 150 and 151 by reacting 2,6-diaminopurine with 2-hydroxy-3-methoxybenzaldehyde

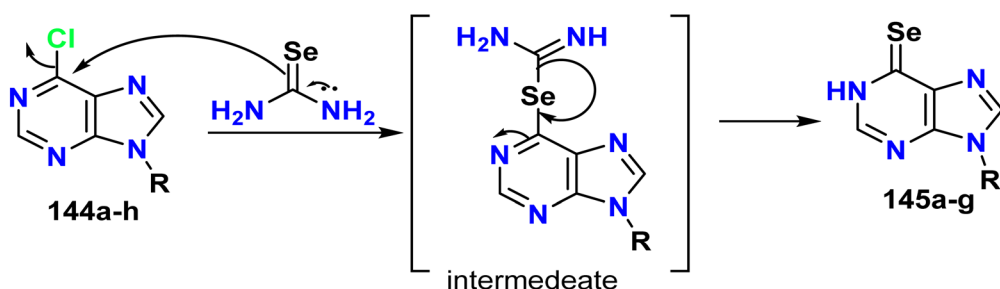
and chromone-3-carboxaldehyde. The reaction was carried out in methanol without any catalyst under reflux and stirring conditions for 6 hours. The authors used these two Schiff bases as the starting material to prepare new copper, zinc, and cobalt metal complexes with targeted DNA-binding activity (Scheme 40).⁶⁶

Furthermore, Afifi *et al.* reported the synthesis of novel hydrazone derivatives based on the purine scaffold. This was achieved by treating 8-hydrazinyl-1*H*-purine-2,6-dione 152 with acetophenone derivatives. Subsequently, the resulting compounds underwent a Vilsmeier reaction using phosphorus oxychloride in DMF, leading to the formation of purine-pyrazolecarbaldehyde derivatives 154a–d. Furthermore, the pyrazolecarbaldehyde derivatives were subjected to Knoevenagel condensation with the activated methylene of 2-thioxothiazole derivatives under basic conditions in dioxane, which

Scheme 37 Amination of 1,3-dimethyl-7-(alkyl)-3,7-dihydro-1*H*-purine-2,6-dione derivatives 122a, b with appropriate amines.



**144a-h and 146a-h; a:R = methyl, b:R = ethyl, c:R = isopropyl, d:R = hexyl,
e:R = benzyl, f:R = cyclobutylmethyl, g:R = cyclohexylmethyl**



Scheme 38 Synthesis of selenotetrazole purine derivatives 146a–g.

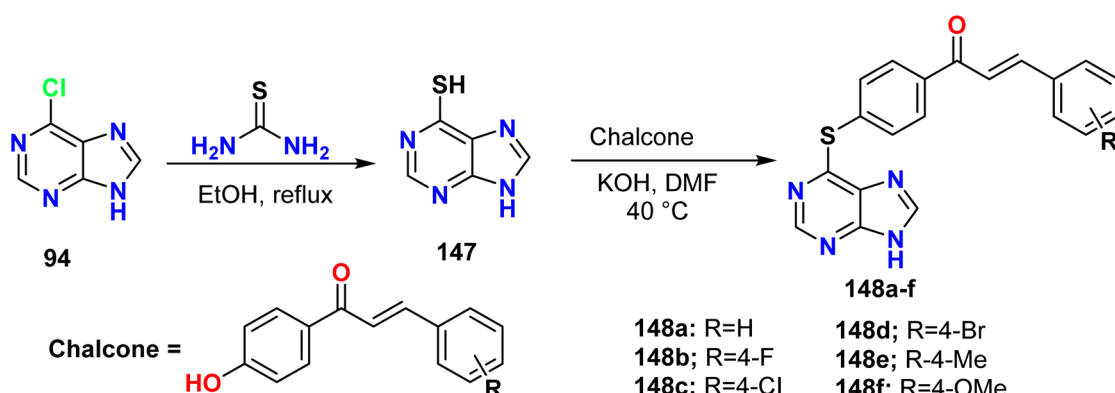
resulted in the formation of the corresponding purine derivatives **155** and **156** (Scheme 41).⁶⁷

3.7. Diazotization and coupling reaction

Khalifa *et al.* illustrated the synthesis of the 8-diazonium purine salt **158** *via* the reaction of 8-aminopurine **157** with nitrous acid; **158** was then coupled with many aryl (phenol, 1-naphthol, and 2-naphthol) and/or hetaryl (3-methyl-6-oxo-thieno[2,3-*b*]pyridine-5-carbonitrile) compounds to afford the diazenyl-purine derivatives **159**, **160**, **161**, and **162** (Scheme 42).⁶⁸

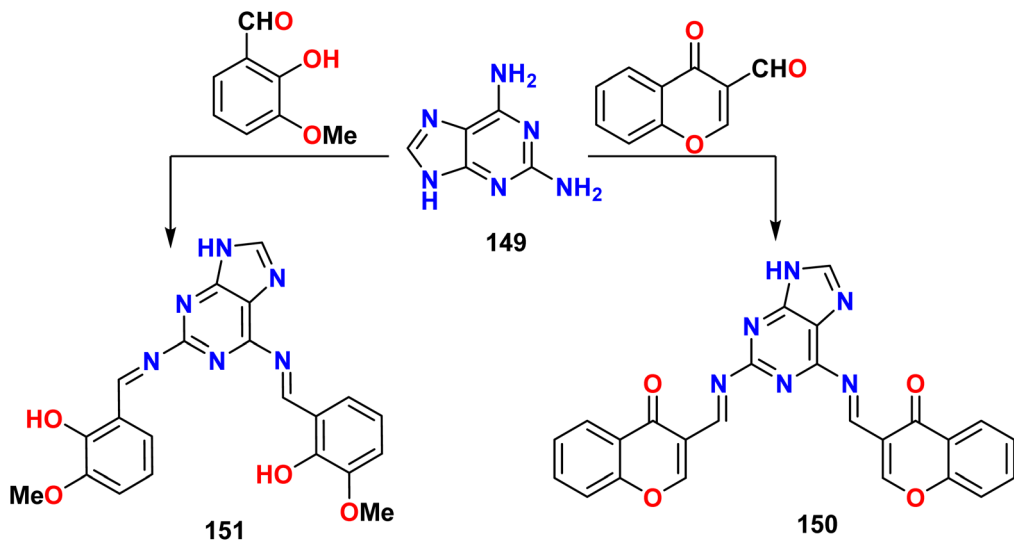
pyridine-5-carbonitrile) compounds to afford the diazenyl-purine derivatives **159**, **160**, **161**, and **162** (Scheme 42).⁶⁸

Furthermore, the diazonium salt of the aminopurine derivative **158** and the 2-phenylthiocarbamide derivative **163** underwent a Japp–Klingemann reaction and afforded a cyano-purine hydrazone derivative **164** by losing the acetyl group. Additionally, the cyclization of the cyano-purine **164** in a bromine solution (Br_2 in ethyl acetate) in pyridine produced the benzothiazolyl acetonitrile derivative **165** (Scheme 43).⁶⁸

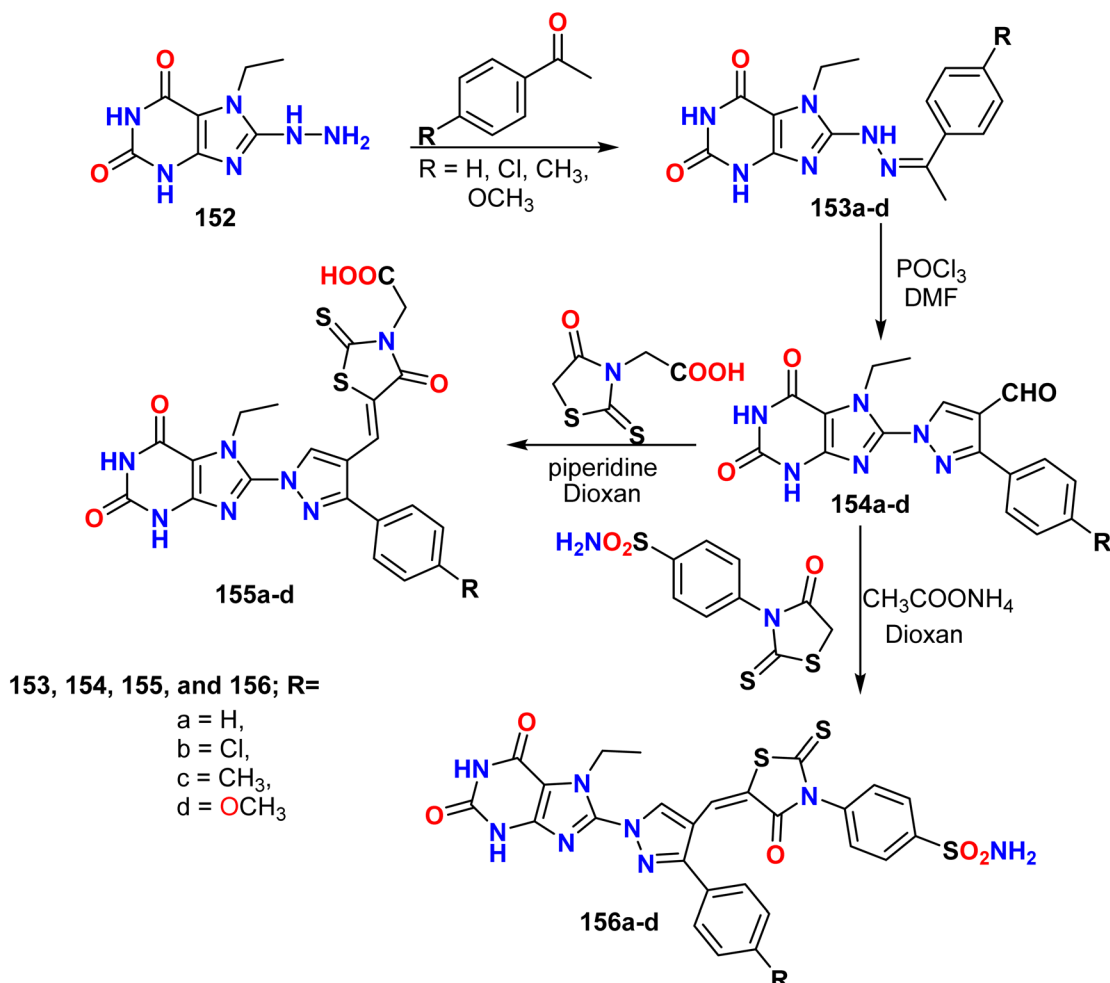


Scheme 39 Synthesis of target 9H-purine-6-thiol **147** and 6-thioalkyl purine derivatives **148a–f**.

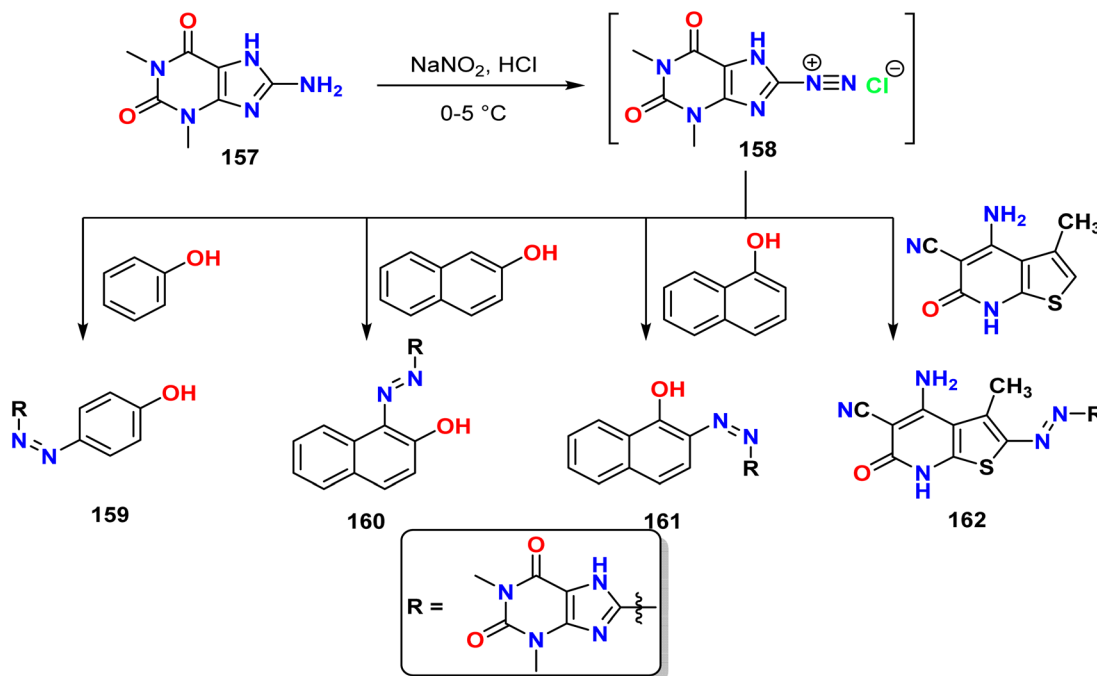




Scheme 40 Synthesis of new Schiff bases by reacting 2,6-diaminopurine 149 with formyl derivatives.



Scheme 41 Synthesis of new Schiff bases based on purine derivatives.



Scheme 42 Synthesis of 8-diazonium purine and its coupling reactions with different reagents.

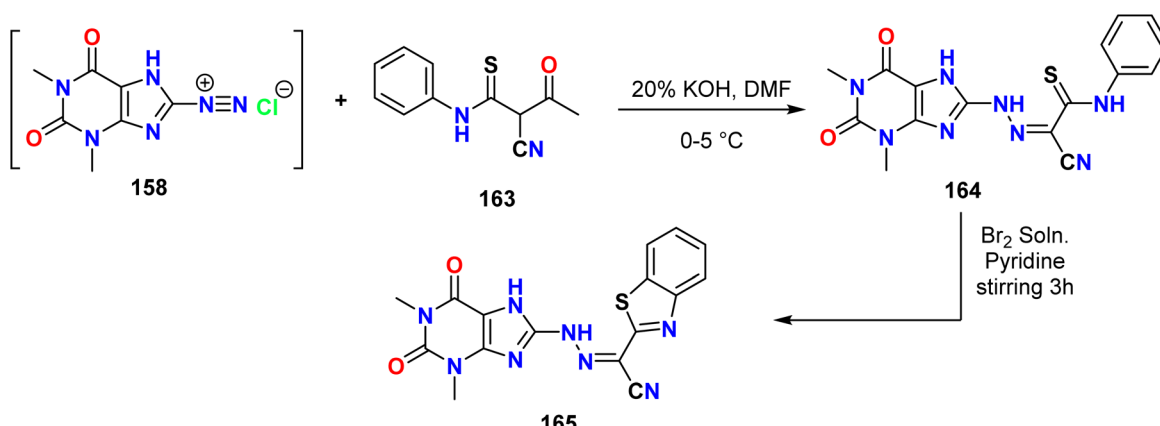
3.8. Miscellaneous reactions

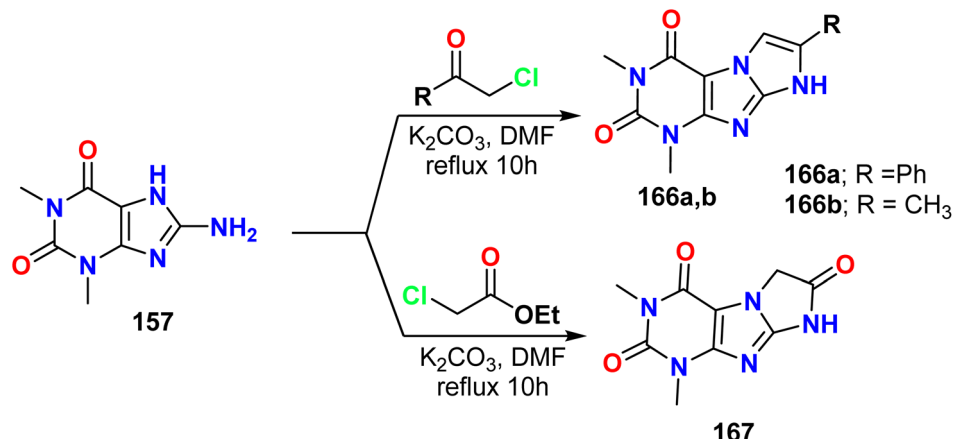
Khalifa described the treatment of 8-amino purine **157** with active α -halo carbonyl compounds, such as phenacyl chloride, chloroacetone, and ethyl chloroacetate, in the presence of anhydrous potassium carbonate; the subsequent cyclization process resulted in imidazopurine derivatives **166a, b** and **167** (Scheme 44).⁶⁸

Furthermore, to synthesize heterocyclic nucleus hybrid with purine nucleus, initially, the purine derivatives **49a-d** containing enaminonitrile-pyridine at C8 were used as starting material for the synthesis of new purines containing heterocyclic fragments at the same carbon, such as pyrido[4,3-*d*]pyrimidine **168a-c**, pyrazolo[4,3-*c*]pyridine **169a-c**, 2-thioxopyrido[4,3-*d*]pyrimidine **170a-c**, 2-oxopyrido[4,3-*d*]pyrimidine **171a-c**, and 2-

oxo-2*H*-pyrano[2,3-*b*][1,6]naphthyridine-3-carbonitrile **172a-c**, by reaction with formic acid, hydrazine hydrate, urea, thiourea, and ethyl cyanoacetate, respectively. All these derivatives were screened for antimicrobial, antiproliferative, and antioxidant activity (Scheme 45).⁴⁴

Hassan *et al.* described the synthesis of chiral-carbon-containing purine derivatives through a one-pot double Mannich-type reaction. The reaction was accomplished by treating the purine derivative **173** with various secondary amines in the presence of an excess amount of formaldehyde (nonenolizable aldehyde) under reflux conditions to afford 1,3,5-thiadiazino[2,3-*f*]purine derivatives **175a-e**. This reaction proceed by double Mannich reaction that involved attach the formaldehyde and led to loss of water molecule and afford methylamine carbocation derivative **174b**, which subsequently

Scheme 43 Synthesis of the benzothiazolyl acetonitrile derivative **165**.



Scheme 44 Synthesis of imidazopurine derivatives 166a, b and 167.

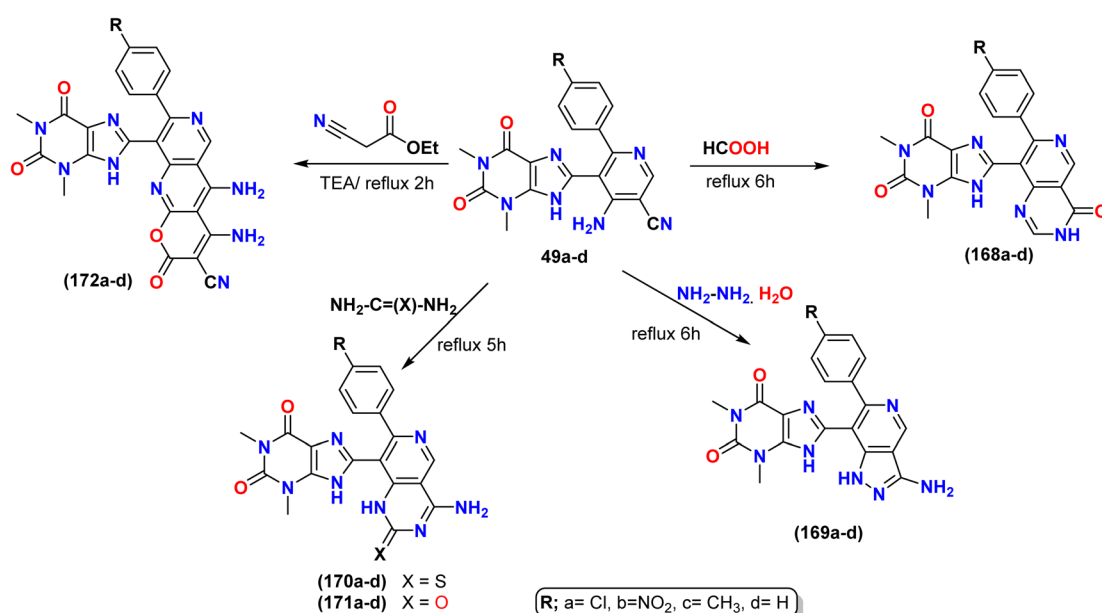
reacted with secondary amine and thiocarbonyl tautomerized to give thio group which *N*-methyl amine derivative 174e and loss the second water molecule leading to formation new thio-heterocyclic ring Scheme 46.⁶⁹

Husseiny *et al.* reported the synthesis of new thiazepino-purines *via* the reaction of 7*H*-purine-6-thiol 147 with arylidenes of malononitrile or ethyl cyanoacetate in a basic medium. The reaction of 7*H*-purine-6-thiol 147 with arylidenes of malononitrile afforded 9*H*-[1,4]thiazepino[4,3,2-gh]purine-8-carbonitrile 176a-d as the sole product. On the other hand, treating 7*H*-purine-6-thiol 147 with arylidenes of ethyl cyanoacetate under reflux conditions revealed two pathways based on the catalyst (trimethylamine or sodium ethoxide) to furnish 2-amino-carboxylate 177a-c or hydroxyl carbonitrile derivatives 178a-c. The reaction proceeded *via* the Michael addition of purine thiol to furnish an olefinic bond in arylidenes, followed by nucleophilic addition to give the desired product (Scheme 47).⁷⁰

4. Biological evaluation of purine derivatives

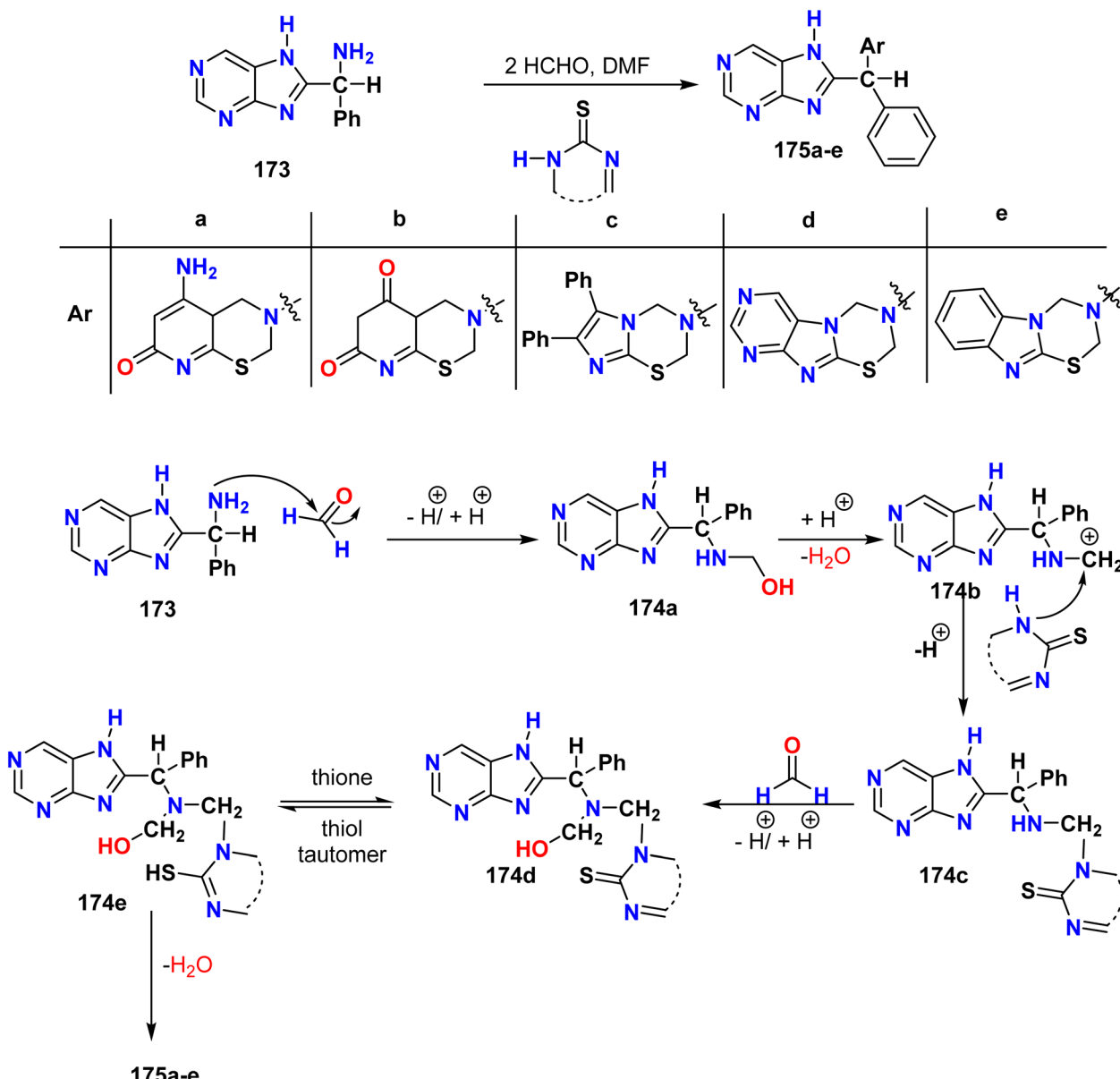
4.1. Anti-cancer activity

Purine derivatives exhibit anticancer activity with different modes of action, but the general mode of action of drugs containing the purine scaffold involves hampering the synthesis of nucleic acids or inhibiting critical enzymes involved in cellular metabolism. It is well-documented that purine analogs have specific targeting abilities and anticancer behavior. For example, tioguanine, also known as 6-thioguanine, is a leukemia drug that has been approved by the FDA. Cytosine methylation in human cells is reduced because it inhibits cytosine residue methylation. Similarly, clofarabine, an FDA-approved medicine based on second-generation purines, exhibits anti-cancer properties by inhibiting ribonucleotide reductase and stopping the elongation of DNA chains.^{71,72}



Scheme 45 Synthesis of many heterocyclic cores with purine as the base nucleus.



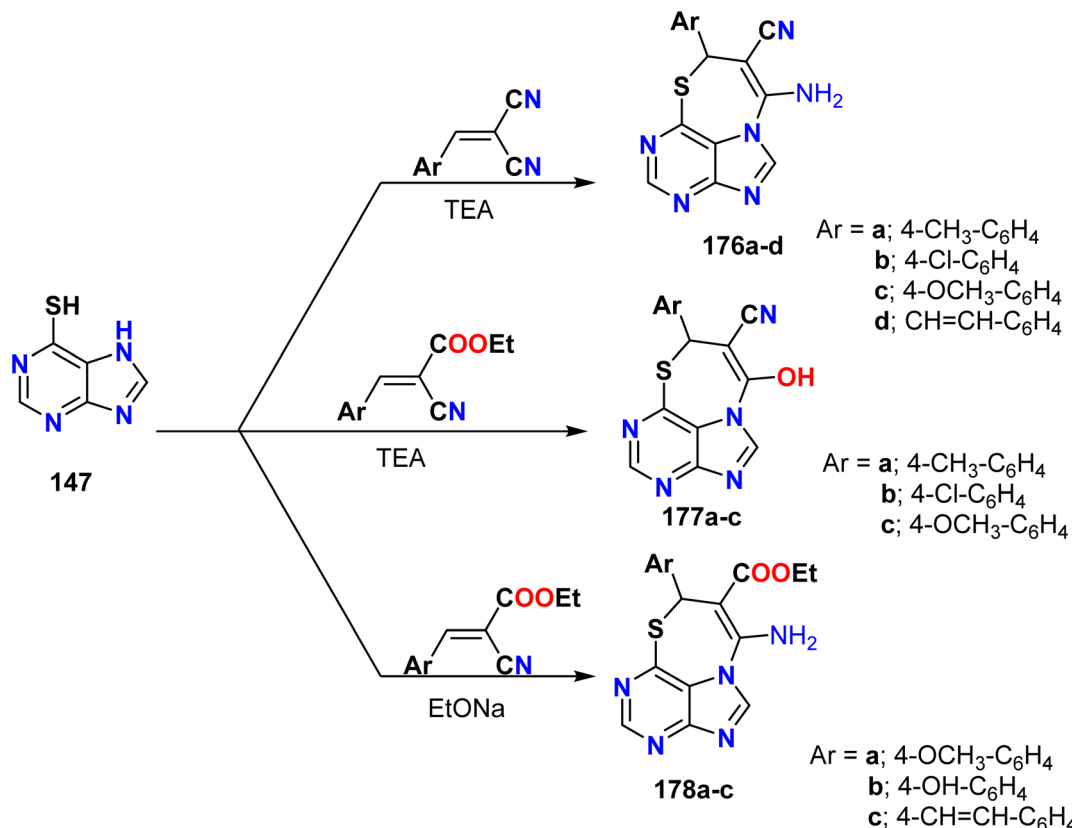


Scheme 46 Formation of new purines attached to chiral-carbon-containing heterocyclic scaffolds and the mechanistic pathway.

Lei *et al.* screened the 9-heterocycl substituted 9*H*-purine derivatives **71a–l** for anti-proliferation activity against four cell lines (HCC827, H1975, A549, and A431) by using the MTT assay, and the results showed their potency against the human lung cancer cell line (HCC827) rather than other tested cells (Fig. 3).⁴⁸ Additionally, **71i** had an IC_{50} value of 0.00088 μ M against HCC827 cells, but for H1975 cells, it was 0.20 μ M. Notably, four derivatives **71d**, **71i**, **71k**, and **71l** exhibited very strong anti-proliferation and EGFR^{L858R/T790M/C797S} inhibition activities. **71i** demonstrated anti-proliferative activity against HCC827 and H1975 cell lines with IC_{50} values of 0.00088 and 0.20 μ M, respectively. Additionally, the most active derivative **71i** suppressed EGFR^{L858R/T790M/C797S} with an IC_{50} of 18 nM. The derivatives **71d**, **71i**, **71k**, and **71l** induced apoptosis at the G0/G1 cell cycle phase, and their percentage of apoptosis in

HCC827 cells were 57.74, 56.91, 60.08, and 55.90%, respectively, at 1 μ M concentration, respectively. The results of mutant EGFR (epidermal growth factor receptor) were compared with the positive control osimertinib, which displayed an IC_{50} value of 110 ± 6.0 nM. The activity was assessed using a western blot assay to better elucidate the mechanism of their anti-proliferative action. Compounds **71d**, **71i**, and **71k** inhibited EGFR phosphorylation in H1975, HCC827, and A549 cell lines in a concentration-dependent manner (Fig. 3).⁴⁸

Polat *et al.* reported the cytotoxicity of tri-substituted purines against different cell lines, including HUH7 (liver), MCF7 (breast), and HCT116 (colon), based on the SRB assay. SAR study demonstrated that substitution with different phenyl moieties at C8 of purine affects the activity; for example, introducing trifluoromethyl phenyl (**79j**, **79k**, **79l**), 4-methoxy



Scheme 47 Synthesis of the new thiazepinopurine derivatives 176–178.

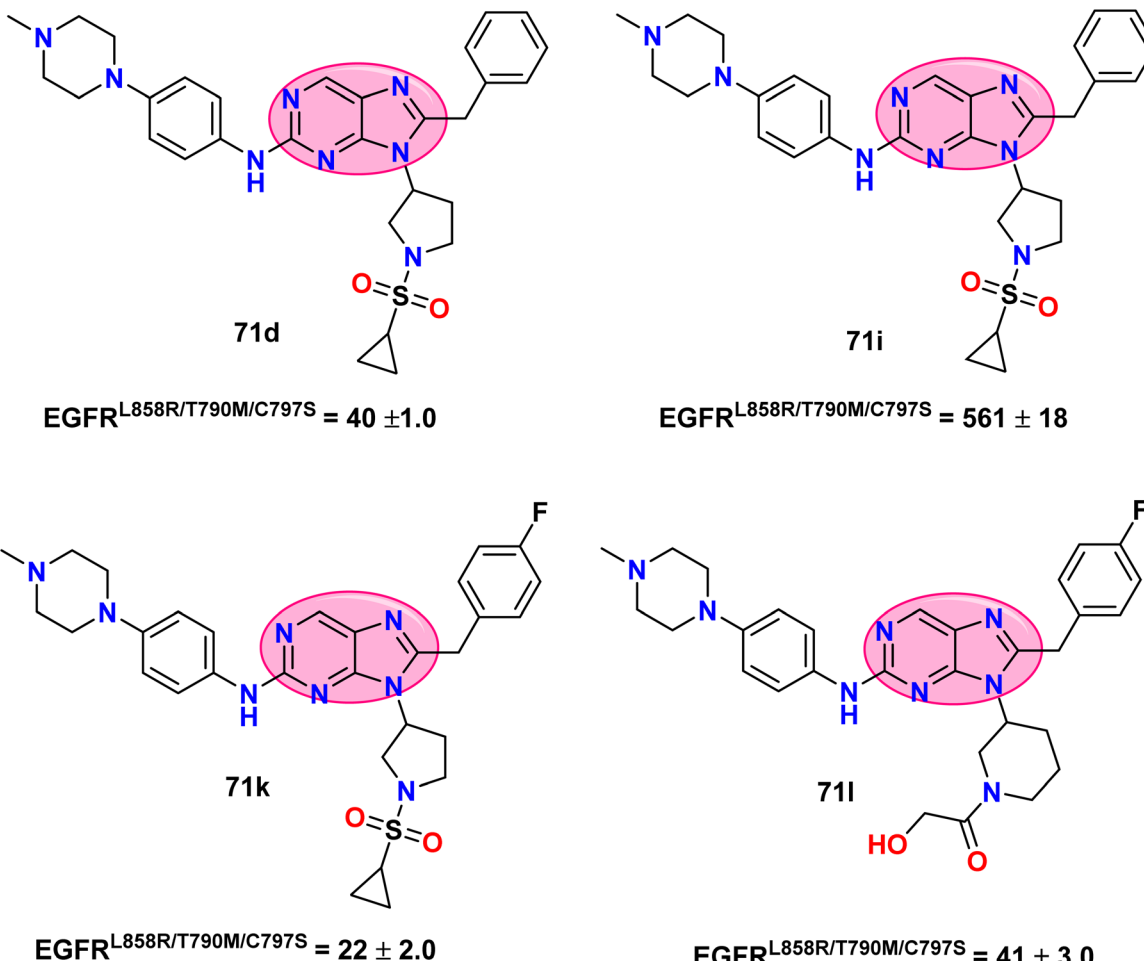
phenyl (**79s**), and 4-fluoro phenyl (**79z**) exhibited IC_{50} values less than 10 μM against liver cell lines (HUH7). Furthermore, the most potent purine derivatives were also tested using the NCI-SRB assay on drug-sensitive hepatocellular carcinoma (HCC) cell lines, including SNU475, SNU387, HepG2, SNU423, Hep3B, SNU182, SNU449, Mahlavu, Huh7, SNU398, FOCUS, and PLC. Compound **79j** had significant anticancer activity with IC_{50} values ranging between (2.9–9.3 μM) against Huh7, FOCUS, SNU475, SNU182, HepG2, and Hep3B cells compared with the positive control fludarabine. In the same way, the substituted purines **79l** and **79s** showed more significant activity than fludarabine against the drug-sensitive HepG2 and Hep3B cells with low IC_{50} values (Fig. 4).⁵⁰

Moreover, Verma *et al.* evaluated the anticancer activity of purine derivative **168b** against four cell lines. The IC_{50} (μM) values against the MCF-7, A549, HeLa, and Panc-1 cancer cell lines were 0.8 ± 0.61 , 1.0 ± 0.3 , 1.2 ± 0.7 , and $0.90 \pm 0.71 \mu\text{M}$ compared with those of doxorubicin (0.92 ± 0.50 , 1.02 ± 0.80 , 1.02 ± 0.72 , and $1.41 \pm 0.58 \mu\text{M}$), respectively, indicating its strong cytotoxic action. Additionally, compounds **168c** and **172c** showed remarkable radical-scavenging action at concentrations between 25 and 100 $\mu\text{g mL}^{-1}$, with ED_{50} values of 3.39 ± 0.3 and $4.27 \pm 0.5 \mu\text{M}$, respectively, comparable to butylated hydroxyanisole (BHA) $5.51 \pm 0.3 \mu\text{M}$ (Scheme 45 and Fig. 5).⁴⁴

Kucukdumlu *et al.* screened the designed di-substituted purines against Huh7 (liver), HCT116 (colon), and MCF7 (breast) cell lines. The results exhibited broad activity against

the tested cells with IC_{50} values ranging from 0.05 to 21.8 μM , except for the compound derived from 4-chlorobenzylamine using 1-((4-trifluoromethyl)phenyl)piperazine, which displayed weak activity (Scheme 21). Additionally, compounds **82f** and **82p** exhibited significant activity against all cell lines, with IC_{50} values of (0.13 ± 0.12 and $0.08 \pm 0.06 \mu\text{M}$), (0.42 ± 0.08 and $0.04 \pm 0.004 \mu\text{M}$), and (0.4 and $0.05 \mu\text{M}$) against Huh7, HCT116, and MCF7, respectively, compared with those of 5-FU (30.6 ± 1.8 , 4.1 ± 0.3 , and $3.5 \pm 0.7 \mu\text{M}$) and cladribine (0.9 ± 0.7 , <0.1 , and $2.4 \pm 2.4 \mu\text{M}$) against the same cell lines. Several liver cancer cell (HCC) lines, including Huh7, HepG2, Mahlavu, and FOCUS, were also used to test the cytotoxic activity of purine analogs. Compounds **82f** and **82s** demonstrated high cytotoxic activity against Huh7 cells, with IC_{50} values in the 0.08 – $0.13 \mu\text{M}$ range, which were comparable to CPT and superior to cladribine, fludarabine, and 5-FU (Scheme 21 and Fig. 6).⁵¹

Attiogbe *et al.* reported the cytotoxicity of **179** against different cell lines, and the results exhibited strong activity against the growth of melanoma, breast, and lung cancer cells; it displayed more sensitivity to HCC827 and H1975 lung cancer cells and T47D breast cancer cells. Surprisingly, the *in vivo* results confirmed that **179** inhibited the proliferation of HCC827 and H1975 tumors. Compound **179** inhibits the EGFR pathway by downregulating p-EGFR, p-Akt, and p-MAPK, as confirmed by western blotting analysis. Apoptosis and cell cycle analyses were conducted on HCC827 and H1975 cell lines. The results showed that the purine derivative **179** could enhance



Positive control Osimertinib = 110 ± 6.0

Fig. 3 Structures of the most active 9-heterocyclyl substituted 9H-purine derivatives and their values against the EGFR^{L858R/T790M/C797S} compared to osimertinib as a positive control.

apoptosis in both early- and late-stage cancer compared with the control. Additionally, purine derivative **179** was found to induce cell cycle arrest at the S phase (Fig. 7).¹⁸

Husseiny *et al.* screened the synthesized thiazepinopurine derivatives against three cancer cell lines (HepG2, MCF-7, and PC-3) and one normal cell line (WI38). The IC₅₀ of the thiazepinopurines exhibited broad activity against the tested cell lines. A significant antiproliferative effect was observed for compounds **176b** and **176c**, whose IC₅₀ values ranged from 5.52 to 17.09 μM compared with roscovitine (9.32 to 13.82 μM). Moreover, both derivatives exhibited good selectivity indexes, and compound **176b** showed the best selectivity index. Compound **176b** showed CDK2 inhibitory potential with an IC₅₀ 0.219 μM . Furthermore, **176b** was found to arrest MCF-7 cells at the S phase and induce apoptosis by suppressing Bcl-2 expression, as well as increasing the expression of Bax and caspases-8 and 9. The SAR study is summarized in Fig. 8.⁷⁰

Rad *et al.* synthesized new 8-((1-alkyl-1*H*-1,2,3-triazol-4-yl)piperazin-1-yl)-1*H*-purine-2,6-dione **180a-o** and screened the designed derivatives against two cancer cell lines, including A-

375 (malignant melanoma) and MCF7 (common breast cancer), using the MTT assay. The results revealed that compounds **180i**, **180j**, and **180k** demonstrated IC₅₀ values of (371 \pm 2.5, 323 \pm 2.6, and 367 \pm 3.4 μM) and (260 \pm 2.2, 245 \pm 2.3, and 175 \pm 3.2 μM) against A-375 and MCF7, respectively. Additionally, screening the synthesized compounds against the normal cell line HEK-293 indicated non-toxic properties with IC₅₀ values above that of methotrexate (MTX) (IC₅₀ = 199 \pm 2.4 μM). Based on the SAR study, the derivatives could be summarized into four categories: (1) compounds with simple aryl-alkyl substituents, such as **180a** and **180c-180f**; (2) compounds with alkyl-ester moieties; (3) compounds with alkyl-imide moieties, such as **180l-180o**; and finally, (4) compounds containing normal alkyl chain substituents **180h-180k**. While the first three groups exhibited no effect on cancer cells, compounds **180h-180k** responded most favorably to both cancer cell lines (Fig. 9).⁶¹

Wang *et al.* reported that compound **99b** showed the greatest efficacy in inhibiting enzyme activity and displaying anti-proliferative effects against the cancer cell lines. Compound

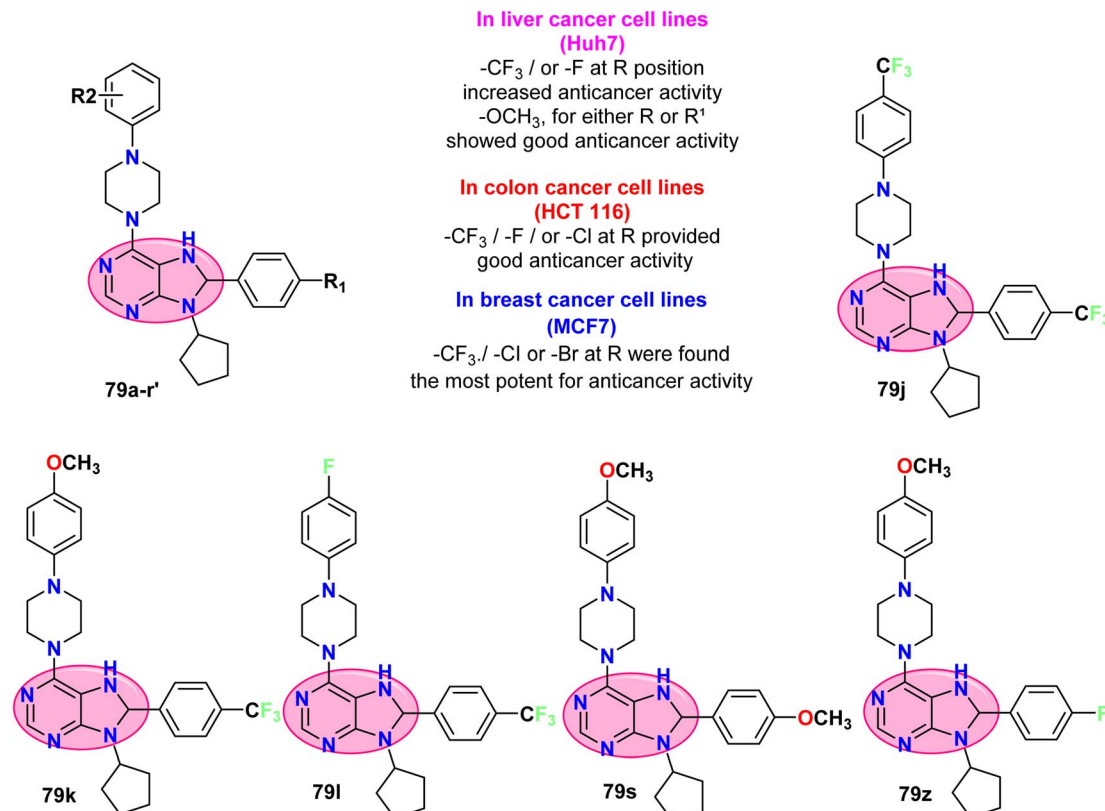


Fig. 4 Structure of the most active tri-substituted purines with cytotoxicity against hepatocellular carcinoma (HCC) cell lines.

99b exhibited kinase activity against fibroblast growth factor receptors (FGFRs), especially FGFR1 ($IC_{50} = 0.20 \pm 0.02$ nM) and FGFR4 ($IC_{50} = 0.40 \pm 0.03$ nM), compared with fexagrinatin (AZD4547), showing an IC_{50} value of 0.95 ± 0.03 nM for FGFR1 and 369.46 ± 26.94 nM for FGFR4, which illustrates that this compound formed irreversible covalent bonds with FGFR1 and FGFR4 proteins, thus effectively inhibiting their enzyme activity. Furthermore, it regulated the FGFR-mediated signaling pathway and the mitochondrial apoptotic pathway, promoting cancer cell apoptosis and hindering cancer cell invasion and metastasis. Moreover, **99b** demonstrated good metabolic

stability and showed significant anti-tumor activity in the MDA-MB-231 xenograft tumor mice model (Fig. 10).⁵⁵

4.2. Anti-microbial activity

Verma *et al.* revealed the antimicrobial activity of 1,3-dimethyl-2,6-dioxo-1*H*-purine derivatives. The SAR study of antimicrobial activity revealed that electron-withdrawing groups, such as nitro and chloro, enhanced the activity greater than electron-donating groups because the hydrophobic nature of nitro and halogen groups changes the physicochemical properties of

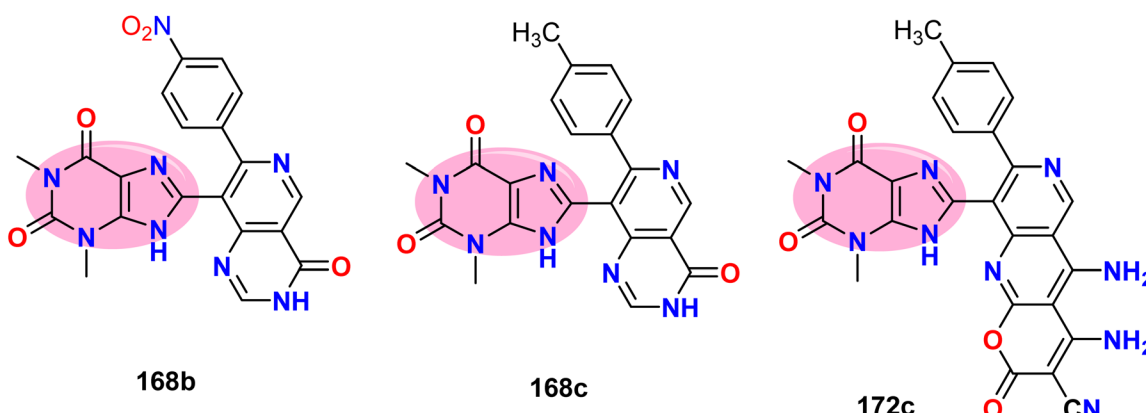


Fig. 5 Structure of 8-substituted purine derivatives attached to heterocyclic scaffolds as anticancer agents.

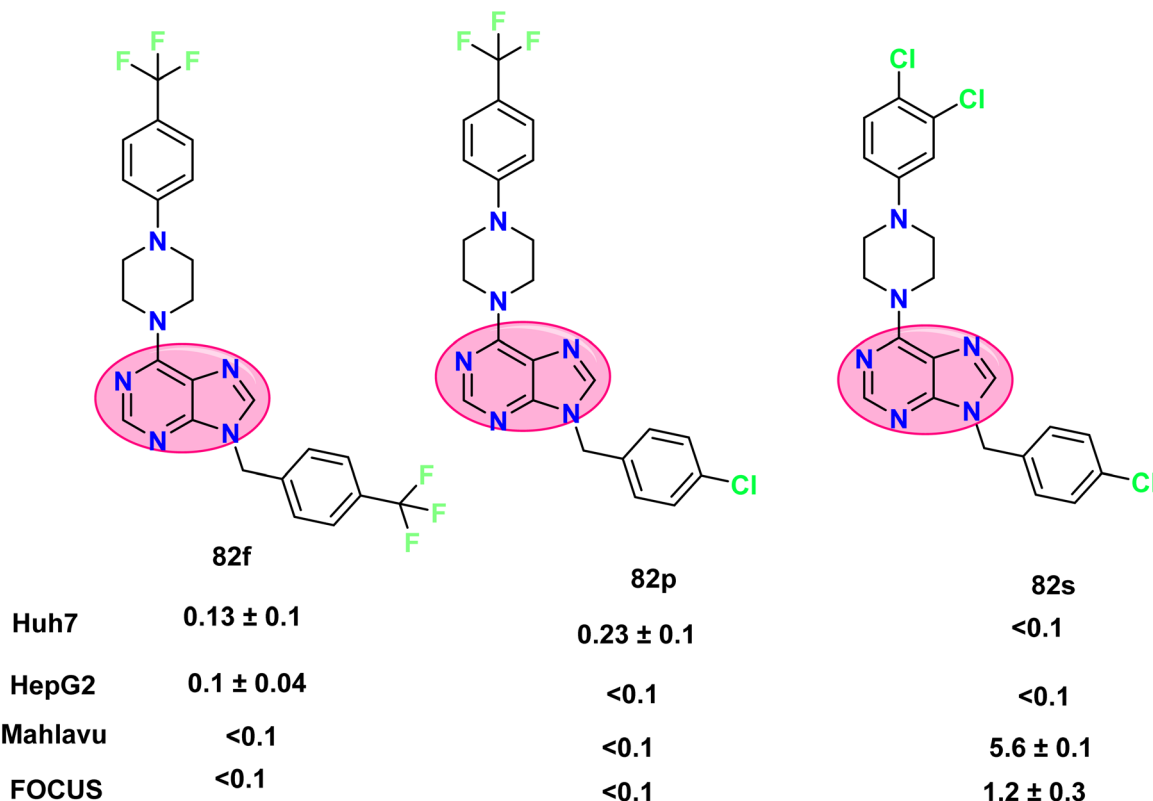


Fig. 6 The most active 6,8-disubstituted purine derivatives **82f**, **82p**, and **82s** against hepatocellular carcinoma (HCC) cell lines: (Huh7, HepG2, MAHLAVU, and FOCUS).

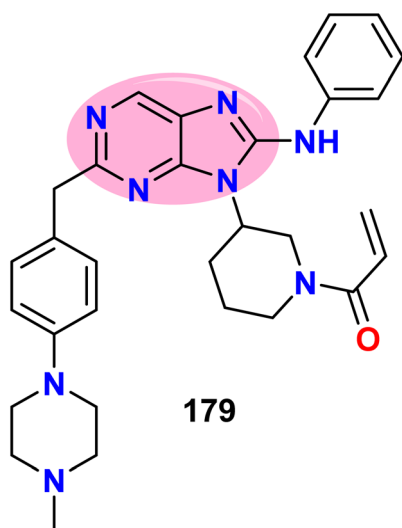


Fig. 7 Structure of the 2,8,9-trisubstituted purine (179).

these compounds to transect microbial membranes. The 8-(7-(4-chlorophenyl)-4-oxopyrido[4,3-*d*]pyrimidin-8-yl)-1,3-dimethyl-1*H*-purine-2,6-dione derivative **168a** showed strong action against Gram-negative bacteria, whereas 8-(6-(4-nitrophenyl)-1*H*-pyrazolo[4,3-*c*]pyridin-7-yl)-1*H*-purine-2,6-dione **169b** showed greatest activity against Gram-positive bacteria. Compound **168a** exhibited the most potent MIC value of 1.5 μ g

mL^{-1} against *Escherichia coli* and *Klebsiella pneumoniae* compared with ciprofloxacin (3.12 and 1.5 $\mu\text{g mL}^{-1}$). Similarly, compound **169b** showed MIC values of 12.5 and 25 $\mu\text{g mL}^{-1}$ against *Staphylococcus aureus* and *Bacillus subtilis*, which are greater than the MIC values of ciprofloxacin (3.12 and 1.5 $\mu\text{g mL}^{-1}$), respectively. As for antifungal activity, purine derivative **171b** showed MIC values of 3.12, 1.5, 1.5, and 3.12 $\mu\text{g mL}^{-1}$ compared to fluconazole (MIC = 1.5, 3.12, 1.5, 3.12 $\mu\text{g mL}^{-1}$) against *Aspergillus niger*, *Aspergillus oryzae*, *Candida albicans*, and *Penicillium chrysogenum*, respectively (Fig. 11).⁴⁴

Hu *et al.* evaluated the antimicrobial activity of purine azole derivatives against five Gram-positive and six Gram-negative isolates. A purine nucleus hybrid with metronidazole compound **181** exhibited significant inhibitory activity, with a MIC value of 6 μ M, which is nearly four times higher than that of norfloxacin (MIC = 25 μ M). Additionally, compound **181** displayed no toxic activity against normal mammalian cells (RAW 264.7). Compound **181** could disrupt the MRSA cell membrane and also get inserted into the MRSA DNA to generate a stable complex known as compound **181**-MRSA DNA. This complex could inhibit the replication and proliferation of MRSA. Finally, it was found that compound **181** exhibited antimicrobial activity *via* a dual-targeted inhibitory action, that is, damaging the MRSA cell membranes and causing changes in the DNA double helix (Fig. 12).⁷³

Paulsen *et al.* conducted a screening to investigate the anti-microbial potential of synthesized 6-(hydroxylimino)-9-methyl-

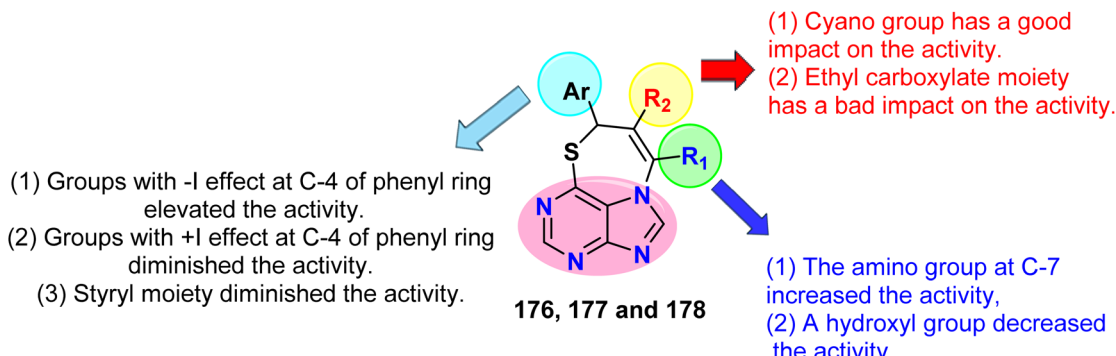


Fig. 8 Illustration of the SAR study of thiazepinopurine derivatives using cancer cell lines (HepG2, MCF7, and PC-3).

1H-purin-7-ium derivatives. The study identified two derivatives **182** and **183**, which exhibited antimicrobial activity against various pathogenic bacteria and protozoa. Notably, compounds **182** and **183**, characterized by larger lipophilic side chains, demonstrated good to very good activity against all microorganisms, except for *E. coli*. Furthermore, these compounds displayed the highest potency, with IC_{50} (μ M) values of 1.89 and 1.84 μ M against *S. aureus*, respectively. Additionally, compounds **182** and **183** exhibited IC_{50} (μ M) values of 0.54 and 0.53 μ M against *T. cruzi*, and an IC_{50} value of 0.50 μ M against *T. rhodesiense*. Importantly, these derivatives demonstrated non-toxic activity against mammalian MRC-5sv2 (human lung fibroblast) cells and exhibited the ability to reduce bacterial biofilm formation by varying percentages. Compounds **182** and **183** demonstrated a significant 90% decrease in *S. epidermidis* biofilm formation at concentrations of 125 and 63 μ M, respectively. In contrast, at the same concentrations (125 and 63 μ M),

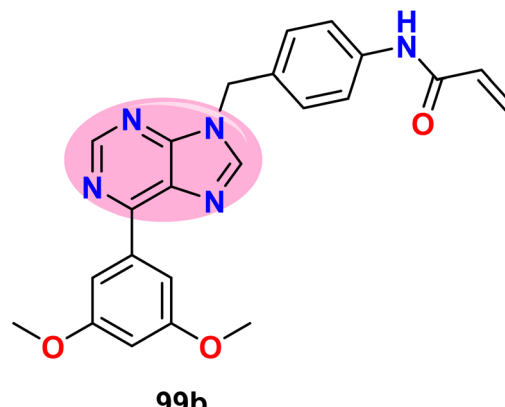
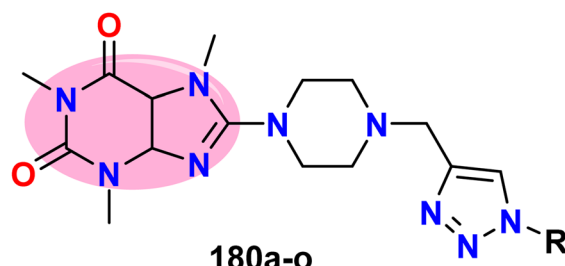


Fig. 10 Structure of compound **99b** with inhibitory activity against fibroblast growth factor receptors (FGFRs).



- a:** R= -CH₂Ph
- b:** R-CH₂CO₂CH₂Ph
- c:** R=-CHPh₂
- d:** R=-(CH₂)₂Ph
- e:** R= -(CH₂)Ph
- f:** R-CH₂Ph-Me(p)
- g:** R=-(CH₂)₂CO₂Et
- h:** R=-n-C₇H₁₅
- i:** R=-n-C₆H₁₃
- j:** R-n-C₈H₁₇
- k:** R-11-C₁₀H₂₁
- l:** R=-(CH₂)₅-(N)-phthalimidyl
- m:** R= -(CH₂)₄-(N)-saccharinyl
- n:** R= -(CH₂)₃-(N)-saccharinyl
- o:** R=-(CH₂)₅(N)-saccharinyl

Fig. 9 Structure of 8-((1-alkyl-1*H*-1,2,3-triazol-4-yl)piperazin-1-yl)-1*H*-purine-2,6-dione derivatives **180a-o**.



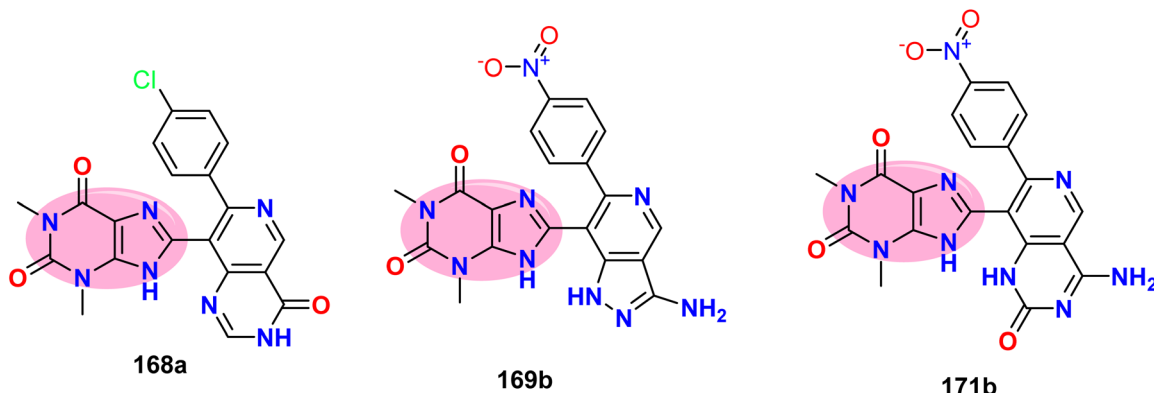


Fig. 11 Structure of 8-purine derivatives with heterocyclic fragments.

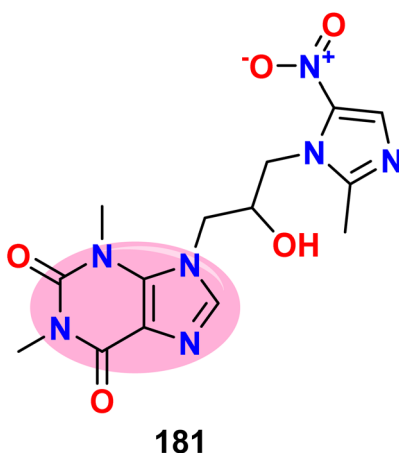


Fig. 12 Purine-metronidazole derivative **181** as a dual-targeting MSRA inhibitor.

the bacterial growth was reduced by 50% and 15%, respectively (Fig. 13).⁷⁴

Nadaf *et al.* synthesized 9-alkyl-6-(4-(4-propoxyphenyl)piperazin-1-yl)-9*H*-purine derivatives and tested their antimycobacterium (antimycobacterial), antibacterial, and antifungal activities. As for antimycobacterial activity, compounds **184a**, **184b**, **184c**, and **184d** showed MIC values of 6.2, 3.125, 3.125,

and 6.25 $\mu\text{g mL}^{-1}$, respectively, while other derivatives showed MIC values of 12.5 $\mu\text{g mL}^{-1}$. Similarly, ciprofloxacin, pyrazinamide, and streptomycin revealed MIC values of 3.125, 3.125, and 6.25 $\mu\text{g mL}^{-1}$, respectively. To test the antimicrobial activity, the designed derivatives were evaluated against *Staphylococcus aureus*, *Bacillus subtilis*, *Escherichia coli*, and *Pseudomonas aeruginosa*. Compounds **184a-f** revealed potent antibacterial activity against the tested strains, with MIC values ranging from 2–4 $\mu\text{g mL}^{-1}$, while other derivatives **184g-j** displayed MIC values between 8 and 64 $\mu\text{g mL}^{-1}$, displaying comparable activity to tetracycline or higher (MIC = 2–4 $\mu\text{g mL}^{-1}$). As for antifungal activity, the designed purine derivatives were screened against *Aspergillus flavus*, *Trichoderma harzianum*, *Penicillium chrysogenum*, and *Candida albicans*, and the same results were observed. Compounds **184a-f** showed good antifungal activity against the tested strains, with MIC values ranging between 1 and 8 $\mu\text{g mL}^{-1}$. For compounds **184g-j**, the MIC ranged from 16 to 64 $\mu\text{g mL}^{-1}$ compared to nystatin and fluconazole (MIC = 2–4 $\mu\text{g mL}^{-1}$). Finally, the SAR study illustrated that the increased length of the alkyl chain decreased the activity of the compound (Fig. 14).⁷⁵

4.3. Anti-inflammatory activity

Hassan *et al.* demonstrated that the [1,3,5]thiadiazino[2,3-*f*] purine derivative **175d** exhibited anti-inflammatory activity by inhibiting the COX-2 enzyme. The IC₅₀ value of this purine

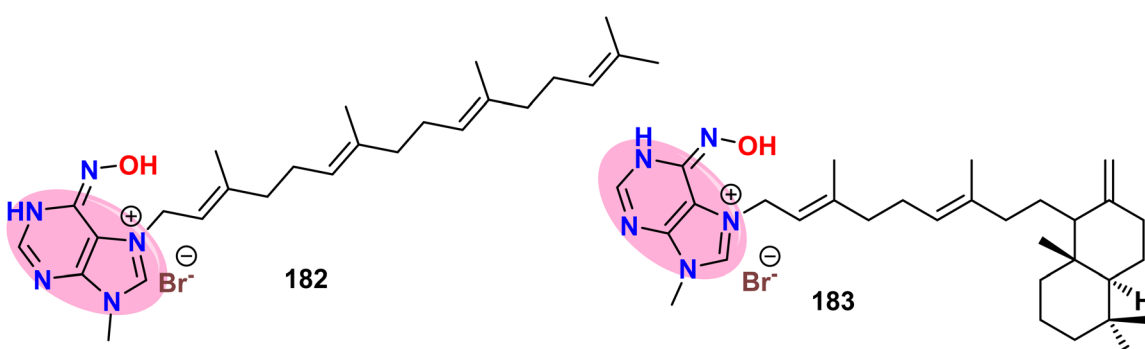


Fig. 13 Structure of the most active 6-(hydroxymino)-9-methyl-1*H*-purin-7-ium derivatives.

**R = a; Et,
b; 'Pr,
c; Pr,
d; Bu,
e; Pentyl,
f; Hexyl,
g; Heptyl,
h; Octyl,
i; Nonyl,
j; Decyl**

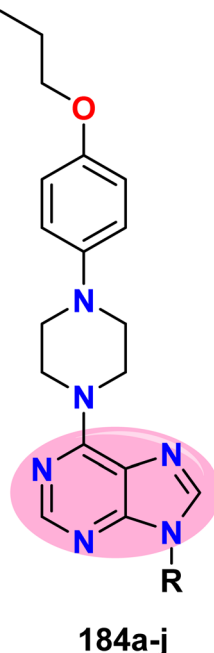


Fig. 14 New 6,9-disubstituted purine derivatives exhibited anti-mycobacterial, antibacterial, and antifungal activity.

derivative was 89.92 ± 2.17 nM, whereas the IC_{50} value of Celecoxib was 53.76 ± 2.05 nM (Scheme 46 and Fig. 15).⁶⁹

Similarly, lipoxygenases (Lox) are a class of oxidative enzymes that contain a non-heme iron atom in their active site. Lox regulates inflammatory responses by producing leukotrienes as pro-inflammatory mediators and lipoxins as anti-inflammatory mediators.⁷⁶ Aifi et al. tested the anti-inflammatory action of the designed purine-pyrazole derivatives **154a-d**, **155a-d**, and **156a-d** against 15-LOX. The IC_{50} of all tested compounds ranged from 1.96 to 6.12 μ M, indicating potent 15-LOX inhibition comparable to zileuton ($IC_{50} = 3.98$ μ M), quercetin ($IC_{50} = 6.87$ μ M) and meclofenamate sodium ($IC_{50} = 5.64$ μ M). Purine derivatives **156a** exhibited the highest potency, while **154d** showed the least activity. The SAR study elucidated that the test pyrazole-carboxaldehydes **154a-d** had

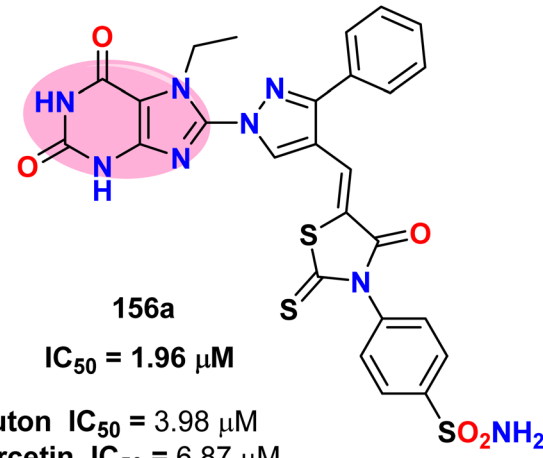


Fig. 16 Structure of the purine analog with the most potent 15-LOX inhibitory action.

moderate activity. A general observation was that the derivatives obtained from condensation with rhodanine derivatives **156a**, **156b**, **156d**, **155a**, **155b**, and **155d** were more potent than the starting pyrazole carboxaldehydes. Moreover, purine derivatives containing acetic acid as a side chain (**155a**, **155b**, and **155d**) exhibited greater inhibitory activity against 15-LOX in comparison with their benzene sulphonamide counterparts **156a**, **156b**, and **156d** (Scheme 41 and Fig. 16).⁶⁷

4.4. Anti-viral activity

Mohammed et al. synthesized a series of tricyclic penciclovir (PCV) derivatives that showed promising antiviral activity, especially against the herpes simplex virus (HSV). Among the synthesized derivatives, the 9*H*-imidazo[1,2-*a*]purin-9-one derivative **185** exhibited potent antiviral activity, with $EC_{50} = 1.5$, 0.8, and 0.8 μ M comparable to cidofovir (CDV) $EC_{50} = 2.0$, 2.0, and 5.0 μ M and aciclovir (ACV) $EC_{50} = 0.9$, 0.9, and 100 μ M against HSV-1, HSV-2, and HSV-1 TK + VZV Oka strains, respectively (Fig. 17).⁷⁷

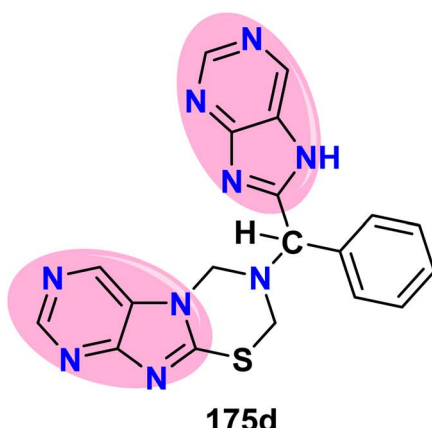


Fig. 15 Structure of the 1,3,5-thiadiazino[2,3-f]purine derivative **175d**, which acts as a COX-2 inhibitor.

COX-2 inhibition

$IC_{50} = 89.92 \pm 2.17$ nM

Celecoxib $IC_{50} = 53.76 \pm 2.05$ nM

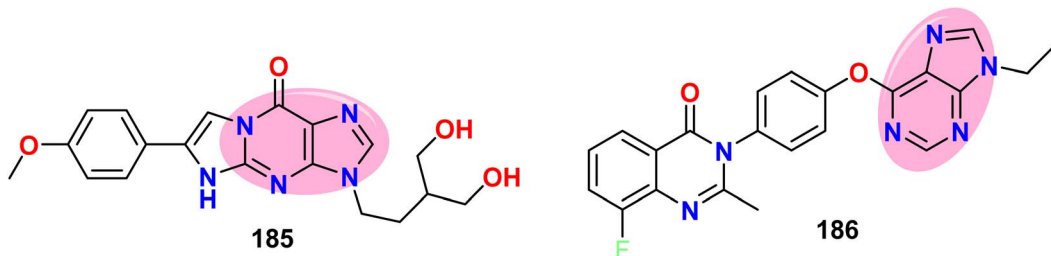


Fig. 17 Structure of purine derivatives with antiviral activity.

Furthermore, Deng *et al.* described the synthesis of new purine hybrids with quinazoline and then evaluated their activity against the tobacco mosaic virus. In the antiviral bioassays against plant viruses, the *in vivo* antiviral activity of some purine-quinazoline derivatives against tobacco mosaic virus (TMV) was higher than that of the commercial drug ribavirin. To our surprise, compound **186** containing 8-fluoro quinazoline (500 mg L^{-1}) showed curative activity and protective inhibitory action up to 65.2% and 60.2%, respectively, higher than those of ribavirin (50.1% and 57.2%). Similarly, the *in vivo*

study of TMV showed that the EC_{50} value of compound **186** (162.3 mg L^{-1}) was greater than that of ribavirin (314.45 mg L^{-1}), indicating that the compound had a significant therapeutic effect (Fig. 17).⁷⁸

4.5. Anti-oxidant activity

Mangasuli *et al.* synthesized new coumarin-purine hybrids and screened them for *in vitro* antioxidant activity using DPPH. By substituting OH at C7 of the coumarin ring, the most active derivative with excellent DPPH scavenging properties was obtained. Compound **187** exhibited radical scavenging activity (%) values of $30.09 \pm 1.16\%$, $43.90 \pm 2.39\%$, $62.51 \pm 0.92\%$, $75.24 \pm 1.78\%$, and $87.04 \pm 1.54\%$ at concentrations of 20, 40, 60, 80, and $100 \mu\text{g mL}^{-1}$, respectively, compared to ascorbic acid, which showed values of $40.36 \pm 0.75\%$, $58.60 \pm 0.916\%$, $75.40 \pm 2.12\%$, $85.23 \pm 1.21\%$, and $95.15 \pm 1.91\%$ at the same concentrations, respectively (Fig. 18).⁷⁹

Valdes *et al.* modified some purine derivatives (adenosine) and evaluated their antioxidant activity using DPPH and ABTS assays. Compounds **188**, **189**, and **190** had a powerful antioxidant effect compared with the reference compound ascorbic acid. As for DPPH, the purine derivatives **188**, **189**, and **190** demonstrated IC_{50} values of 77.25 ± 1.5 , >100 , and $17.12 \pm 1.9 \mu\text{g mL}^{-1}$, respectively, much higher than that of ascorbic acid

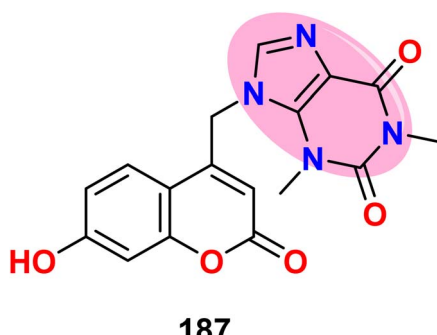
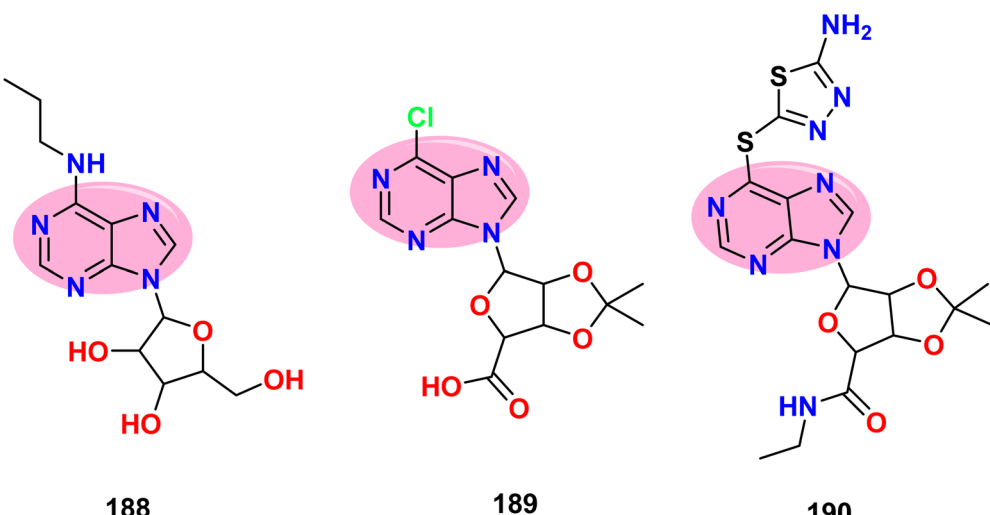
Fig. 18 Structure of the 9-(coumarin)-purine derivative **187** with antioxidant activity.

Fig. 19 Structures of some modified adenosine purine analogs exhibiting anti-oxidation potential.



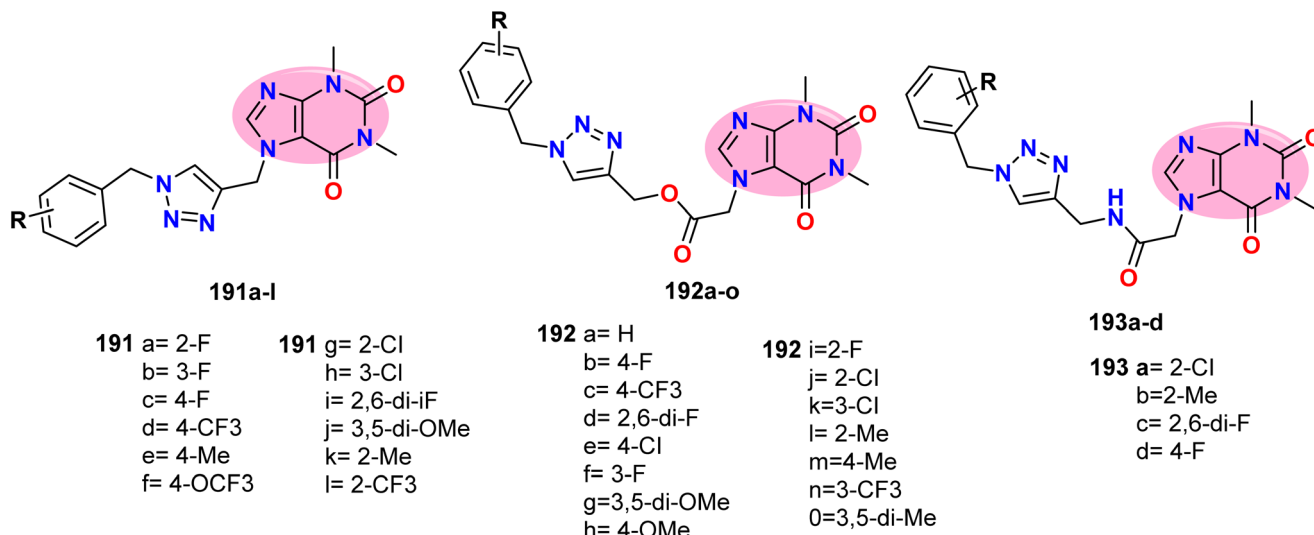


Fig. 20 Structure of caffeine-based triazoles as AChE and BChE inhibitors.

($IC_{50} = 1.5 \pm 0.2 \mu\text{g mL}^{-1}$). On the other hand, these derivatives revealed IC_{50} values of 7.25 ± 1.5 , 83.24 ± 2.2 , and $20.05 \pm 2.5 \mu\text{g mL}^{-1}$, respectively, which were much lower compared to that of ascorbic acid ($IC_{50} = 27.62 \pm 3.5 \mu\text{g mL}^{-1}$) in the ABTS assay (Fig. 19).⁸⁰

4.6. Anti-Alzheimer activity

Sharma *et al.* synthesized three series of caffeine-based triazoles starting from a 1,3-dimethyl-1*H*-purine-2,6-dione derivative. These three series differed only in the linker substituted at N9 of the purine ring: compounds with methylene are denoted as **191a-l**, while those with alkylmethyl acetate are **192a-o** and compounds with *N*-(alkyl)acetamide are **193a-d**. All the synthesized derivatives were screened *in vitro* against AChE and BChE at $10 \mu\text{M}$ and exhibited good to potent inhibitory activity. Compounds with high inhibitory activity were further selected for IC_{50} value determination. The results showed that the purine derivative **192d** showed promising activity with dual potential against AChE and BChE, exhibiting IC_{50} values of 1.43 and $10.9 \mu\text{M}$, respectively. Cryptolepine $IC_{50} = 0.26 \pm 0.13 \mu\text{M}$ and rivastigmine $IC_{50} = 40.57 \pm 0.69 \mu\text{M}$ were used as positive controls for AChE, while β -secretase inhibitor-IV was used as the positive control for BChE ($IC_{50} = 0.74 \pm 0.19 \mu\text{M}$) (Fig. 20).⁵

5. Conclusion

In drug development, purine is a promising lead molecule due to its ability to interact with various essential biomolecules involved in metabolic processes. Consequently, synthesizing novel derivatives and structural modifications of purine has become a significant area of research because it is considered a building block of nucleic acids and implicated in cellular energy transfer, and signaling pathways, many drug modifications, modified nucleosides, *etc.* This review focuses on the recently developed synthetic methods, chemical modifications of purine scaffolds, and some pharmacological activities,

including their structure–activity relationships and modes of action. It hopes to pave the way for researchers to develop purine nuclei and explore the effect of different substituents in many biological evaluations. Finally, this review is expected to serve as a valuable reference for researchers involved in the investigation of novel purine scaffolds.

Abbreviations

HOMA	Harmonic oscillator model of aromaticity
DNA	Deoxyribonucleic acid
RNA	Ribonucleic acid
ATP	Adenosine triphosphate
BChE	Butyrylcholinesterase
AChE	Acetylcholinesterase
mTOR	Mammalian target of rapamycin
VEGFR	Vascular endothelial growth factor receptor
VEGF	Vascular endothelial growth factor
PI3K	Phosphoinositide-3 kinases
BRAF	V-Raf murine sarcoma viral oncogene homolog B1
JAK2	Janus kinase 2
BRD4	Bromodomain-containing protein 4
DAMN	2,3-Diaminomaleonitrile
TEA	Triethyl amine
DAFN	Diaminofumaronitrile
AICN	Amino imidazole carbonitrile
THF	Tetrahydrofuran
DPPA	Diphenylphosphoryl azide
<i>p</i> -TsOH	Toluenesulfonic acid
DMSO	Dimethyl sulfoxide
AMNS	Aminomalononitrile <i>p</i> -toluenesulfonate
TOA	Triethyl orthoacetate
TOF	Triethyl orthoformate
TMSCN	Trimethylsilyl cyanide
DABCO	Diazabicyclo[2.2.2]octane
KO <i>t</i> Bu	Potassium <i>tert</i> -butoxide



ADC	Acceptorless dehydrogenative coupling
DMF	Dimethylformamide
NOESY	Nuclear Overhauser effect spectroscopy
HMBC	Heteronuclear multiple bond correlation
DMB	Dimethylbenzamide
MWI	Microwave irradiation
SNAr	Aromatic nucleophilic substitutions
KOH	Potassium hydroxide
TFA	Trifluoroacetic acid
DIPEA	<i>N,N</i> -Diisopropylethylamine
CuAAC	Cu(i)-catalyzed azide–alkyne cycloaddition
NBS	<i>N</i> -Bromosuccinimide
DMAP	Dimethylaminopyridine
FDA	Food and Drug Administration
MTT	3-[4,5-Dimethylthiazol-2-yl]-2,5-diphenyl tetrazolium bromide
IC ₅₀	Half-maximal inhibitory concentration
EC ₅₀	Half maximal effective concentration
EGFR	Epidermal growth factor receptor
SRB	Sulforhodamine B
SAR	Structure–activity relationship
HCC	Hepatocellular carcinoma
BHA	Butylated hydroxyanisole
5-FU	5-Fluorouracil
CPT	Camptothecin
WI38	Human fetal lung fibroblast cells and its normal cell line
CDK2	Cyclin-dependent kinase 2
HEK-293	Human embryonic kidney cells
MTX	Methotrexate
FGFRs	Fibroblast growth factor receptors
MIC	Minimum inhibitory concentration
MSRA	Methicillin-resistant <i>Staphylococcus aureus</i>
RAW	Normal mammalian cells and macrophage cell line
264.7	
COX-2	Cyclooxygenase-2
15-LOX	15-Lipoxygenase
HSV	Herpes simplex virus
CDV	Cidofovir
ACV	Aciclovir
TMV	Tobacco mosaic virus
DPPH	2,2-Diphenyl-1-picrylhydrazyl
ABTS	2,2-Azino-bis-3-ethylbenzothiazoline-6-sulphonic acid

Data availability

All data will be made available on request.

Conflicts of interest

The author declares no conflicts of interest.

References

- 1 G. Chakraborty, R. Mondal, A. K. Guin and N. D. Paul, *Org. Biomol. Chem.*, 2021, **19**, 7217–7233.
- 2 F. Doganc, A. S. Aydin, E. Şahin and H. Göker, *J. Mol. Struct.*, 2023, **1272**, 134200.
- 3 N. Abad, S. Buhlak, M. Hajji, S. Saffour, J. Akachar, Y. Kesgun, H. Al-Ghulikah, E. Hanashalshahaby, H. Turkez and A. Mardinoglu, *J. Mol. Struct.*, 2024, **1311**, 138400.
- 4 T. Cheviet, I. Lefebvre-Tournier, S. Wein and S. Peyrottes, *J. Med. Chem.*, 2019, **62**, 8365–8391.
- 5 M. Sharma, A. Sharma, V. K. Nuthakki, S. Bhatt, U. Nandi and S. B. Bharate, *Drug Dev. Res.*, 2022, **83**, 1803–1821.
- 6 A. Chaurasiya, S. K. Wahan, C. Sahu and P. A. Chawla, *J. Mol. Struct.*, 2023, **1274**, 134308.
- 7 A. R. Mohamed, A. M. El Kerdawy, R. F. George, H. H. Georgey and N. M. A. Gawad, *Bioorg. Chem.*, 2021, **107**, 104569.
- 8 Y. Guo, Y. Zou, Y. Chen, D. Deng, Z. Zhang, K. Liu, M. Tang, T. Yang, S. Fu, C. Zhang, W. Si, Z. Ma, S. Zhang, B. Peng, D. Xu and L. Chen, *Bioorg. Chem.*, 2023, **132**, 106386.
- 9 M. A. Bhat, B. Tüzün, N. A. Alsaif, A. A. Khan and A. M. Naglah, *J. Mol. Struct.*, 2022, **1257**, 132600.
- 10 Y. Y. Yang, W. L. Wang, X. T. Hu, X. Chen, Y. Ni, Y. H. Lei, Q. Y. Qiu, L. Y. Tao, T. W. Luo and N. Y. Wang, *Bioorg. Chem.*, 2023, **132**, 106356.
- 11 A. K. Maddheshiya, M. Kumar, A. Tufail, P. S. Yadav, Y. Deswal, N. Yadav, T. P. Yadav and A. Dubey, *ACS Appl. Bio Mater.*, 2024, **7**(9), 5906–5924.
- 12 P. Salas-Ambrosio, S. Vexler, R. P. S. I. A. Chen and H. D. Maynard, *ACS Bio Med Chem Au*, 2023, **3**, 189–200.
- 13 M. Ali, E. N. Sholkamy, A. S. Alobaidi, M. K. Al-Muhanna and A. Barakat, *ACS Omega*, 2023, **8**, 47304–47312.
- 14 F. He, J. Shi, Y. Wang, S. Wang, J. Chen, X. Gan, B. Song and D. Hu, *J. Agric. Food Chem.*, 2019, **67**, 8459–8467.
- 15 I. Schino, M. Cantore, M. de Candia, C. D. Altomare, C. Maria, J. Barros, V. Cachatra, P. Calado, K. Shimizu, A. A. Freitas, M. C. Oliveira, M. J. Ferreira, J. N. C. Lopes, N. A. Colabufo and A. P. Rauter, *Pharmaceuticals*, 2023, **16**(1), 54.
- 16 J. Liu, S. Hong, J. Yang, X. Zhang, Y. Wang, H. Wang, J. Peng and L. Hong, *J. Ovarian Res.*, 2022, **15**, 93.
- 17 A. Chaurasiya, C. Sahu, S. K. Wahan and P. A. Chawla, *J. Mol. Struct.*, 2023, **1280**, 134967.
- 18 M. K. I. Attiogbe, H. y. Zhao, J. Wang, T. t. Huang, P. p. Yan, Y. n. Liu, W. Li, L. Cao, S. q. Zhang and Y. x. Cao, *Life Sci.*, 2024, **336**, 122308.
- 19 T. Manna, S. Maji, M. Maity, B. Debnath, S. Panda, S. A. Khan, R. Nath and M. J. Akhtar, *Mol. Divers.*, 2024, **29**(1), 81–848, DOI: [10.1007/s11030-024-10870-4](https://doi.org/10.1007/s11030-024-10870-4).
- 20 D. D. Umesh, P. K. Nagaraj and L. K. Karadigere, *Int. J. Pharm. Invest.*, 2025, **15**, 19–29.
- 21 S. Sharma, S. Mehndiratta, S. Kumar, J. Singh, P. M. S. Bedi and K. Nepali, *Recent Pat. Anti-Cancer Drug Discov.*, 2015, **10**, 308–341.
- 22 J. Linden, F. Koch-Nolte and G. Dahl, *Annu. Rev. Immunol.*, 2019, **37**, 325–347.
- 23 G. Burnstock, *Neuropharmacology*, 1997, **36**, 1127–1139.
- 24 N. Rana, P. Grover and H. Singh, *Curr. Top. Med. Chem.*, 2024, **24**, 541–579.



25 A. A. Abu-Hashem, O. Hakami, M. El-Shazly, H. A. S. El-Nashar and M. N. M. Yousif, *Chem. Biodivers.*, 2024, **21**, e202400050.

26 S. Benkirane, H. Misbahi, M. Boudkhili, Y. K. Rodi, N. K. Sebbar and E. M. Essassi, *Curr. Org. Chem.*, 2023, **27**, 1683–1696.

27 B. D. Cheson, D. A. Vena, F. M. Foss and J. M. Sorensen, *J. Clin. Oncol.*, 2024, **12**, 2216–2228.

28 A. Ragab, S. A. Fouad, Y. A. Ammar, D. S. Aboul-Magd and M. S. Abusaif, *Antibiotics*, 2023, **12**, 128.

29 A. Ragab, M. S. Abusaif, N. A. Gohar, D. S. Aboul-Magd, E. A. Fayed and Y. A. Ammar, *Bioorg. Chem.*, 2023, **131**, 106307.

30 A. Ragab, M. S. Abusaif, D. S. A. Magd and M. M. S. Wassel, *Drug Dev. Res.*, 2022, **83**, 1305–1330.

31 M. M. Abdelgalil, Y. A. Ammar, G. A. M. E. Ali, A. K. Ali and A. Ragab, *J. Mol. Struct.*, 2023, **1274**, 134443.

32 R. Ayman, M. S. Abusaif, A. M. Radwan, A. M. Elmetwally and A. Ragab, *Eur. J. Med. Chem.*, 2023, **249**, 115138.

33 B. M. Bizzarri, A. Fanelli, S. Cesarini and R. Saladino, *Eur. J. Org. Chem.*, 2022, **2022**, e202200598.

34 I. Reva, H. Rostkowska and L. Lapinski, *Photochem.*, 2022, **2**, 448–462.

35 N. J. Green, J. Xu and J. D. Sutherland, *J. Am. Chem. Soc.*, 2021, **143**, 7219–7236.

36 M.-R. Huang, Y.-L. Hsu, T.-C. Lin, T.-J. Cheng, L.-W. Li, Y.-W. Tseng, Y. Chou, J.-H. Liu, S.-H. Pan, J.-M. Fang and C.-H. Wong, *Eur. J. Med. Chem.*, 2019, **181**, 111551.

37 Y.-W. Tseng, T.-J. Yang, Y.-L. Hsu, J.-H. Liu, Y.-C. Tseng, T.-W. Hsu, Y. Lu, S.-H. Pan, T.-J. R. Cheng and J.-M. Fang, *Eur. J. Med. Chem.*, 2024, **265**, 116042.

38 R. Mazzucato, M. Roberti, A. M. Capelli, F. Rancati, M. Biagetti, C. Fiorelli, P. Bruno, P. Ronchi, S. Bertolini, M. Corsi and D. Pala, *Eur. J. Med. Chem.*, 2023, **254**, 115331.

39 A. P. Bettencourt, M. Castro, J. P. Silva, F. Fernandes, O. P. Coutinho, M. J. Sousa, M. F. Proença and F. M. Areias, *Med. Chem.*, 2019, **15**, 341–351.

40 M. Pretze, C. Neuber, E. Kinski, B. Belter, M. Köckerling, A. Caflisch, J. Steinbach, J. Pietzsch and C. Mamat, *Org. Biomol. Chem.*, 2020, **18**, 3104–3116.

41 J. M. Gonçalves, J. N. D. Gonçalves, A. S. Pêra, N. R. Senhorães, A. R. O. Rodrigues, R. Oliveira, P. J. G. Coutinho, E. M. S. Castanheira and A. M. Dias, *Eur. J. Org. Chem.*, 2023, **26**, e202300176.

42 B. M. Bizzarri, A. Fanelli, L. Botta, M. De Angelis, A. T. Palamara, L. Nencioni and R. Saladino, *RSC Adv.*, 2021, **11**, 30020–30029.

43 Z. Tber, N. G. Biteau, L. Agrofoglio, J. Cros, S. Goffinont, B. Castaing, C. Nicolas and V. Roy, *Eur. J. Org. Chem.*, 2019, **2019**, 5756–5767.

44 V. A. Verma, B. Halu, A. R. Saundane and R. S. Meti, *Polycycl. Aromat. Compd.*, 2022, **42**, 3694–3716.

45 S. El-Kalyoubi, F. Agili, W. A. Zordok and A. S. A. El-Sayed, *Int. J. Mol. Sci.*, 2021, **22**, 1–36.

46 S. El-Kalyoubi, F. Agili, I. Adel and M. A. Tantawy, *Arab. J. Chem.*, 2022, **15**, 103669.

47 V. V. Fedotov, E. N. Ulomsky, K. V. Savateev, E. M. Mukhin, D. A. Gazizov, E. B. Gorbunov and V. L. Rusinov, *Synthesis*, 2020, **52**, 3622–3631.

48 H. Lei, S. Fan, H. Zhang, Y. J. Liu, Y. Y. Hei, J. J. Zhang, A. Q. Zheng, M. Xin and S. Q. Zhang, *Eur. J. Med. Chem.*, 2020, **186**, 111888.

49 Á. Lorente-Macías, I. Iañez, M. C. Jiménez-López, M. Benítez-Quesada, S. Torres-Rusillo, J. J. Díaz-Mochón, I. J. Molina and M. J. P. de las Infantas, *Arch. Pharm.*, 2021, **354**, 2100095.

50 M. F. Polat, I. D. Şahin, P. Kul, R. C. Atalay and M. Tuncbilek, *Bioorg. Med. Chem. Lett.*, 2024, **106**, 129775.

51 A. Kucukdumlu, M. Tuncbilek, E. B. Guven and R. C. Atalay, *Acta Chim. Slov.*, 2020, **67**, 70–82.

52 J. M. Orduña, N. del Río and M. J. Pérez-Pérez, *Org. Biomol. Chem.*, 2023, **21**, 5457–5468.

53 S. Bigonah-Rasti, S. Sheikhi-Mohammareh, K. Saadat and A. Shiri, *Polycycl. Aromat. Compd.*, 2022, **42**, 2644–2654.

54 R. T. Attia, M. A. Ewida, E. Khaled, S. A. Fahmy and I. M. Fawzy, *ACS Omega*, 2023, **8**, 37864–37881.

55 Y. Wang, Y. Pan, Z. Lv and S. Gou, *Eur. J. Med. Chem.*, 2024, **271**, 116415.

56 V. Petrov, R. J. Dooley, A. A. Marchione, E. L. Diaz, B. S. Clem and W. Marshall, *Beilstein J. Org. Chem.*, 2020, **16**, 2739–2748.

57 Y. Fu, D. Liu, H. Zeng, X. Ren, B. Song, D. Hu and X. Gan, *RSC Adv.*, 2020, **10**, 24483–24490.

58 A. Villegas, R. Satheeshkumar, A. Ballesteros-Casallas, M. Paulino, A. Castro, C. Espinosa-Bustos and C. O. Salas, *J. Heterocycl. Chem.*, 2022, **59**, 97–111.

59 A. Bistrović Popov, A. B. Popov, R. Vianelo, P. Grbčić, M. Sedić, S. K. Pavelić and S. Raić-Malić, *Molecules*, 2021, **26**, 3334.

60 S. Konduri, J. Prashanth, V. S. Krishna, D. Sriram, J. N. Behera, D. Siegel and K. P. Rao, *Bioorg. Med. Chem. Lett.*, 2020, **30**, 127512.

61 M. N. S. Rad, S. Behrouz, K. Shahbazkhani, M. Behrouz, E. Zarenezhad and A. Ghanbariasad, *RSC Adv.*, 2023, **13**, 24656–24673.

62 A. Q. A. Nadaf, S. Dixit, M. Yaseen, S. Mantur, M. S. Najare, S. Joshi, S. Vootla and I. A. M. Khazi, *ChemistrySelect*, 2020, **5**, 8635–8643.

63 V. P. Krasnov, G. L. Levit, V. V. Musiyak, D. A. Gruzdev and V. N. Charushin, *Pure Appl. Chem.*, 2020, **92**, 1277–1295.

64 A. Zagórska, A. Czopek, A. Jaromin, M. Mielczarek-Puta, M. Struga, D. Stary and M. Bajda, *Materials*, 2021, **14**(15), 4156.

65 G. Dilek, I. O. Tekin, B. Coban, A. Disli and Z. Gercek, *Med. Chem. Res.*, 2021, **30**, 84–97.

66 A. Singh, S. K. Maiti, H. P. Gogoi and P. Barman, *Polyhedron*, 2023, **230**, 116244.

67 O. S. Afifi, O. G. Shaaban, H. A. A. El Razik, S. E.-D. A. Shams El-Dine, F. A. Ashour, A. A. El-Tombari and M. M. Abu-Serie, *Bioorg. Chem.*, 2019, **87**, 821–837.

68 M. E. Khalifa, *J. Mol. Struct.*, 2021, **1229**, 129843.

69 A. Y. Hassan, E. S. Abou-Amra and S. A. El-Sebaey, *J. Mol. Struct.*, 2023, **1278**, 134930.



70 E. M. Husseiny, H. S. Abulkhair, A. Saleh, N. Altwaijry, R. A. Zidan and F. G. Abdulrahman, *Bioorg. Chem.*, 2023, **140**, 106789.

71 W. C. Hahn, J. S. Bader, T. P. Braun, A. Califano, P. A. Clemons, B. J. Druker, A. J. Ewald, H. Fu, S. Jagu and C. J. Kemp, *Cell*, 2021, **184**, 1142–1155.

72 A. Chaurasiya, S. K. Wahan, C. Sahu and P. A. Chawla, *J. Mol. Struct.*, 2023, **1274**, 134308.

73 Y. Hu, S. Hu, G. Pan, D. Wu, T. Wang, C. Yu, M. F. Ansari, R. R. Y. Bheemanaboina, Y. Cheng, L. Bai, C. Zhou and J. Zhang, *Bioorg. Chem.*, 2021, **114**, 105096.

74 B. Paulsen, K. A. Fredriksen, D. Petersen, L. Maes, A. Matheeussen, A. O. Naemi, A. A. Scheie, R. Simm, R. Ma, B. Wan, S. Franzblau and L. L. Gundersen, *Bioorg. Med. Chem.*, 2019, **27**, 620–629.

75 A. Q. A. Nadaf, M. S. Najare, M. Garbhagudi, S. Mantur, M. G. Sunagar, S. Gaonkar, S. Joshi and I. A. M. Khazi, *Chem. Biodivers.*, 2020, **17**(5), e2000053.

76 A. Ohler, P. E. Taylor, J. A. Bledsoe, A. T. Iavarone, N. C. Gilbert and A. R. Offenbacher, *ACS Catal.*, 2024, **14**, 5444–5457.

77 A. F. Mohammed, G. Andrei, A. M. Hayallah, S. G. Abdel-Maty, R. Snoeck and C. Simons, *Bioorg. Med. Chem.*, 2019, **27**, 1023–1033.

78 Y. Deng, M. Chen, J. Yi and Y. Zheng, *Phytochem. Lett.*, 2024, **59**, 10–14.

79 S. N. Mangasuli, K. M. Hosamani and P. B. Managutti, *Helijon*, 2019, **5**, e01131.

80 F. Valdes, N. Brown, A. Morales-Bayuelo, L. Prent-Peñaloza and M. Gutierrez, *Antioxidants*, 2029, **8**(10), 468.

